



University of Pannonia

Doctoral School of Chemical Engineering and Material Sciences

**Submitted for the degree of
Doctor of Philosophy
of the University of Pannonia, Hungary**

**Author: Wenjing Quan
Supervisor: Dr. habil. Gusztáv Fekete Dr. Tamás Korim**

Dissertation Title: Effect of footwear drop on running biomechanics and finite element analysis in recreational runners

DOI:10.18136/PE.2023.862

**Veszprém
2023**

EFFECT OF FOOTWEAR DROP ON RUNNING BIOMECHANICS AND FINITE
ELEMENT ANALYSIS IN RECREATIONAL RUNNERS

Thesis for obtaining a PhD degree in the Doctoral School of Chemical Engineering and
Material Sciences of the University of Pannonia

in the branch of Material Sciences and Technologies

Written by Wenjing Quan

Supervisor: Dr. habil. Gusztáv Fekete

Co-supervisor: Dr. Tamás Korim

propose acceptance (yes / no)

propose acceptance (yes / no)

.....
Dr. habil. Gusztáv Fekete
Supervisor

.....
Dr. Tamás Korim
Co-supervisor

As reviewer, I propose acceptance of the thesis:

Name of Reviewer: Dr. yes / no

.....
1st reviewer

Name of Reviewer: Dr. yes / no

.....
2nd reviewer

The PhD-candidate has achieved% at the public discussion.

Veszprém,

.....
Chairman of the Committee

The grade of the PhD Diploma (..... %)

Veszprém,

.....
Chair of the UDHC

Submitted with 95 pages and 186 references

The Dissertation contains 38 Figures, and 15 Tables

Supervision

Dr. habil. Gusztáv Fekete	Supervisor	PhD supervisor, Doctoral School of Chemical Engineering and Material Sciences, University of Pannonia. Senior Research Fellow at Vehicle Industry Research Center, Széchenyi István University
Dr. Korim Tamás	Co-supervisor	PhD supervisor, Doctoral School of Chemical Engineering and Material Sciences, University of Pannonia.

Acknowledgments

First and foremost, I would like to express my sincere appreciation to my supervisor, Dr. Gusztáv Fekete, for his consistent guidance, support, and encouragement throughout this research endeavor. His extensive expertise and insightful suggestions have played a critical role in shaping the outcome of this study, and his unwavering confidence in my abilities has served as a constant source of motivation. Additionally, I would like to extend my deepest gratitude to my co-supervisor, Dr. Tamás Korim, for his invaluable advice, constructive critiques, and unwavering backing. His relentless pursuit of excellence and generous knowledge-sharing have significantly enriched this work and contributed to its success.

I am profoundly grateful to Prof. Yaodong Gu for providing me with the opportunity to pursue my doctoral degree and for his comprehensive support during both my master's and doctoral studies. Your unwavering belief in my capabilities and exceptional guidance as a mentor has left an indelible impression on me. I would also like to convey my heartfelt thanks to Prof. Feng Ren. Your enthusiastic support was always there to uplift me whenever I encountered obstacles. It has been an honor to have you as my supervisor.

Secondly, I am incredibly fortunate to be part of such an extraordinary team. I sincerely appreciate the Research Academy of Grand Health at Ningbo University and Pannonia University's invaluable contributions to this research.

I want to express my gratitude to Jinna Ding and Shizheng Feng. In the ten years of knowing and accompanying each other, I sincerely appreciate your unwavering companionship and support. I am confident that our bond will endure the test of time and continue to thrive.

I cannot overlook the unwavering support of my family. Despite the physical distance that separated us, their unshakable belief in me never wavered. Their love and encouragement have been the cornerstone of my inner strength.

Lastly, I would like to acknowledge the financial assistance provided by the Stipendium Hungaricum Programme, Tempus Public Foundation, and China Scholarship Council (CSC).

Content

Acknowledgments	I
Abstract	III
Abbreviations	VI
List of Figures	VII
List of Tables	IX
1. Introduction	1
1.1 Overview of running	1
1.2 Running shoes biomechanical characters	11
1.3 Opensim simulation modeling in human movements.....	17
1.4 Anatomy of the Human Foot.....	21
1.5 Aims and Objectives	25
2 Materials and methods	27
2.1 Experiments	27
2.2 Musculoskeletal modeling	38
2.3 Data analysis	39
2.4 Finite element modeling simulation.....	43
2.5 Data analysis	45
3 Results	46
3.1 Gait fatigue biomechanics variables	46
3.2 Gait analysis of Minimalist and normal shoes	52
3.3 Finite element model simulation.....	57
4 Discussion	64
4.1 Gait fatigue biomechanics variables	64
4.2 Gait analysis of Minimalist and normal shoes	66
4.3 Finite element model simulation.....	69
5 Conclusions and future work	71
5.1 Conclusions.....	71
5.2 Recommendations for future works.....	72
Thesis points	73
List of publications	77
References	80

Abstract

Running can be considered one of the most popular recreational physical activities worldwide that promote aerobic capacity and reduce the risk of cardiovascular disease. However, running-related injuries have been identified as a common overuse injury in competitive and recreational runners.

The first research question of this thesis is: Joint mechanics are permanently changed using different intensities and running durations. These variations in intensity and duration also influence fatigue during prolonged running. Little is known about the potential interactions between fatigue and joint mechanics in female recreational runners.

The first objective of this thesis is to describe and examine kinematic and joint mechanical parameters when female recreational runners are fatigued after long-distance running. The analysis used the Partial Least Square Algorithm (PLSR) to investigate if a linear relationship existed between the initial joint angle, ankle joint work, and knee joint work. The first hypothesis was that ankle work would decrease due to fatigue after prolonged running. The second hypothesis was that joint work would have a greater relationship with the initial angle of the ankle and knee.

The second research question of this thesis is: Previous studies always focus on the kinematics and kinetic variables of running in barefoot, minimalist shoes and conventional shoes. However, little work has investigated how negative heel-to-toe drop affects lower extremity muscle force variables during the running stance.

The second objective of this thesis: This section was to create musculoskeletal modeling and simulation techniques to compare the muscle force, kinematics, and kinetic variables of habitually rearfoot runners while wearing the heel-to-toe drop of negative 8mm shoes (minimalist shoes) and the heel-to-toe drop of positive 9mm shoes (normal shoes) during the running stance phase. This section focused on the immediate effect of kinematic and kinetic variables during the running stance with different heel-to-toe drop shoe conditions.

The third research question of this thesis is: Previous studies have shown that the finite element model was considered an accurate approach to analyzing the foot stress distributions in the model of the foot and footwear under running stance phase conditions and in biomechanical investigations. However, few studies have focused on internal foot biomechanics while running with different heel-drop shoes during different running stances.

The third objective of this thesis is to investigate the internal stress in the metatarsals and midfoot with the different heel-drop shoes (normal and minimalist shoes) during the running stance phase. Two finite element models were developed from a reactional runner, and four conditions were simulated and compared: (1) initial contact, (2) midstance phase, (3) push off

(4) toe-off.

Long-distance running is a widely embraced athletic activity that gains popularity among countless individuals globally. With the increased number of runners, overuse of running injuries has increased. According to epidemiological investigations, the risk of running injuries increases by 79% yearly. Studies have demonstrated that amateur runners face a greater susceptibility to running injuries in the lower limbs compared to those engaged in competitive running. Several variables contribute to the occurrence of such injuries, including foot strike patterns, level of running experience, and the factor of fatigue. Nonetheless, the precise mechanisms linking running fatigue, minimalist footwear, and running experience to these injuries remain unclear.

Therefore, the first section's thesis used the Partial Least Squares Algorithm (PLSR) to investigate if a linear relationship existed between the initial joint angle, ankle joint work, and knee joint work for female fatigue running. The second section of the thesis was to investigate the lower limb extremity muscle characteristics in minimalist shoes and normal shoes. Finally, utilize the FE model to identify the stress distribution of minimalist and normal shoes in the four different running stance phase conditions.

This thesis's first section showed moderate reductions in absolute positive ankle power, total ankle energy dissipation, dorsiflexion at initial contact, max dorsiflexion angle, and ROM (range of motion) of the joint ankle after fatigue following prolonged running. Knee joint mechanics, joint angle, and joint power remained unchanged after prolonged running. Nevertheless, with the decreased ankle joint work, negative knee power increased. At the hip joint, the extension angle was significantly decreased. The range of motion of the hip joint, hip positive work, and hip positive power were increased during the prolonged running.

The second section of this thesis revealed differences in the sagittal ankle and hip angles and sagittal knee moments between the different heel-to-toe drops of running shoes. Specifically, it showed that the negative 8 mm running shoes led to significantly smaller values than the positive 9 mm running shoes in terms of the angle of ankle dorsiflexion, ankle eversion, knee flexion, hip flexion, and hip internal and external rotation. The peak ankle dorsiflexion moment, ankle plantarflexion moment, ankle eversion moment, knee flexion moment, knee abduction moment, and knee internal rotation decreased obviously with the minimalist running shoes. Simultaneously, the lateral gastrocnemius, Achilles tendon, and extensor hallucis longus muscles were significantly greater in the minimalist shoes compared to normal shoes. The vastus medialis, vastus lateralis, and extensor digitorum longus muscles were smaller in the minimalist shoes.

The results of the third section of the thesis showed that the minimalist shoes showed larger von Mises stresses in the metatarsal segment during the four running stance phases compared to normal shoes. This difference was the most significant in the push-off phase, where 12%

higher von Mises stress was found compared to normal shoes. Concerning stress distribution, 74% higher von Mises stress was found in the midfoot segment when minimalist shoes were compared to normal shoes during the mid-stance phase. The results suggest that minimalist shoe design should consider midfoot support and cushioning to reduce the pressure distribution during running. Therefore, I could generally conclude that shoes with lower drop increase stress levels in the metatarsal and midfoot, particularly during the push-off phase.

This study presents an innovative multidisciplinary approach combining biomechanics, machine learning, and finite element analysis. An established workflow that integrates experimental and computational simulations to model the work done during running fatigue, the muscle contribution when running with different heel drop shoes, and the mechanism and results of stress distribution in the foot's finite element.

Abbreviations

IC: initial contact	VL: vastus lateralis
3D: three-dimensional	BF: biceps femoris
EMG: Electromyography	MF: maximum force
RRIs: Running Related Injuries	CRS: conventional running shoes
BMI: mass index	MS: minimalist shoes
RFS: rearfoot strike	MP: maximum pressure
MFS: midfoot strike	RE: Running economy
FFS: forefoot strike	IK: inverse kinematics
GRF: ground reaction forces	ID: inverse dynamics
VILR: vertical loading rate	RRA: residual reduction algorithm
ITBS: Iliotibial band syndrome	CMC: computed muscle control
PFP: patellofemoral pain syndrome	FE: finite element
RPE: Ratings of Perceived Exertion Scale	FHL: flexor hallucis longus
VGRF: vertical ground reaction force	EDL: extensor digitorum longus
ROM: range of motion	TP: tibialis posterior
PFJ: patellofemoral joint	PLSR: Partial Least Square Algorithm
iEMG: integrated EMG	SPM1d: one-dimensional statistical parametric mapping
MPF: mean power frequency	MVIC: maximal voluntary isometric contraction
VILR: vertical instantaneous loading rate	
HTD: heel-to-toe drop	
RMS: root mean square	
TA: tibialis anterior	
GM: gastrocnemius medialis	
AT: Achilles tendon	
PTF: knee patellofemoral tracking force	
PP: patellofemoral pressure	
ILR: instantaneous load rate	
PL: peroneus longus	
SL: soleus muscle	

List of Figures

<i>Figure 1 The overview of a gait cycle includes stance and swing phases [5].</i>	2
<i>Figure 2 Overview of the stance phase[9].</i>	2
<i>Figure 3 Running foot strike (A-Forefoot strike B-midfoot strike C rearfoot strike).</i>	6
<i>Figure 4 Simulation steps with Opensim.</i>	18
<i>Figure 5 Anatomy of the Human Foot.</i>	22
<i>Figure 6 The extrinsic foot muscle and the intrinsic foot muscle.</i>	23
<i>Figure 7 Build a 3D-coupled foot-shoe finite element model process[147].</i>	24
<i>Figure 8 3D Infrared Motion Capture System.</i>	28
<i>Figure 9 The machine of the force plate.</i>	29
<i>Figure 10 The machine of smart speed.</i>	29
<i>Figure 11 The Delsys surface electromyography devices.</i>	30
<i>Figure 12 The machine of heart rate monitor.</i>	30
<i>Figure 13 The CT scanner in this study (GE Healthcare, Chicago, United States).</i>	31
<i>Figure 14 Experimental set-up (not on scale). Outlined in this illustration, the left running shoe has the- 8 mm HTD (minimalist shoes) and the right running shoe has with 9 mm HTD (normal shoes).</i>	32
<i>Figure 15 Marker placement on the lower limb and trunk.</i>	33
<i>Figure 16 Placement of test equipment.</i>	34
<i>Figure 17 Static model collection and dynamic model in the data collection.</i>	34
<i>Figure 18 EMG (Electromyography) Muscle Data Collection Diagram.</i>	35
<i>Figure 19 Borg Scale RPE.</i>	36
<i>Figure 20 Workflow of finite element in this study.</i>	37
<i>Figure 21 Data collection and foot model simulation in the FE analysis section, A: kinematics parameters collection, B:FE model building, C: FE model with the minimalist shoes.</i>	37
<i>Figure 22 Comparison of muscle activations from static optimization estimated (blue line) and filtered electromyography (EMG) signals measured from the subjects during the same trial of normal walking, jogging and running. Note. EMG and activations were normalized from zero to one for each subject based upon the minimum and maximum values over the stance phase.</i>	38
<i>Figure 23 FE simulations at four different running gait instants: initial contact(at 20% of the stance phase), midstance stance (40% of the stance phase), push-off (60% of the stance phase), toe-off (80% of the stance phase).</i>	45
<i>Figure 24 Comparing the mean values of ankle, knee and hip joint angle from all participants between fatigue conditions (pre-fatigue; post-fatigue). *P ≤ 0.05.</i>	46
<i>Figure 25 Comparing the mean values of ankle, knee and hip joint moment from all participants between fatigue conditions (pre-fatigue; post-fatigue). *P ≤ 0.05.</i>	48
<i>Figure 26 Training (left) and testing (right) accuracy of special skills assessment results of observed and predicted from the PLSR model in the female runners.</i>	50
<i>Figure 27 The predicted results of the response variables base on the PLSR model. Ankle positive work (Y1), ankle negative work(Y2), total work of the ankle (Y3), knee positive work (Y4), knee negative work (Y5) and total work of the knee (Y6).</i>	51

<i>Figure 28 Illustration of the MS and NS lower limb results shows the statistical parametric mapping outputs for the angle of the ankle, knee, and hip during the running stance phase. MS, minimalist shoes, NS, normal shoes.</i>	<i>53</i>
<i>Figure 29 Illustration of the MS and NS lower limb results showing the statistical parametric mapping outputs for the moment of the ankle, knee, and hip during the running stance phase. MS, minimalist shoes, NS, normal shoes.</i>	<i>55</i>
<i>Figure 30 Illustration of the results between the MS and NS lower limb showing the statistical parametric mapping outputs for the muscle force during the running stance phase. MS, minimalist shoes, NS, normal shoes.</i>	<i>56</i>
<i>Figure 31 Validation of the FE foot model by comparing the predicted ground reaction force with experimental measurement.</i>	<i>58</i>
<i>Figure 32 Foot-ground angle between the two running shoes condition. MS: minimalist running shoes, NS: normal shoes.</i>	<i>59</i>
<i>Figure 33 Extrinsic lower limb muscle force estimated by the OpenSim musculoskeletal model. MS: minimalist shoes, NS: normal shoes.</i>	<i>60</i>
<i>Figure 34 Metatarsal von mises stress distribution during the different running stances between the MS and NS conditions.</i>	<i>61</i>
<i>Figure 35 First metatarsal von mises stress to fifth metatarsal von mises stress distribution during the different running stances between the MS and NS conditions.</i>	<i>62</i>
<i>Figure 36 Mid-bone von mises stress distribution during the different running stances between the MS and NS conditions.</i>	<i>63</i>
<i>Figure 37 Muscle force changed between the MS and NS running.</i>	<i>74</i>
<i>Figure 38 3D-footwear Finite Element model analysis.</i>	<i>75</i>

List of Tables

<i>Table 1 Detailed comparison of minimalist shoes and normal shoes.</i>	32
<i>Table 2 The average value (X_{ave}), maximum value (X_{max}), minimum value (X_{min}) and the difference between the maximum and minimum values (X_{dif}) of predictive variables X.</i>	42
<i>Table 3 The predictors of each predictive variable.</i>	42
<i>Table 4 Material properties of the components in the finite element model.</i>	43
<i>Table 5 Lower extremity joint kinematics pre-fatigue running and post-prolonged fatigue running ($x \pm SD$).</i>	46
<i>Table 6 Lower extremity joint moment, power pre-fatigue running and post-prolonged fatigue running ($x \pm SD$).</i>	48
<i>Table 7 Lower extremity joint work pre- fatigue running and post-prolonged fatigue running ($x \pm SD$).</i>	49
<i>Table 8 Lower limb joint kinematics during the running stance of two running shoes (minimalist vs. normal shoes).</i>	53
<i>Table 9 Lower limb joint moment during the running stance of two running shoes (minimalist vs. normal shoes).</i>	55
<i>Table 10 Normalized peak muscle force data during the running stance of two running shoes (minimalist vs. normal shoes).</i>	57
<i>Table 11 Ground reaction force variables of MS and NS conditions between FE prediction and experimental measurement.</i>	57
<i>Table 12 Running gait variable during the running stance.</i>	58
<i>Table 13 The musculoskeletal model calculated muscle forces used to define the loading and boundary conditions of the FE model at four different gait instants in the running stance phase of MS.</i>	59
<i>Table 14 Musculoskeletal model calculated muscle forces used to define the loading and boundary conditions of the FE model at four different gait instants in the running stance phase of NS.</i>	60
<i>Table 15 First metatarsal von mises stress to fifth metatarsal von mises stress distribution during the different running stances between the MS and NS conditions.</i>	61

1. Introduction

1.1 Overview of running

1.1.1 Running gait cycle

Recreational physical activities, like running, are highly favored across the globe. Consistent engagement in running aids in combatting chronic illnesses like cardiovascular disease and obesity [1,2]. The convenience it offers makes long-distance running a favored choice among many individuals, as it not only enhances cardiopulmonary functionality but also alleviates mental strain [3]. One of the most popular endurance activities is marathon running, and competitions have been prevalent worldwide. Amateur runners view the distance as a physical challenge and want to reap the numerous health benefits of consistent endurance training. The number of participants engaged in running throughout the world has increased in recent years. Thirty-five million people in the United States have engaged in running sports. The Athletics Association registers as many as 49 marathon events in China annually. In Beijing, there are about 2 million runners. A standard marathon competition was defined as a distance of 42.15 km, which can be run on tarmac roads (e.g., paved, etc.), an athletic track, or off-road [4].

Running is a periodic movement consisting of multiple local movements, such as the upper limbs swaying back and the lower limbs taking alternating steps. Gait is a biological concept that refers to the posture of the human body while walking or running, and it is a periodic phenomenon that defines the characteristics of individuals walking or running. Regarding the lower limb, the running gait can be categorized into the stance and swing phases (as shown in Figure 1) [5]. The running gait cycle initiates when one foot touches the ground and concludes when the same foot touches the ground again [6,7]. The stance phase is considered over once the foot is no longer in contact with the ground. The swing phase of the gait cycle commences when the foot lifts off the ground [8]. During the running cycle, the swing phase accounted for 40% of the entire duration. This particular phase, which commenced from the toe-off stage of the cycle, contributed significantly to the overall motion.

The stance phase of running is a crucial component of the running gait cycle and covers 60% of the running cycle. The stance phase can be divided into four periods: the loading response, the mid-stance phase, the terminal stance and the pre-swing phase, as illustrated in Figure 2 [9]. During the initial contact phase (IC), the foot first touches the ground. Notably, approximately 75% of runners exhibit a habitual rearfoot-strike pattern, in which the heel is the first part of the foot to touch the ground [10]. At the initial contact phase, the foot may absorb the shock to maintain whole-body balance and stability. The stance phase of running is a crucial component of the running gait cycle.

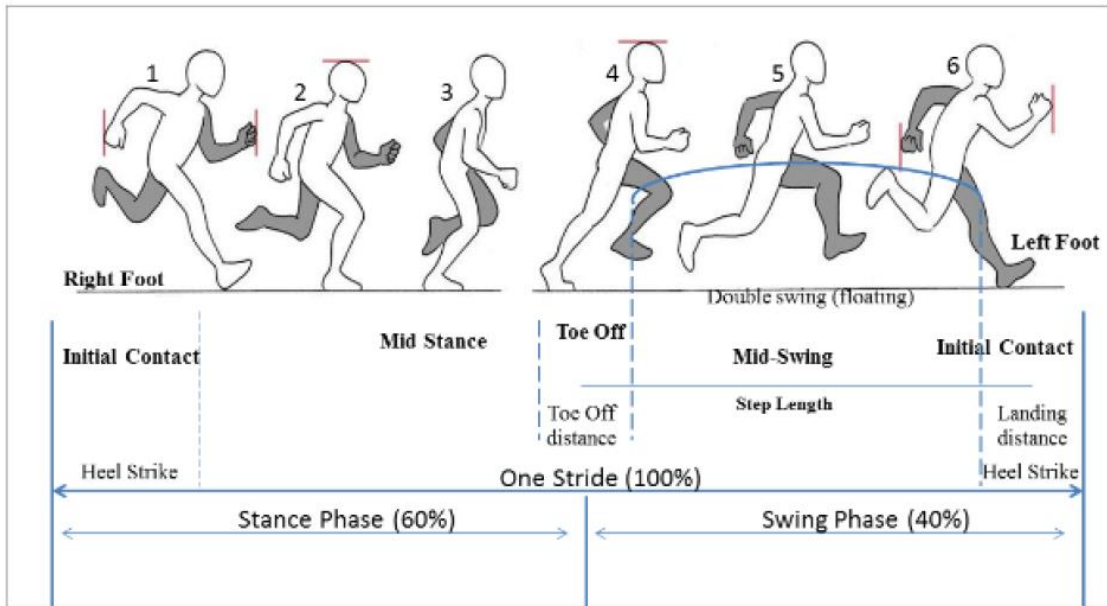


Figure 1 The overview of a gait cycle includes stance and swing phases [5].

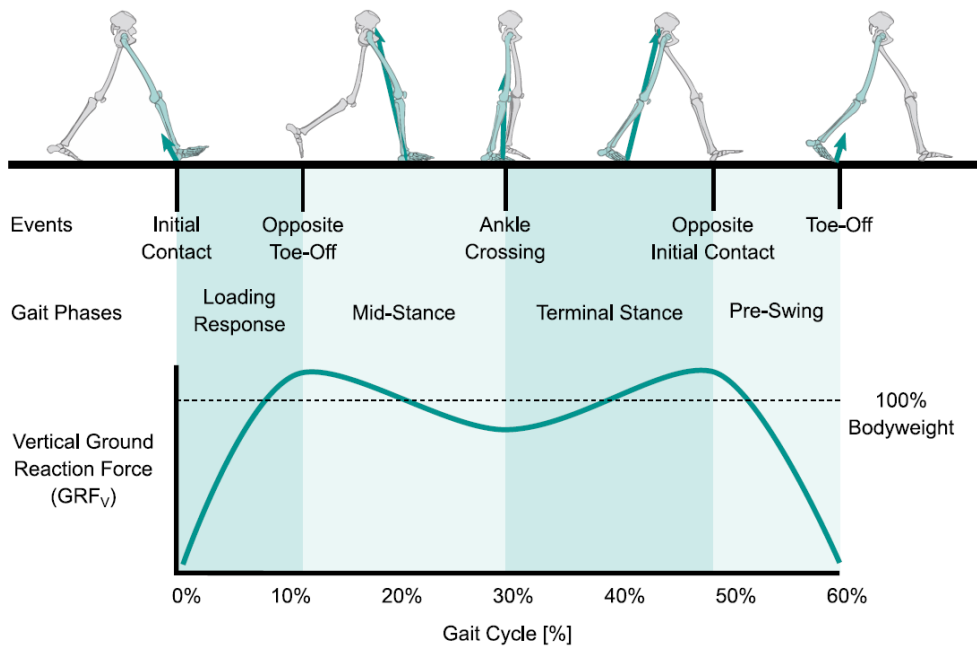


Figure 2 Overview of the stance phase[9].

Gait analysis refers to the kinematic observation and dynamic analysis of limb and joint activities during walking and running by applying mechanical principles and processing techniques. The biomechanical measurement was the essential measurement of the gait cycle. Numerous instruments have been created to aid in the evaluation of running gait. These encompass three-dimensional (3D) motion systems that collect the movement track, force

plates that measure the forces, and electromyography (EMG) that calculates muscle activity during movement. Generally, motion analysis facilitates a numerical depiction of bodily segments during movement but does not involve measuring forces. Force platforms typically measure vertical force, anterior-posterior force, and medial-lateral force. More recently, compact, portable sensors have been designed and effectively utilized to gauge running gait parameters. These consist of accelerometers, electro-goniometers, gyroscopes, and in-sole pressure sensors. These instruments have been effectively employed to examine shoe [11-13] and orthotic [14] performance, risk factors for injury [15], running performance [16], fatigue effects [17], and gait adaptations to various running techniques [18].

3D motion systems and force plate equipment can capture the gait kinematics and kinetics variables. Basic kinematic parameters included the joint angle and angular velocity. In addition, the kinetics included the joint moment, power, and ground reaction force. Therefore, using the biomechanical analysis method might contribute to a better understanding of gait mechanisms and, subsequently, a lower injury incidence.

1.1.2 The injury from long-distance running

The health advantages of frequent running are well known, yet there have been reports of alarming numbers of running-related injuries, which have associated difficulties and economic consequences. However, the incidence of running injuries was still high among runners. A review of the incidence and determinants of lower extremity running injuries in long-distance running has shown that lower limb running injuries were 19.4%–79.3% [19]. According to the findings of Videbæk et al., the occurrence of injury during 1000 hours of running was observed. The injury rate for novice runners was 17.8%, whereas for recreational runners, it was 7.7%, and for ultramarathon runners, it was 7.2% [20]. Out of all running populations, novices experience a significantly elevated injury rate. The injury rate among novices surpasses that of recreational, competitive, and marathon runners [21]. Despite the diligent efforts of scientific researchers and clinical personnel in mitigating running-related injuries, the incidence of such injuries has persisted at a high level for an extended period.

Running is a widespread activity often associated with a high risk of overuse injuries in the lower back and lower extremities. These injuries can be quite severe and can severely impact an individual's ability to participate in physical activities. Therefore, it is vital for individuals who engage in running to be aware of the potential risks and take appropriate measures to prevent and treat these injuries [22,23]. There is no uniform standard for the definition of running-related injuries (RRIs), primarily due to the varying levels of runners who participated in the survey, the varying training burdens, and the varying diagnostic criteria. A previous study defined RRIs as musculoskeletal injuries to the lower extremities or spine that impact running

speed or distance for a week [24]. Another study discovered that running during a running training session causes discomfort in the bones, muscles, joints, and tendons; significantly reduced running pace, frequency, distance, and time; or symptoms like muscle soreness [25].

1.1.2.1 Risk factors for running-related injuries

Meanwhile, there are numerous causes of overuse running injuries. The research investigated risk factors for injuries due to repetitive strain RRIs and examined extrinsic and intrinsic factors [26]. Callahan (2014) documented extrinsic risk factors such as training variables, warm-ups and stretches, running barefoot or with minimalist shoes, locomotion, strength and biomechanics, nutrition and supplementation, and psychology. On the other hand, anatomy, gender, and age were categorized as intrinsic factors [27]. The influence of gender has been regarded as an essential factor in the potential for injuries associated with running. Ferber et al. have shown that female runners have higher peak hip adduction, hip internal rotation, and knee abduction angles than male runners, which may increase the risk of lower limb injury [28]. Sinclair et al. also investigated knee loading in female and male recreational runners. Female runners showed larger knee extension and abduction moments, patellofemoral contact forces, and patellofemoral contact pressure than males.

Consequently, this finding also indicated that the prevalence of running injuries among female runners may be greater than that of male runners. The current investigation also provided insight into the incidence of patellofemoral pain [29]. With increased age, lower extremity injuries were higher in elderly populations than in younger populations, mainly due to the age-related deterioration in musculoskeletal function and joint stability [30,31]. Elderly runners, on the other hand, have been found to experience a higher incidence of injuries than young runners [32]. According to previous studies, anthropometric factors such as height, weight, body fat percentage, and body mass index (BMI) play a combined role in running-related injuries [33-36]. BMI is an indicator of body obesity. Previous studies have found that novice runners with a BMI greater than 30 have a higher risk of sports injuries [37].

Training factors are considered important causes of RRIs, including volume, duration, frequency, and intensity [38]. A previous study reported that 61% of male and 56% of female injured runners continuously increased their weekly running volume by approximately 30% at least once a week during the month before the injury. The main finding of this study was that a sudden increase in distance or intensity might increase the risk of RRIs injuries [39]. Simultaneously, Macera et al. conducted a 12-month follow-up survey of 583 recreational runners and found that runners who ran more than 64 km per week and had a running experience of less than three years were more likely to develop RRIs [34]. Sports equipment, professional running shoes and protective gear were essential for the runners. A systematic

analysis of the structural composition of athletic footwear has found that employing softer midsoles might decrease the impact on the ground and the rate at which it is absorbed while engaged in running. On the other hand, opting for thicker midsoles could potentially enhance shock absorption. Additionally, embracing minimalist footwear might bolster the cross-sectional dimensions and rigidity of the Achilles tendon, although it may concurrently augment the forces exerted on the ankle, metatarsophalangeal joint, and Achilles tendon [40].

The muscle was the most crucial structural element during the movement. Evidence has shown that running uses nearly every muscle in the lower extremities [8]. Nevertheless, lower muscle strength may reduce the ability of surrounding muscles to absorb shock and lead to decreased control of joint motion, thereby increasing the risk of RRIs [41]. Recently, a study explored the muscle strength associated with running injuries in high school cross-country runners. This research demonstrates that individuals who exhibit the lowest levels of muscle strength in the hip abductor, knee extensor, and knee flexor regions are more likely to experience anterior knee pain among the running population [42].

1.1.2.2 Biomechanical factors for running-related injuries

Comprehending the biomechanical aspects of running has generated implications for mitigating running injuries. Medial tibial stress syndrome, fractures, Achilles tendinitis, patellar pain syndrome, and plantar fasciitis were the most prevalent running-related injuries [25-28]. The high loading force causes these RRIs during the repetitive running cycle [18]. Some studies have reported that 70%–80% of running disorders are caused by overuse injuries, predominantly affecting the knee, ankle/foot, and shank anatomic sites [25,26]. Nevertheless, recent studies reported that the vertical impact peak was not associated with the RRIs between injured and uninjured female recreational runners [27,28].

According to the foot strike pattern, there are three main types of running patterns: rearfoot strike (RFS), midfoot strike (MFS), and forefoot strike (FFS) (Figure 3) [43]. The FFS is the metatarsal forefoot area contacting the ground before the heel, the MFS is the midfoot area and metatarsal area landing simultaneously, and the RFS is the heel. The heel touches the ground first during the running process. Research about the running strike pattern found that 75% of runners were habitually rearfoot strikers [10]. In RFS running, strike pattern technologies were also associated with running injuries, which might increase the impact loading rate and knee power. However, the forefoot strike pattern would increase ankle power and Achilles tendon force [44].

Moreover, barefoot group runners had the highest calf injury rates and lower plantar fasciitis incidence than shod group runners [45]. A previous study found that running barefoot may increase ankle plantarflexion and knee flexion angles. However, the barefoot group

experienced reduced ground reaction forces (GRF). These changes in biomechanical variables were believed to contribute to preventing RRIs [46]. Nevertheless, insufficient evidence exists to establish a clear relationship between running strike patterns and the risk of running injuries. Further prospective studies are necessary to determine the impact of different running styles on RRIs.

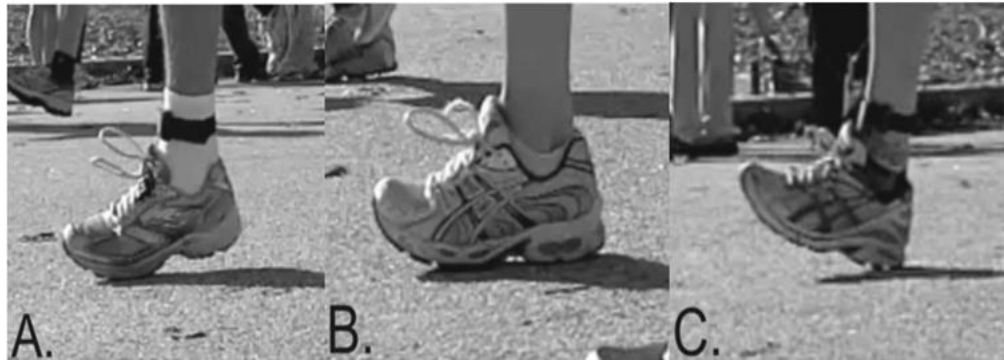


Figure 3 Running foot strike (A-Forefoot strike B-midfoot strike C rearfoot strike)

In running, it is commonly believed that kinematic characteristics such as joint angle, range of motion, and angular velocity of the lower extremities are related to RRIs. During running biomechanical analysis, hip adduction, knee flexion, and ankle valgus are frequently associated with developing RRIs. The relationship between hip adduction angle and RRIs has been inconsistent in studies [47]. Dudley et al. found that maximal hip adduction is not a risk factor for RRIs in college cross-country runners [48]. Nevertheless, Noehren et al. indicated that iliotibial band syndrome (ITBS) and patellofemoral pain syndrome (PFP) were the most common RRI caused by the increased hip adduction angle in recreational female runners [49,50].

The evidence indicates that the reduction in knee flexion angle does not appear to be the primary contributing factor to the risk of RRIs. Hein et al. observed a decreased knee flexion angle among male and female runners during running. This finding suggests a potential association between a reduced knee flexion angle and the development of Achilles tendinopathy [51]. In addition, another study has revealed that peak knee internal rotation and external femoral rotation relative to the global coordinate system are important kinematic factors in the development of ITBS in female recreational runners [50].

In addition, some studies have reported ankle and foot kinematic variables. Messier et al. found that ankle eversion range motion is not essential for the RRIs between male and female recreational runners [52]. However, three prospective studies found that an increased ankle eversion angle may be a risk factor for Achilles tendinitis [51]. Meanwhile, smaller ankle eversion may be associated with iliotibial band syndrome [50].

1.1.3 Biomechanical characteristic of the lower limb in fatigue running

Fatigue is a complex issue resulting from the interaction of multiple factors. In 1982, the 5th International Sports Biochemistry Conference defined exercise-induced fatigue as "the physiological process of the body that cannot continue to function at a specific level or maintain a predetermined intensity." Fatigue can be divided into general fatigue and local fatigue. Muscle fatigue is defined as the fatigue of the entire body during physical exertion, which can contribute to a decrease in muscle strength, alterations in athletic performance, and a loss of motor control [53]. In most cases, a single muscle or muscle group produces localized fatigue. Local and general fatigue can reduce athletic performance, muscle strength, and motor control [54,55].

Currently, programs to assess running fatigue rely primarily on general fatigue programs as interventions, monitoring the runner's heart rate and using a subjective fatigue scale (Ratings of Perceived Exertion Scale, RPE) to determine exercise fatigue. The subjective fatigue scale ranges from 6 to 20, with higher numbers indicating more significant fatigue. Studies have indicated that fatigue may decrease running performance and increase the likelihood of running-related sports injuries [56].

Previous studies have utilized a running protocol in which all the participants wore uniform running shoes and ran at a speed of 6 km/h, then increased the speed by 1 km/h every 2 minutes until the RPE reached 17 or 90% of the maximum heart rate [57]. Dierks et al. utilized a fatigue protocol in which participants ran at a self-selected cadence on a treadmill for an extended period until their RPE reached 17 and their maximal heart rate reached 85% [58]. Bazuelo et al. used a fatigue intervention that involved two sets of exercises: first, subjects ran up and down stairs for 5 minutes, then performed five sets of alternating jumps on a step, with each set lasting 1 minute and a 30-second rest between sets. These two exercises were repeated with a 1-minute rest between each exercise until the subject's RPE reached 18, and their maximum heart rate reached 90% [59]. Willson et al. concluded that fatigue intervention involved runners running on a treadmill at a speed of 3.5 m/s and rating their fatigue on a scale every two minutes until their RPE reached 17, defined as a state of fatigue [60].

Fatigue might considerably influence lower limb biomechanical parameters, with a repetitive loading rate to the lower extremities, which may cause RRIs risks [58]. Several studies have researched how fatigue affects running kinematics and kinetic variables. Understanding the running mechanic's changes was essential to scientific training and running injury prevention. In 1999, Dutto et al. reported that after fatigued running, dorsiflexion at heel contact was more reduced than pre-fatigue; in 1981, Elliot et al. showed an increase in rearfoot motion after prolonged running, possibly due to fatigue [61,62]. Dierks et al. investigated the

effect of running in an exerted state on lower limb extremity kinematic variables and joint timing. The study's findings showed that certain kinematic variables in the lower extremities, such as peak angles, excursions, and peak velocities of eversion, tibial internal rotation, and knee internal rotation, were found to be increased after exerted running. This suggests that running in a state of exertion could impact these specific movement patterns. However, no significant differences were observed in knee flexion, hip internal rotation, or joint timing variables. These results imply that while exerted running may affect certain aspects of kinematics, it may not significantly influence other variables such as knee flexion, hip internal rotation, or joint timing. The most significant change was observed in eversion, indicating that this particular movement may be more susceptible to alteration during exerted running than other kinematic variables [58].

The study by Allison et al. analyzed the biomechanics of the dominant limb while running under conditions of exhaustion. This study focuses on solving unilateral pathology, a condition commonly encountered by physical therapists. The restoration of symmetry is a frequently used clinical benchmark by these therapists. In this study, the researchers found no noticeable differences in the movement and force characteristics of the non-dominant legs while running on flat ground. These results were observed among individuals who were in excellent physical shape. Hence, physical therapists don't have to consider limb dominance when solving lower extremity symmetry as a therapy objective [63].

The study conducted by Dominic et al. aimed to analyze the vertical ground reaction force (VGRF) and ankle joint motion of runners during the initial 50% of the running stance. After undergoing a localized muscle fatigue intervention, the participants were instructed to run at a speed of 2.9 m/s on a treadmill. Surprisingly, no variations in rearfoot motion parameters were observed. However, running in a fatigued state resulted in a significant reduction in dorsiflexion during heel contact and a decrease in the magnitudes of the impact peak and push-off peak. The decline rate of the impact peak force was also found to be affected. Therefore, this research clearly demonstrates that localized muscle fatigue can substantially impact loading rates, peak magnitudes, and ankle joint motion during the running stance phase. Furthermore, it highlights the significant role of localized muscle fatigue in developing common running injuries [58].

Brianne et al. researched the effect of fatigue on running mechanics in older and younger runners, hypothesizing that running in an exerted state would expose different gait adaptations exhibited by older runners compared to young runners. This study recruited 15 young and 15 older runners as participants to run in a fatigue protocol. The main finding of this study was that no interaction was observed between fatigue and age. The author concluded that knee range

of motion (ROM) and hip extension moments significantly decreased when all runners were exhausted [64].

Felipe et al. researched how fatigue alters step characteristics and stiffness during running. The main finding of this study was that a 60-minute trial run could cause fatigue, which could alter the spatiotemporal characteristics of running and lower limb stiffness after fatigued running. The authors concluded that the changes in step variability (i.e., contact time, flight time, step frequency, and step length) and leg stiffness were due to fatigue from running. Similarly, the findings reported that contact time increased, flight time decreased, and leg stiffness decreased with the fatigue running protocol [65]. Additionally, Möhler et al. investigated fatigue-related kinematics and kinetic parameter changes for expert runners during a middle-distance run. They reported that expert runners exhibit greater stance time and shorter flight time after fatigued running. Simultaneously, the leg stiffness, the vertical stiffness, and the center of mass decreased in post-fatigue running compared to pre-fatigue running [66].

Willwacher et al. researched the kinematic changes on the frontal and transverse planes in recreational and competitive runners during a 10-kilometer treadmill run. The results concluded that the kinematics parameters adapt in post-fatigue running, particularly in ankle eversion, knee valgus, and hip adduction angles. According to this finding, the author also speculated that strengthening ankle invertors and hip abductors might prevent fatigue-related running injuries [67].

In their study, Willson et al. explored the impact of exhaustive running on the disparities between sexes in running mechanics and patellofemoral joint kinetics. The findings of this research indicated that engaging in exhaustive running could potentially amplify the loading rate of peak patellofemoral joint (PFJ) contact force, stress loading rate of PFJ, excursion of hip adduction, angular impulse of hip abduction, angular impulse of knee abduction, loading rate of average vertical ground reaction force, step length for both female and male runners [60].

Hajiloo et al. investigated the effect of fatigued running on the synergy of lower limb muscles. Furthermore, the synergy pattern and relative muscle weight were compared between pre- and post-fatigue running. This study's main finding was that the number of muscular synergies did not change in fatigued running conditions. However, the relative weight of the muscles changed during the fatigued running condition compared to the pre-fatigued running condition. Therefore, fatigue did not affect the structure of muscular synergy [65]. Stress fractures were runners' most common running injury, with 50% reported to occur in the tibia.

Additionally, the examination conducted by MIZRAHI et al. explored the correlation between fatigue during running and the imbalance in loading on the shank. The primary

discoveries of the study indicated that, on average, there was a decrease in both the average integrated EMG (iEMG) and the mean power frequency (MPF) of the tibialis anterior muscle from the initial stages to the conclusion of the running process. Nevertheless, it was observed that the MPF experienced a significant increase throughout the running activity, while no notable change was identified in the iEMG of the gastrocnemius muscle. Based on the alterations observed in these variables, the authors inferred that fatigued running not only triggers an imbalance in muscle contractions within the shank but also elevates the acceleration of shock experienced by the shank [68].

Concerning kinematic parameters, previous studies have pointed out that exertion while running affects ankle, knee, and hip joint mechanics. More importantly, ankle eversion, knee adduction, internal rotation, and hip internal rotation were significantly greater in the exertion running. However, after exhaustive running, the plantarflexion and external rotation moments decreased [69].

1.1.4 The characteristics of energy change during long-distance running

From a mechanical perspective, mechanical energy is generally used to represent energy, which is the ability of the body to do work during the process of movement. The conversion between various mechanical energies follows the energy conservation law [70]. Previous investigations have reported that ankle energy generation significantly decreased in recreational runners but not in the case of competitive runners. With increased running distance, the positive work contribution could shift from distal (ankle) to proximal (knee, hip) joints. The possible interpretation of this phenomenon is that if a person is fatigued due to intensive sports activities such as running, the ankle and plantar flexors reduce ankle energy generation and ankle joint moment [71]. This evidence shows that a redistribution occurs in joint work, a primary factor in improving the metabolic cost during prolonged running. Simultaneously, the muscular capacity of competitive runners was significantly greater than that of recreational runners, which might result in less plantar flexor after fatigued running. Evidence has demonstrated that the foot and ankle play an essential role during running, constituting more than 50% of joint absorption and energy generation [72,73].

Interestingly, a previous study found that well-trained rearfoot strike runners did not exhibit a proximal positive joint work shift after extensive running [74]. It is worth mentioning that different running strike pattern designs were used in the study, which may have caused different results. However, there is little research about joint work in fatigue running biomechanics. Future studies should consider the type of race and distance when calculating the changes in joint work following fatigue induced by prolonged running [74].

As for the kinematics variables, it has been shown that the ankle and knee initial contact

angle is crucial for joint stability [59]. Regarding IC (initial foot contact), contradictory studies have been published, where some authors claim that the ankle angle is linearly influenced by joint absorption during running [75]. In contrast, others stated that the connection was nonlinear [76]. There is limited research on how the initial angle affects joint work. Bastiaan Breine et al. found that the foot angle at initial contact during the rearfoot strike had the highest correlation with the vertical instantaneous loading rate (VILR) [77]. This indicates that a greater foot angle or more pronounced rearfoot strike corresponded with a lower VILR. Furthermore, following exhaustive treadmill running, knee flexion at foot contact was significantly increased [17]. Therefore, lower limb kinematics' modification following fatigue-induced running was associated with ankle initial foot contact and joint energy.

1.2 Running shoes biomechanical characters

1.2.1 Heel-to-toe shoes biomechanical characters

Sports shoes appeared in the 1970s with various shoe designs to improve athletic performance and reduce sports injuries. In modern sports shoe design, the shoe's midsole represents the core technology of sports shoes. The critical technologies of various sports shoe brands are also reflected, mainly in the midsole technology. The sole is an essential aspect of functional running shoe design, and any change in any part of the midsole may affect the shoe's performance.

After decades of research on running shoes, people have identified several key features that a good running shoe should have to minimize ground reaction force during the first 30 to 50 ms after initial ground contact. This period has the most significant potential for injuries [78,79]. The shoe should also improve the stability of the medial and lateral midsoles, which might affect the runner's foot control during the running process [80,81]. Furthermore, wearing running shoes might prevent excessive inward rolling during running landings, as excessive inward rolling is believed to be related to Achilles tendon injuries [82].

The heel-to-toe drop (HTD) is the difference between the heel height and the heel forefoot of a shoe. The heel-to-toe drop is essential in determining the risk of running injuries. The heel-to-toe drop (HTD) of the running shoes is an essential factor in plantar sensations and may be crucial in the change in foot strike pattern between shod and barefoot running. The normal heel-to-toe drop of running shoes was approximately 12 mm; in some cases, it was as high as 15–19 mm. However, the drop of minimalist shoes ranges from 0-8 mm.

So far, several studies have analyzed the effect of shoe drops on the biomechanical variables during the running stance phase. Chambon et al. conducted a study investigating the impact of midsole thickness on running patterns. The study involved fifteen participants who ran barefoot with five different midsole thicknesses (0 mm, 2 mm, 4 mm, 8 mm, and 16 mm) in running

shoes overground at a speed of 3.3 m/s. The findings revealed that contact time increased significantly with a midsole thickness of 16 mm. However, no significant differences were observed in ground reaction force or tibial acceleration [83].

Zhang et al. investigated the impact of different heel-to-toe drop variations in running shoes on the stress experienced by the patellofemoral joint during running. The experimental setup included running shoes with 15 mm, 10 mm, and 5 mm drops and shoes without any drops. The study's results demonstrated that running with shoes featuring drops of 15 mm and 10 mm may increase stress on the patellofemoral joint compared to running without any drop. Additionally, the knee flexion angle was higher when individuals ran with running shoes with drops of 15 mm, 10 mm, and 5 mm. These findings suggest that running with heel-to-toe drops greater than 5 mm is correlated with higher peak stress on the patellofemoral joint, primarily due to an augmented knee extension moment [84]. Simultaneously, a previous study also concluded that heel-to-toe drop increases the running injury risk of leisure-time runners. The author found that shoes with a lower heel-to-toe drop of 0 mm and 6 mm instead of 10 mm were less likely to injure occasional runners than regular runners [85]. Therefore, the heel-toe drop is vital for runners to prevent running injuries.

A study by Chambon et al. examined the impact of shoe drops on running patterns during overground and treadmill running. The findings indicated that loading rates were reduced when running without shoes or on the ground compared to wearing shoes with the greatest drop. However, running barefoot on the treadmill resulted in significantly higher loading rates. Consequently, it can be concluded that shoe drops play a critical role in shaping running patterns. However, its influence on VGRF differs depending on the running task (treadmill versus overground) and requires careful consideration [86].

In addition, several studies have demonstrated that the heel drop would change the running foot strike pattern. Horvais et al. compared the effects of heel height and heel-to-toe drop differences on the foot-strike pattern and running kinematics, finding that the foot-strike pattern was associated with the lower heel-toe drop. The results demonstrated a positive correlation between the drop of shoes and running contact time during the running stance phase. The lower shoe drop decreased the foot angle at contact and contact time [87]. Chambon et al. reported that running with lower heel-toe drop shoes may influence the foot strike pattern. For example, running in shoes with 0 mm might lead the rearfoot strike into a midfoot strike pattern [83]. Furthermore, the negative heel-to-toe drop of running shoes will change the strike pattern into a midfoot strike pattern during the running stance [88].

Electromyography is an essential parameter for characterizing muscle activity during running. Lower limb muscles may provide proper joint alignment, stability, stiffness and

propulsion to propel the body forward while running. Yong et al. concluded that RMS (root mean square) activity in the tibialis anterior in FFS runners was considerably reduced compared to RFS runners during the final swing phase. In FFS runners, on the other hand, the medial and lateral gastrocnemius demonstrated much larger RMS (root mean square) activity during the terminal swing phase [89]. Fernandes Ervilha et al. showed that the iEMG of the TA (tibialis anterior) was increased when running in shoes utilizing rear-foot strike patterns compared to in shoes utilizing forefoot strike patterns and barefoot running.

Moreover, the iEMG of soleus and GM (gastrocnemius medialis) were significantly smaller when running in the shoes using rearfoot strike patterns [90]. A previous study found that plantar flexor muscles were stimulated 11% earlier and for 10% longer in FFS runners than in RFS runners [91]. There are several differences in muscle activation while running barefoot versus shod. In barefoot runners, medialis gastrocnemius, lateralis gastrocnemius and soleus muscle activity were significantly increased [92].

1.2.2 Minimalist running shoes and normal shoes biomechanical

The main objective of minimalist running shoes is to simulate the sensation of running barefoot while providing minimal protection. In contrast to traditional running shoes, minimalist footwear diminishes the heel's height, the height disparity between the heel and forefoot, and motion control and stabilization mechanisms, thereby minimizing any disruption to the foot's natural motion [93,94]. Minimalist shoes exhibit a low drop, remarkable lightness, enhanced flexibility, and reduced cushioning, among other features. According to Esculier et al., a uniform definition of minimalist running shoes exists. The researchers demonstrated that the minimalist index evaluation comprises aspects such as weight, flexibility, heel-to-toe drop, stack height, and motion control and stability mechanisms, with each factor carrying equal significance [93].

According to the foot strike pattern, there are three main types of running patterns: RFS, MFS and FFS [10,43]. Strike pattern technologies were also associated with running injuries. In RFS running, there may be increases in the loading rate of the impact and knee power. However, the forefoot strike pattern would increase ankle power and Achilles tendon force [44]. In addition, a good pair of running shoes is essential and desirable for runners. In 30 years, running shoes with cushioned and comfortable features have reduced running injuries [95].

Moreover, a previous study reported that changing the running strike pattern and controlling the running distance might induce running overuse injuries [96]. Thus, many shoe manufacturers have also begun to focus on barefoot running, in which Vibram Five Fingers, Nike Free, and minimalist shoes are produced using the forefoot strike pattern [97,98]. Several studies focus on how minimalist running shoes affect the running strike pattern for runners [99-

101]. These studies demonstrated that minimalist running might habitually change rearfoot strike patterns in runners into midfoot strike patterns. However, it could not change the runners into forefoot strike patterns [102-105]. Minimalist running shoes might keep the runners still using rearfoot or midfoot strike patterns.

Moreover, ankle plantarflexion showed a noticeable increase when running with minimalist shoes and barefoot [100]. Simultaneously, compared to traditional shoes, running with minimalist shoes led to larger contact times and swing and stride phases [100,106-108]. It was also determined that minimalist running shoes resulted in a significant elevation in the angle of ankle plantarflexion during the IC phase of running. Unlike conventional running shoes, minimalist running shoes induce a smaller angle between the foot and the ground while aligning the pressure center closer to the forefoot [107,109,110]. Firminger et al. conducted a comparative analysis of minimalist footwear and stride length reduction by assessing lower extremity running mechanics and cumulative loading. The findings indicated that when running with minimalist running shoes, the metatarsophalangeal and ankle joints experienced substantial increases, while knee loading decreased. The cumulative impulses were also amplified at the ankle but diminished at the knee [99]. Previous studies have shown that metatarsal strains increased by 28.7% when running in minimalist shoes [102].

Two recent experiments compared the kinematics and kinetics of the lower limb and the mechanics of the lower limb when running in conventional, barefoot, and minimalist running shoes. Zhang et al. aimed to investigate the ankle mechanics and the Achilles tendon's mechanical properties during running with minimalist and conventional running shoes. The main result of this study showed a significant increase in ankle moment, peak force of the Achilles tendon (AT), force impulse of the AT, peak AT loading rate, average loading rate, AT stress, strain, peak AT stress rate, and strain rate when running in minimalist shoes. This suggests that runners who habitually use a rearfoot strike pattern may gradually adapt to minimalist shoes for running. To prevent knee injuries, they should avoid long-distance running with heavy loads in the initial stages [109]. Running barefoot and using minimalist footwear increased ankle kinematics and the stress on the Achilles tendon compared to conventional shoes. The findings also indicated that running barefoot and using minimalist barefoot footwear reduced knee patellofemoral tracking force (PTF) and patellofemoral pressure (PP) compared to running in conventional footwear [111]. Lu et al. concluded that running in running shoes with a negative heel-to-toe drop decreased ankle dorsiflexion angle, knee flexion velocity, ankle dorsiflexion moment extension, knee extension moment, knee extension power, and knee flexion. This suggests that novice runners or patients with Achilles tendon issues should not use running shoes with a negative heel-to-toe drop [112].

Sinclair et al. conducted a study to determine the effects of different types of running shoes on limb and knee stiffness. The study found that running in barefoot and minimalist shoes increased peak ankle plantar flexor moment and knee-limb stiffness compared to cushioned footwear. On the other hand, running in cushioned footwear resulted in a significantly larger peak knee extensor moment. These findings enhance our understanding of the various mechanisms contributing to running injuries when using different running shoes [110]. A meta-analysis comparing the running economy of barefoot, minimalist, and standard running shoes discovered that running in barefoot minimalist shoes requires less oxygen utilization [113].

A separate investigation conducted by Nordin and colleagues investigated the impact of minimalist footwear on variables related to ground reaction forces (GRF). The examination explored the loading rate-time features in three dimensions (X, Y, and Z) for two distinct categories of running shoes (cushioned and minimalist) and three variations of running strike patterns (forefoot, midfoot, and rearfoot). The findings uncovered that cushioned footwear reduced the magnitude of impact loads in the vertical direction. In contrast, minimalist footwear led to diminished impact loads in the anterior-posterior and medial-lateral directions [114]. Different foot strike patterns when using their habitual footwear conditions were examined. It was observed that both barefoot and minimalist shoe conditions exhibit a more anterior foot strike than regular footwear.

Moreover, the impact peak GRF loading rates were higher in barefoot and minimalist shoe conditions than regular footwear [115]. Additionally, Hannah et al. conducted a study on runners and investigated the resultant instantaneous load rate (ILR) when using different foot strike patterns with their habitual footwear conditions. The study concluded that running in minimalist shoes with a forefoot strike leads to smaller vertical, lateral, and medial ILR than running in standard shoes with either foot strike [116].

Electromyography is a vital parameter to characterize muscle activity during exercise. Previous studies have researched how shoe conditions affect the muscle activity of the lower extremities. No differences were found in tibialis anterior (TA), peroneus longus (PL), gastrocnemius medialis (GM), soleus muscle (SL), vastus lateralis (VL), and biceps femoris (BF) muscle activity when running in barefoot and shod running. However, TA PL, GM, SL, VL, and BF were lowest in the barefoot compared to the shod [117,118].

The study's findings, as mentioned above, indicate that the level of muscle activity observed in individuals who transitioned immediately to minimalist running shoes is more similar to that of individuals who wear traditional running shoes as opposed to those who run barefoot. The study found a correlation between landing patterns and lower extremity muscle activity. Specifically, it was observed that ankle dorsiflexion led to an increase in anterior tibial muscle

activity during rearfoot landing. In contrast, adopting a forefoot landing technique heightened the activation of the gastrocnemius and hallux valgus muscles. Promptly adopting minimalist running shoes yielded restricted outcomes in altering landing patterns. Runners who habitually landed on their hindfoot did not encounter significant modifications in their landing patterns. Furthermore, the activation patterns of muscles did not undergo significant changes upon initial exposure or short-term use of minimalist running shoes.

In a study conducted by Willson et al. in 2013, the impact of running with minimalist shoes on lower extremity running mechanics was examined for two weeks. The results revealed that the knee flexion angle experienced an increase during initial contact. Notably, no significant differences were observed regarding the hip flexion angle during initial contact. Nevertheless, no significant variations were observed in the hip flexion angle at initial contact. More importantly, the two-week minimalist shoe intervention did not change the runner's strike pattern, who habitually wears RFS. Nevertheless, after two weeks of minimalist shoe intervention, the vertical loading rate was three times larger for the RFS runners [119]. According to Warne et al., their study found that a four-week minimalist shoe intervention did not appear to alter the runner's strike pattern. They observed that maximum force (MF) decreased significantly in both conventional running shoes (CRS) and minimalist shoes (MS) after the four-week MS training, along with a reduction in heel pressure. However, during over-testing, it was noted that the maximum pressure (MP) in the MFW condition was higher [120].

Endurance capacity can be reliably assessed using running economy (RE). Numerous research investigations have devoted considerable attention to distinguishing the variances in RF when comparing conventional shoes with barefoot or minimalist footwear [97,121-123]. It has been shown that the MS and re-training interventions did not affect RF. In addition, eight weeks of gait-retraining increased the step frequency of running in MS more than in CRS [124]. Likewise, runners undergoing six weeks of intervention gait retraining may increase the loading rate and vertical stiffness. Combining different interventions has the potential to reduce the impact parameters. Nevertheless, it should be noted that in the case of minimalist footwear with a higher initial loading rate, there may be an increased risk of injury [125].

Research has demonstrated that minimalist running shoe intervention for six weeks led to a significant decrease in the activity of the anterior tibialis muscle. In contrast, there was a noteworthy increase in gastrocnemius muscle activity during the pre-activation and stance phases [126]. Using minimalist running shoes over an extended period also caused adaptive changes in muscle activity in the lower extremities. Specifically, it resulted in considerable growth in the cross-sectional area of the abductor hallucis [127,128]. It generated relatively insignificant changes in the cross-sectional area and volume of the abductor digits in the foot.

1.3 Opensim simulation modeling in human movements

1.3.1 Introduction of OpenSim software

Stanford University created OpenSim, which is open-source software. The platform can be used for visual modeling, dynamic simulation of the human body, animal, robot, and environment, and analysis of their motion and interaction effects. OpenSim software has extensive and powerful functions and can be applied in many fields, such as gait dynamics analysis, sports performance research, surgical process simulation, rehabilitation medical device design, etc. It also provides an application programming interface, which can expand other software, such as C++, Matlab, Python, etc., and research and development personnel can use it to expand the functions of Opensim software.

Opensim enables the quantification of mechanical attributes associated with human motion, which prove challenging to assess in vivo, such as joint reaction forces and muscle-tendon forces. These measures often inform various fields, including orthopedic surgery, injury prevention, performance enhancement, and prosthetic device design. As a result of its extensive research capabilities, accurate biological and mechanical representation of musculoskeletal models and their constituents becomes crucial.

As for the simulation process in OpenSim comprises four essential steps: scaling, inverse kinematics (IK), residual reduction algorithm (RRA), and computed muscle control (CMC) (Figure 4).

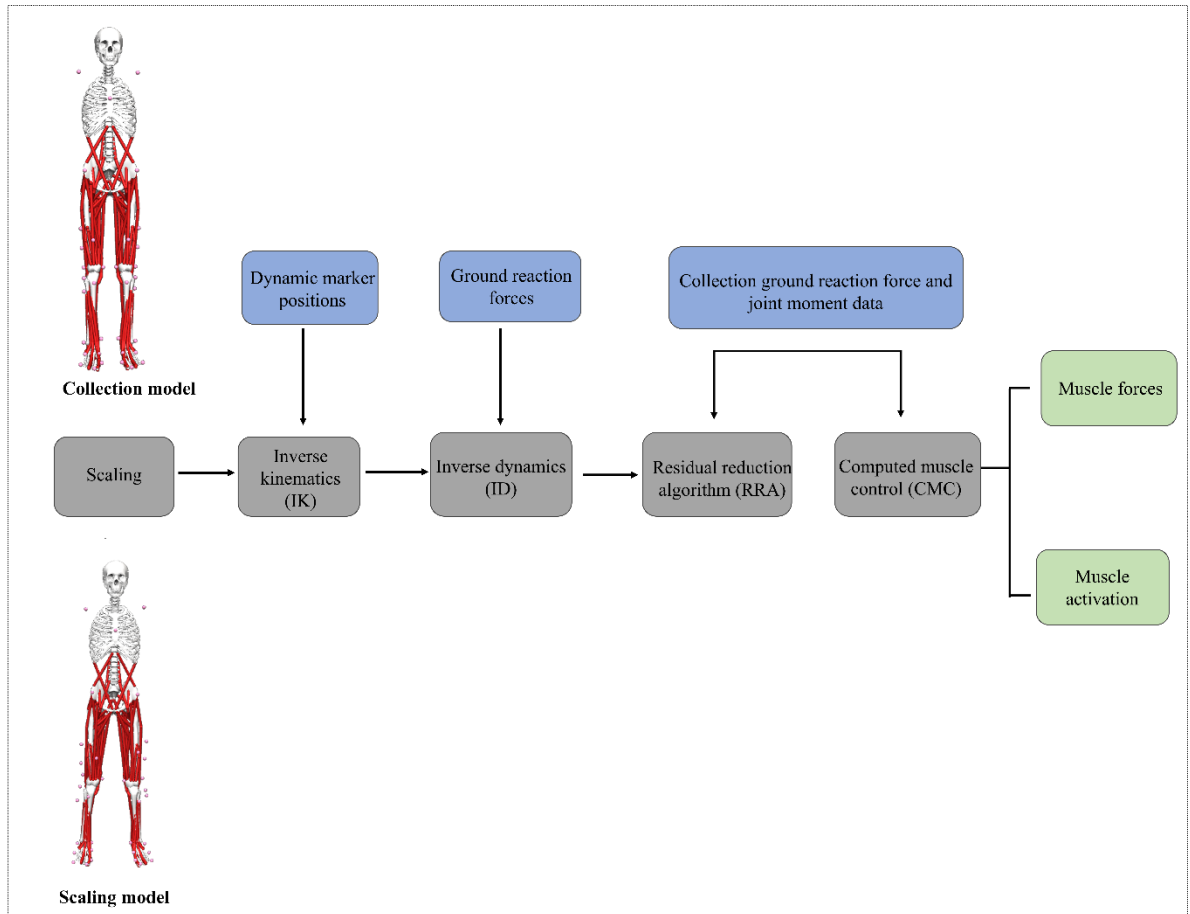


Figure 4 Simulation steps with Opensim.

In modeling environments, the first step involves scaling individual anthropometrics by matching them with adjusted muscle attachments, length properties, and moment arms. The static trial model is chosen for scaling, where the size of each body part is adjusted based on the distance between pairs of markers from a 3D infrared motion capture system and the placement of virtual markers in the model. The error between the model's control marker and theoretical mark is particularly important during scaling. The problem of reducing the difference between the measured and placed markers in the model is solved using the least squares method [129]. Inverse kinematics calculates the joint angle with the collection mark in the second step. This step involves solving a least-squares problem to minimize the difference between the measured markers and their placement in the model while considering other factors [129]. In order to improve the accuracy of inverse kinematics, RRA was used to adjust the simulation results. RRA is a methodology that involves a forward kinematics simulation with a tracking controller to follow the model kinematics generated by inverse kinematics. Inverse dynamic analysis can be conducted by combining the inertial parameters of the human body with the ground reaction force using RRA [130]. Computed muscle control (CMC) generates a series of coordinated muscle excitations, enabling a muscle-driven simulation of

the subject's movement [131].

1.3.2 Human gait applied in the Opensim

Recently, there has been an increase in biomechanical research focused on the human musculoskeletal system. One prominent application in this field is the OpenSim model, which primarily examines normal human gait characteristics and biomedical aspects. The OpenSim simulation tool can provide a musculoskeletal model that estimates muscle activation and muscle force during running gait. Musculoskeletal models elucidate the dynamics of multiple rigid body segments linked through articulations, unveiling their intricate interactions. The conglomeration of inertial traits from such constituents as muscles, tendons, and bones forms the composite inertia for each segment in the model. Consequently, OpenSim simulation can calculate the muscle force and activities using kinematics and kinetics parameters.

Previous studies have shown a strong agreement between muscle activation computed by OpenSim and electromyographic muscle activations [132-134]. Liu et al. conducted a study investigating the muscle's contribution to support and progression across various walking speeds. They utilized the OpenSim software to evaluate the muscle contribution of participants walking at very slow, slow, free, and fast speeds. The study's main finding was that the muscle activity measured by the OpenSim simulation aligned with the EMG activity. Furthermore, the study revealed increased muscle contribution with walking speed, particularly in the vastus muscle between slow and free walking [132]. Similarly, Ursula et al. employed two mathematical methods to compare muscle activation during different walking speeds. Their findings also demonstrated the consistency between simulation muscle activities and EMG recordings [134]. Therefore, these previous studies provide strong evidence for the exceptional accuracy of muscle activation levels achieved by the OpenSim software.

The effect of muscle activity and muscle force during the running gait has recently been studied. A previous study used a musculoskeletal model to estimate the muscle and joint reaction forces in barefoot running. The results indicated a decreased hip and knee joint reaction force compared to the control groups wearing shoes. Based on these findings, the design of running shoes can take into account strike patterns to prevent lower limb injuries [135]. Zhou et al. investigated the difference in muscle force between normal and bionic shoes during walking and running. The results demonstrated that the muscle control ability in bionic shoes was superior to that in normal shoes during the walking and running stance phases. These findings contribute to our understanding of the muscle mechanics associated with different types of running shoes [136].

Furthermore, the exploration conducted by Yu et al. involved an amalgamation of finite element analysis and OpenSim simulation to examine the correlation between the interaction

of human movement and the musculoskeletal system. Specifically, the authors directed their attention toward comparing loadings in the patellofemoral joint when executing directional lunges in individuals involved in badminton. To accomplish this objective, the investigators gathered data on the trajectories of dynamic markers and the forces exerted on GRF, which were then employed to calculate joint angles and muscle forces. Subsequently, these numerical values were implemented as constraints in the finite element simulation to determine the loadings experienced by the patellofemoral joint. The findings demonstrated that badminton players with right-side dominance encountered increased loadings in their right patellofemoral joint while performing left-side (backhand) lunges. Gaining insights into these loadings could potentially impact badminton footwork training by emphasizing musculature development, thus reducing load accumulation on the cartilage and preventing anterior knee pain[137].

Moreover, OpenSim simulation was also applied to analyze clinical gait, explicitly evaluating the lower limb muscle strength in subjects with diabetic neuropathy compared to healthy individuals. The study found significant differences in lower limb muscle force and activation between the two groups. Healthy subjects exhibited greater muscle strength in the tibialis posterior muscle, soleus muscle, hallucis flexor, toe flexor, and toe extensor compared to diabetic subjects. These findings contribute to a deeper understanding of the physiological disparities between individuals with diabetic neuropathy and healthy individuals, potentially informing the development of targeted rehabilitation interventions [138].

Recently, simulation analyses have indicated that individuals who have had a stroke show decreased contributions from their paretic soleus and gastrocnemius muscles when it comes to forward propulsion compared to individuals who have not had a stroke. This finding suggests that rehabilitation strategies that aim to increase paretic forward propulsion and swing initiation in individuals post-stroke have the potential to improve their gait performance significantly. This conclusion is supported by similar simulation results involving post-stroke populations with average walking speeds of 0.55 and 0.92 m/s. These findings highlight the importance of targeting paretic muscle function in post-stroke rehabilitation interventions to enhance gait performance and improve overall mobility in this population [139].

The OpenSim stimulation method can also be used to analyze and assess the muscle mechanics of children's lower limbs. In a study conducted by Lerner et al., the impact of pediatric obesity on compressive and shear hip joint contact forces during walking was examined. The authors found a significant positive correlation between total body mass and hip joint contact forces. Obese children exhibited higher compressive and shear contact forces and loading rates. These findings suggest increased hip joint loading may contribute to hip pain and pathology [140].

In future research, the utilization of OpenSim for modeling and simulation will primarily concentrate on the following aspects: Exploring the neuromuscular mechanism of abnormal gait, examining the interaction between musculoskeletal systems in human movement by integrating finite element analysis, comprehending the coordination mechanism of human movements, and improving movement techniques and preventing sports injuries through simulation.

1.4 Anatomy of the Human Foot

1.4.1 Foot Bones

The foot is a vital structure in the human body as it directly interacts with the supporting surface. It is a complex part of the musculoskeletal system, consisting of more than one hundred elements, including bones, muscles, tendons, and ligaments. The anatomical structure of the foot is specifically designed to bear the body's weight and facilitate various locomotive activities such as jogging, sprinting, walking, and running. The foot primarily absorbs shocks during the gait and generates forward propulsion [141].

The foot is a complex structure of various bones, joints, muscles, and ligaments [142]. Understanding its anatomical and biomechanical characteristics is crucial to comprehend injury mechanisms and associated risk factors. There are 26 bones in the foot, including the phalanges, metatarsals, cuneiform bones, cuboid bone, navicular bone, and the hindfoot's talus and calcaneus bones. In addition to the bones, there are 33 joints, 28 intrinsic muscles, and 107 ligaments in the foot [143,144]. These components work together to support the overall function of the foot and the lower extremities. The foot is divided into three regions: the forefoot, midfoot, and rearfoot (Figure 5). The rearfoot is connected to the midfoot through the talonavicular and calcaneocuboid joints, while the forefoot attaches to the midfoot via the tarsometatarsal joints. Collectively, these bones, ligaments, and tendons form the arch of the foot, which plays an essential role in weight-bearing and walking.

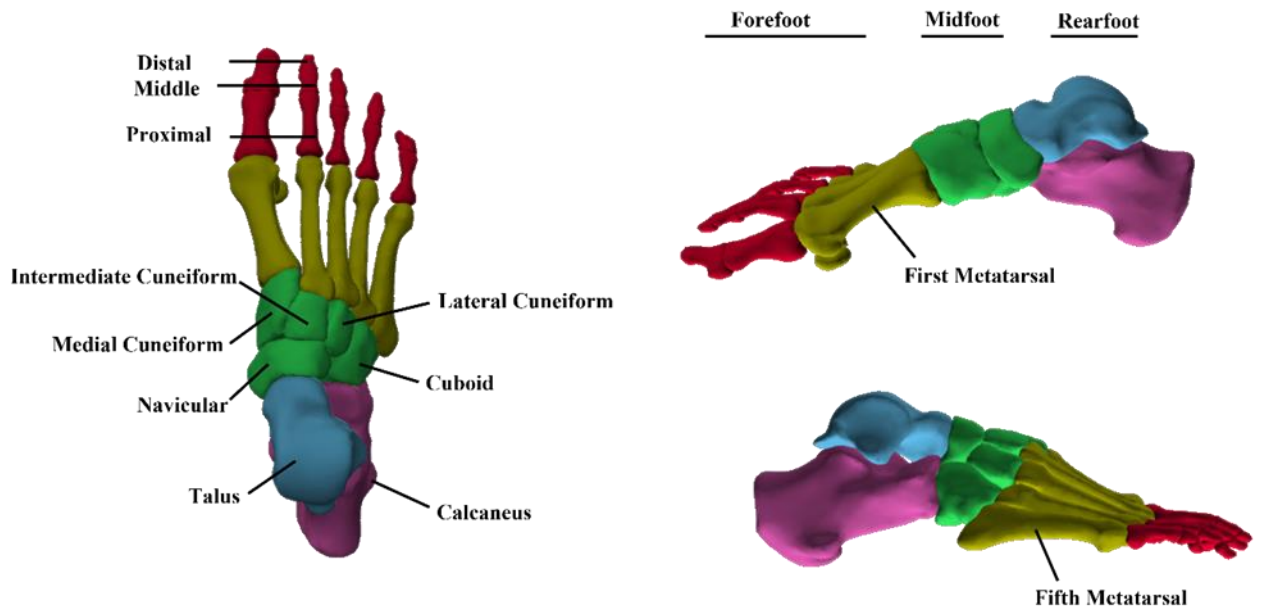


Figure 5 Anatomy of the Human Foot.

1.4.2 Foot muscles

The role of the foot's musculature in human locomotion and equilibrium is crucial. These muscles bear the weight of the body and are involved in various activities such as walking, running, and jumping. The foot muscles can be categorized into two groups: the intrinsic muscle group and the extrinsic muscle group (Figure 6). The intrinsic muscle group primarily functions to position and stabilize the arch of the foot. On the other hand, the extrinsic muscle group primarily contributes to foot-plantar and joint movement functions [145]. The external accessory muscles of the foot originate in the lower leg, wrap around the ankle joint, and extend to the foot. These muscles have a significant cross-sectional area and moment arm, making them the primary movers of the foot and providing stability to the arch [146]. The medial appendage muscles of the foot are located at the beginning and end of the foot. Although these muscles usually have a minor moment arm and cross-sectional area, they play a role in maintaining and controlling arch deformation [146].

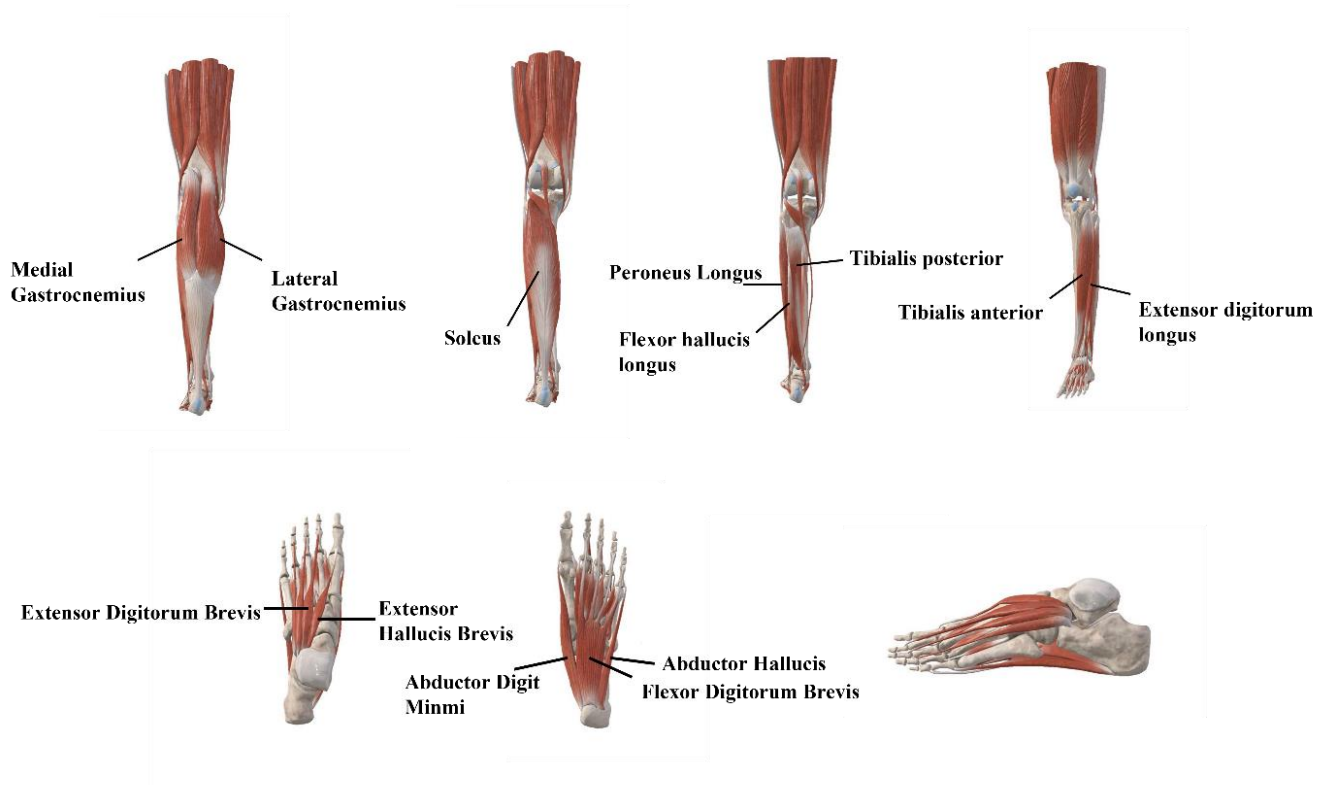


Figure 6 The extrinsic foot muscle and the intrinsic foot muscle.

1.4.3 Development of Finite Element Modelling in Shoe Design

The field of finite element analysis has witnessed substantial growth in recent years and has proven to be a valuable tool for advancing clinical treatment and designing sports equipment. In their study, Cho et al. introduced a 3D model based on the finite element method to investigate the interaction between the foot, shoe, and ground. The accurate representation of this interaction was achieved through the reconstruction of the skeletal structure, soft tissue, and shoe architecture employing CT-scanned images. Figure 7 illustrates the obtained results. By imposing appropriate running kinematics and kinetic parameters as boundary conditions, the authors were able to calculate the required parameters. The developed finite element model was carefully designed to consider realistic loading and boundary conditions [147]. For instance, the researchers employed the finite element (FE) method to assess the impact of different design parameters of running shoes on peak plantar pressure during the rear-foot strike pattern. A foot-shoe finite element model was constructed using reverse engineering and the Taguchi method to simulate peak plantar heel pressure with various shoe parameters accurately. The findings demonstrated that implementing latex material, a 6mm insole, a 100% conforming heel cup, and a midsole hardness of Asker C-45 yielded a highly effective composite, enhancing the cushioning ability during heel landing. These valuable insights contribute to

developing and producing [148].

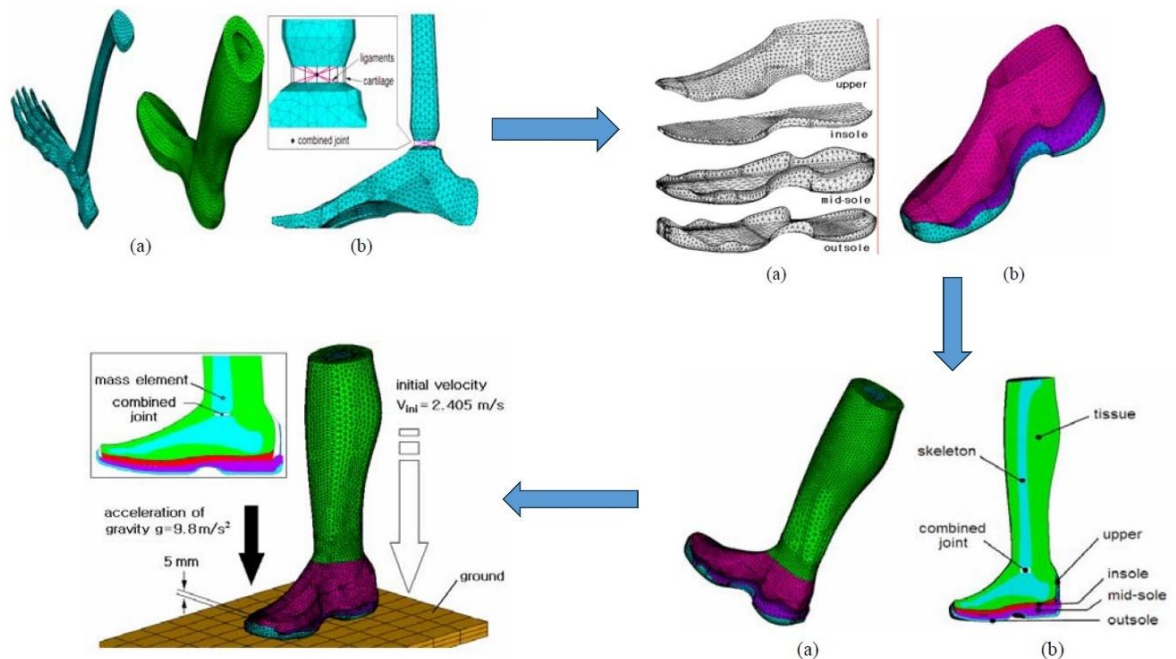


Figure 7 Build a 3D-coupled foot-shoe finite element model process[147].

The investigation of the effects of different designs of foot orthosis on strain in the plantar fascia and pressure on the plantar area in individuals with flatfoot was conducted using the finite element (FE) method. Boundary conditions incorporating data on muscle force stimulation were incorporated to enhance the accuracy of the calculations. The results indicated that higher arch support and an inclination angle towards the medial side reduced the maximum pressure experienced on the plantar area. Moreover, the degree of arch support and stiffness of the material were identified as the key factors affecting the strain on the proximal plantar fascia [149]. In a separate study, Firminger et al. developed a musculoskeletal model based on the finite element method to predict the impact of footwear and stride length on the strain and failure of the metatarsal bones during running. As a result, it was discovered that there were no significant interactions between footwear and stride length. However, running in minimalist shoes led to an increase in the strain experienced by all metatarsals. Specifically, the strain in the fourth metatarsal decreased by 4.2% when running at 90% of the preferred stride length [102]. The finite element simulation proved a non-invasive approach for investigating internal loads on bones and tissue.

Consequently, the FE model was employed to assess the functional effects of a 12-week minimalist footwear intervention on the foot affected by hallux valgus. Xiang et al. employed the FE model to evaluate the long-term impact of a minimalist footwear running protocol on a

patient with mild-to-moderate hallux valgus. The results showed varus realignment of the first metatarsophalangeal joint and a 72.1% and 51.2% decrease in von Mises stress in the first and second metatarsals, respectively, compared to before the intervention. In this regard, the FE mode analysis approach can serve as a valuable reference for clinical foot evaluations [150].

In recent years, there has been a global trend towards different running styles, prompting footwear companies to focus on designing shoes that can modify how runners strike their feet on the ground while running. However, much of the research conducted in this field has mainly centered on the biomechanical aspects of running with barefoot or minimalist shoes. Only a few studies have delved into analyzing running strike patterns using FE foot modeling. For instance, Li et al. developed a 3D finite element model of the human foot to investigate the variations in peak plantar pressure during the weight-bearing phase of landing between barefoot and barefoot running footwear. The results of this study indicated that the coupled model showed lower peak plantar pressure distribution on the forefoot compared to the barefoot model. These findings hold significance for the design of barefoot running shoes [151]. Another research endeavor utilized an effective FE model to compare the stress and energy levels in the foot during forefoot strike (FFS) and rearfoot strike (RFS). The study discovered that the metatarsals experienced higher average stress levels throughout the entire landing cycle in the FFS pattern [152].

Similarly, a study employed an FE model to examine the impact of different habitual foot-strike groups on the stresses experienced by the second metatarsal. The author observed that non-rearfoot strikers exhibited greater external loading and joint contact forces compared to rearfoot runners. However, the stress differences between the two groups were not statistically significant [153]. In addition, a dynamic finite element simulation model was utilized to investigate foot arch deformation and the loading on the plantar fascia during running with rearfoot and forefoot strikes. The research findings indicated that when employing the forefoot strike, there was a decrease of 9.12% in the height of the foot arch and an increase of 2.06% in the angle of the medial longitudinal arch compared to the rearfoot strike. Adopting a forefoot strike pattern causes a significant increase in the stress exerted on the connective tissues of the sole, varying from 18.28% to 200.11%. Moreover, an escalation in the tensile force acting upon the plantar fascia was observed, ranging from 18.71% to 109.10% [154].

1.5 Aims and Objectives

In my thesis, I would like to draw up three research questions unanswered so far in the relevant literature.

The 1st research question:

Joint mechanics are permanently changed using different intensities and running durations. These variations in intensity and duration also influence fatigue during prolonged running. Little is known about the potential interactions between fatigue and joint mechanics in female recreational runners.

Therefore, my 1st objective is:

To describe and examine kinematic and joint mechanical parameters when female recreational runners were subjected to fatigue after long-distance running. The analysis used the Partial Least Square Algorithm (PLSR) to investigate if a linear relationship existed between the initial joint angle, ankle joint work, and knee joint work. Our first hypothesis was that ankle work would decrease due to fatigue after prolonged running. Our second hypothesis was that joint work would have a greater relationship with the initial angle of the ankle and knee.

The 2nd research question:

Previous studies always focus on the kinematics and kinetic variables of running in barefoot, minimalist, and conventional shoes. However, no studies investigating the heel-to-toe drop effects on lower extremity muscle force and biomechanical parameters.

Therefore, my 2nd objective is:

This study was to create musculoskeletal modeling and simulation techniques to compare the muscle force, kinematics, and kinetic variables of habitually rearfoot runners while wearing the heel-to-toe drop of negative 8mm shoes (minimalist shoes) or the heel-to-toe drop of positive 9mm shoes (normal shoes) during the running stance phase. This study focused on the immediate effect of kinematic and kinetic variables during the running stance with different heel-to-toe drop shoe conditions.

The 3rd research question:

The running style is an essential factor influencing the risk of running injuries. In order to decrease the impact force and reduce running injuries, shoe companies design shoes such as minimalist shoes. However, there has been limited research on the effects of different heel drops in finite element (FE) simulations. This study evaluates the stress distribution between minimalist and normal shoes during different running stance phases. To develop an FE foot model using minimalist and normal shoes to address the biomechanics of different heel-drop shoes.

Therefore, my 3rd objective is:

The objectives of this study were to develop a finite element (FE) foot model that incorporates various heel-drop shoes for static simulation of running. Subsequently, the

minimalist and normal shoes were simulated during different running stance phases to compare the von Mises stresses on the metatarsal and mid-bones.

2 Materials and methods

2.1 Experiments

2.1.1 Participants

Section 1: Fifty female recreational runners (23.89 ± 1.27 years, 65.39 ± 22.47 kg, 163.22 ± 15.01 cm) were recruited from the university running clubs, while flyers were distributed around the university campus for this investigation. Participants were screened to include individuals aged between 18 and 27 years who ran between 5 and 10 km per week and had no low-limb musculoskeletal injuries in the previous six months before data collection. All participants were rearfoot strikers 24 hours before data capture without vigorous exercise.

Section 2: Before the test, the present study's sample size was estimated using G*Power (Version 3.1.9.7). Considering the effect size of 0.8, the power value of 0.8, and the alpha level of 0.05, we recruited sixteen healthy recreational male runners (age: 26.00 ± 2.0 , weight: 73.50 ± 4.60 , height: 175.80 ± 0.50 cm) to participate in this study. For runners to qualify as recreational, the following conditions had to be met running using a rearfoot striking pattern and running 2 to 5 kilometers a week [179]. All the male subjects having the target foot length of US size 9 (0.5) and self-reporting as right-leg dominant were included. None of the participants had any lower-limb injuries in the past six months. All the participants had no experience with minimalist running shoes or the negative value of running shoes. In order to avoid subjects changing their strike pattern during the running test, all the participants were not informed of the test's purpose before the study. They were only informed about the experimental methodology.

Section 3: In this section, a healthy male (age: 25 years old; height: 175 cm; weight: 60 kg; and foot length: 265 mm) was recruited from the University for this finite element analysis. The subject reported no musculoskeletal or foot injuries in the past half-year. And the subject has normal foot morphology without any foot deformity. This section mainly collects two sections of data: CT scanning of the subject's foot with the shoes to build the foot model and the running biomechanical variables collection. Before this study, the participant was informed about the experimental conditions and provided written consent.

The Ningbo University Ethics Committee approved all the tests in this dissertation (Authorization No. RAGH20201024). Before participation, all participants were provided information about the aims, experimental techniques, and potential dissertation risks.

2.1.2 Instruments and Materials

The laboratory facilities at the Ningbo University Research Academy of Grand Health are well-equipped for conducting studies in the field of sports biomechanics. All the testing was conducted at the biomechanics lab.

(1) Vicon motion system

The kinematic data was acquired using a British-made Vicon infrared 3D motion capture system (Oxford Metric Ltd., Oxford, UK), including eight high-speed infrared cameras with Nexus analysis software. The sampling frequency for this study was 200 Hz.



Figure 8 3D Infrared Motion Capture System.

(2) Kistler force plate

GRF (ground reaction force) measurements were conducted using a force platform measuring 90*58*10 cm (1000 Hz, 9281B, Winterthur, Switzerland). Figure 9 displays the laboratory coordinate system utilized in this investigation, which replicated the one specified by the International Society of Biomechanics. The system encompassed the following components: a positively oriented X-axis indicating forward movement during gait. The Y-axis denoted a vertical direction with an upward positive sign. The Z-axis was aligned in the medial-lateral direction, with a positive orientation towards the right.



Figure 9 The machine of the force plate.

(3) Smart speed

A device regulating the subjects' speed was placed on either side of the force platform (smart speed, Fusion Sport Inc. of Burbank, California, USA). Equipment for assessing speed was located 3.0 meters away.



Figure 10 The machine of smart speed.

(4) Surface electromyogram (EMG)

The electromyographic test part is used to verify the simulation results. A total of eight muscle collection muscles of the right lower extremity are selected: vastus lateralis (VL),

vastus medialis (VM), gastrocnemius medial (GM), gastrocnemius lateral (GL), soleus muscle (SL), flexor hallucis longus (FHL), extensor digitorum longus (EDL), tibialis anterior (TA) and tibialis posterior (TP). The EMG test instrument used was DELSYS (USA), with 32 leads, a sampling frequency of 1000 Hz, noise of 750 nV, offset of 0.1 mV, and electrode distance of 10.0 mm.

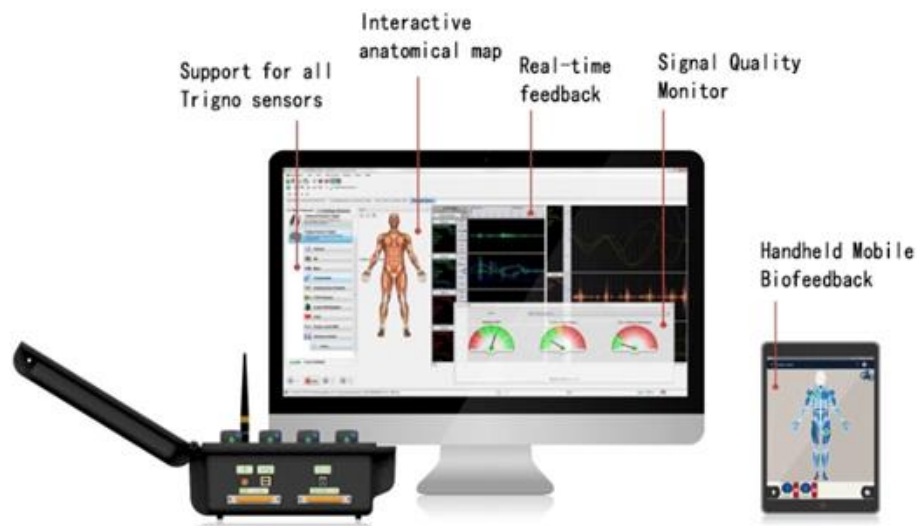


Figure 11 The Delsys surface electromyography devices.

(5) Heart rate monitor

This point was detected by a heart rate monitor (Polar RS100, Polar Electro Oy, Woodbury, NY, USA), which was compulsory for all participants while running on the treadmill.



Figure 12 The machine of heart rate monitor.

(6) Treadmill

A treadmill (h/p/ cosmos, Nussdorf- Traunstein, Nußdorf, Germany) was used in the test collection.

(7) Ankle CT scan

In order to obtain a clear image, the skin surface of the foot and ankle was cleaned before scanning. The subject lay flat on the device during the scan, and a foot brace was used to stabilize the ankle joint and keep the foot in a neutral position. In this study, the subject's right foot was scanned using an Optima Computed Tomography 540 scanner (GE Healthcare, Chicago, United States) at a hospital while wearing minimalist running shoes.



Figure 13 The CT scanner in this study (GE Healthcare, Chicago, United States).

2.1.3 Experimental shoe condition

This study used two pairs of running shoes (AT US 9). The difference between the two running shoes was the heel-toe drop. The heel-to-toe drop in running shoe design is the difference in thickness between the forefoot and heel regions of the sole. Figure 14. shows the test shoes in this study. Heel-to-toe drop differs significantly between regular and negative running shoes, with an offset of -8 mm in negative shoes and 9 mm in normal shoes. It is common for both conventional and negative shoe soles to be comprised of EVA foam.



Figure 14 Experimental set-up (not on scale). Outlined in this illustration, the left running shoe has the- 8 mm HTD (minimalist shoes) and the right running shoe has with 9 mm HTD (normal shoes).

Table 1 Detailed comparison of minimalist shoes and normal shoes.

Variables	Minimalist shoes	Normal shoes
Size (EUR)	9	9
Weight (gram)	264	280
Rearfoot height(mm)	15	32
Forefoot height(mm)	23	23
Offset(mm)	-8	9
Midsole material	EVA	EVA
Midsole hardness (Asker)	53C	53C
Bending stiffness (N/mm)	13.4	13.5

2.1.4 Protocol

The following processes were included in the data-collection protocol:

(1) Interview. When each participant arrived at the laboratory, they were introduced to the laboratory and given a short explanation of the trial procedures. All the participants were informed about the experimental conditions and provided written consent.

(2) Basic measurements measured the participant's body mass, height, and foot length. Before the test, all subjects had to wear uniform pants, T-shirts, socks, and running shoes.

(3) Warm-up. Before the test, all the participants were informed about familiarizing themselves with the test process. During the data collection process, participants were first instructed to warm up with light jogging and stretching, wearing their shoes for five minutes.

(4) Marker placement. Thirty-eight reflective markers (diameter: 14 mm) were attached to the bilaterally lower limbs, torso and head according to the Opensim Gait 2392 mode (see detail in Figure 15). The markers were placed on: Sternum, R. Acromion, L. Acromion, Toe. Head, R. ASIS, L. ASIS, V. Sacral, Thigh. Upper, R. Thigh. Front, R. Thigh. Rear, R. Knee. Lat, R. Knee. Med, R. Shank. Upper, R. Shank. Front, R. Shank. Rear, R. Ankle. Lat, R. Ankle. Med,

R. Heel, R. Midfoot. Sup, R. Midfoot. Lat, R. Toe. Lat, R. Toe. Med, R. Toe. Tip, L. Thigh. Upper, L. Thigh. Front, L. Thigh. Rear, L. Knee. Lat, L. Knee. Med, L. Shank. Upper, L. Shank. Front, L. Shank. Rear, L. Ankle. Lat, L. Ankle. Med, L. Heel, L. Midfoot. Sup, L. Midfoot. Lat, L. Toe. Lat, L. Toe. Med, L. Toe. Tip [155].

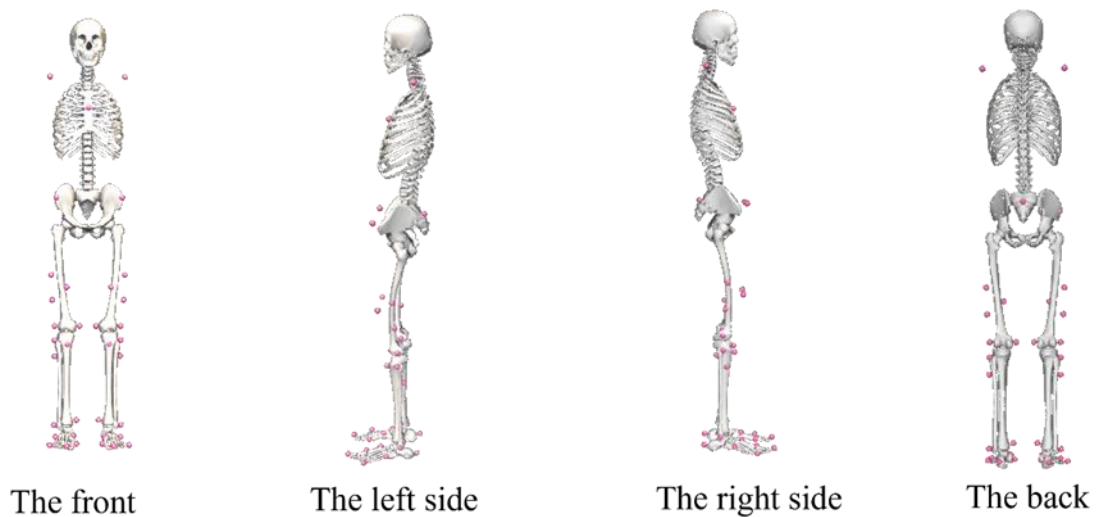


Figure 15 Marker placement on the lower limb and trunk.

(5) Dynamic trials.

During data collection, experience-running shoe orders were randomized among the participants. They were asked to familiarize themselves with each of the running shoes. Then runners were randomized and wore running shoes to run through a 10-metre walkway. A device regulating the subjects' speed was placed on either side of the force platform (smart speed, Fusion Sport Inc. of Burbank, California, USA). Equipment for assessing speed was located 3.0 meters away. Speed was controlled at 3.0 ± 0.5 m/s [32]. During data collection, experience-running shoe orders were randomized among the participants. They were asked to familiarize themselves with each of the running shoes. Then runners were randomized and wore running shoes to run through a 10-metre walkway. A device regulating the subjects' speed was placed on either side of the force platform (smart speed, Fusion Sport Inc. of Burbank, California, USA). Equipment for assessing speed was located 3.0 meters away. Speed was controlled at 3.0 ± 0.5 m/s.

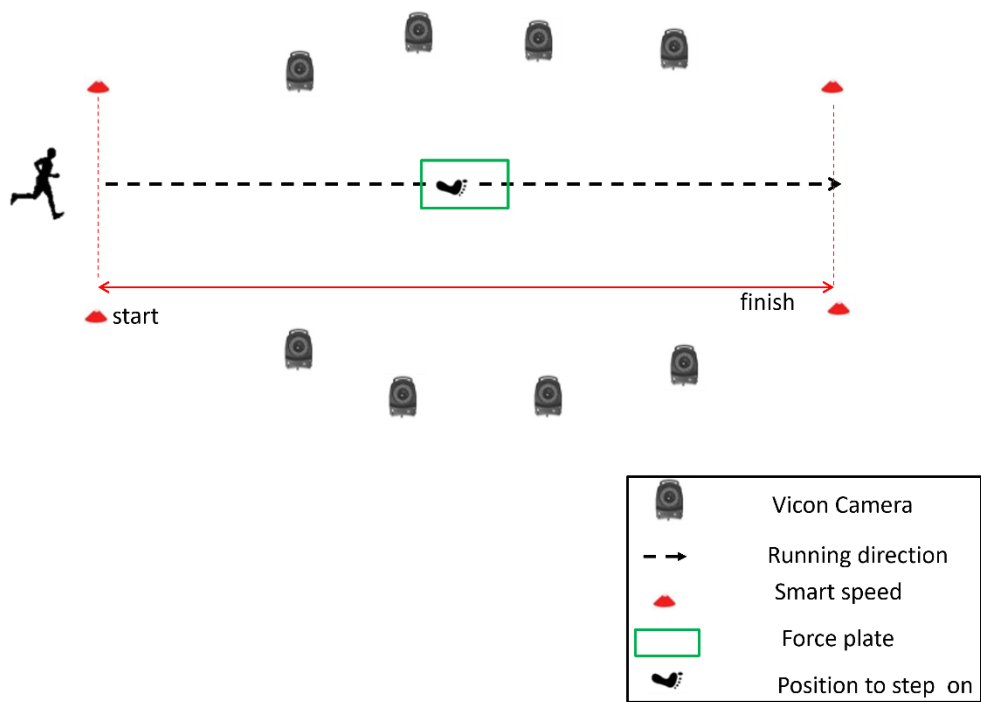


Figure 16 Placement of test equipment.

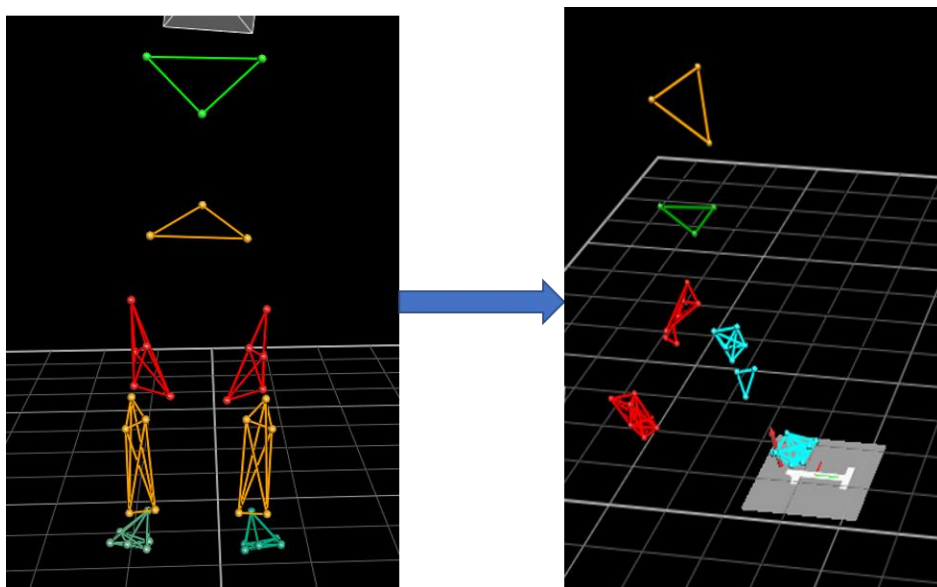


Figure 17 Static model collection and dynamic model in the data collection.

(6) The surface electromyogram (EMG) wireless 32-channel system (Delsys, Boston, MA, USA) collected ten participants' muscle activities during the running phase. The surface

electromyogram (EMG) wireless 32-channel system (Delsys, Boston, MA, USA) collected five participants' muscle activities during the running phase. Muscle activity included vastus lateralis (VL), vastus medialis (VM), gastrocnemius medial (GM), and gastrocnemius lateral (GL), soleus muscle (SL), flexor hallucis longus (EMG) and Extensor digitorum longus (EDL), tibialis anterior (TA) and tibialis posterior (TP) (Figure 18). was collected at a frequency of 1000 Hz. Following a previously established protocol, the muscles' max voluntary contractions (MVC) were performed to normalize muscle activity (0-100%).

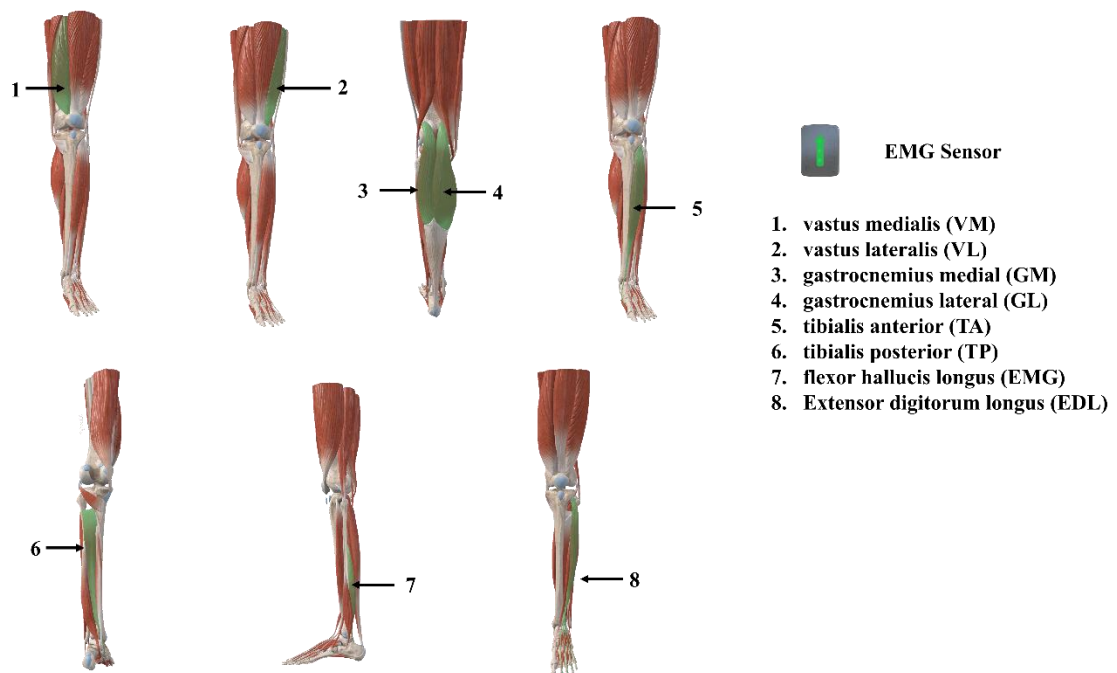


Figure 18 EMG (Electromyography) Muscle Data Collection Diagram.

(7) Running fatigue protocol. Before data collection, subjects were familiarized with the running protocol and the Borg Scale RPE 6–20. The Borg Scale RPE 6–20 and heart rate monitor were used to record subjective fatigue and heart rate changes during the running intervention. First, the subjects warmed up at 6 km/h for 3 minutes. Then, the operator increased the treadmill speed to 14.4 km/h. Subjects were required to run at 14.4km/h on the treadmill until they could not continue. They were then considered in a fatigued state. Fatigue was defined when all the following conditions were met: (1) the heart rate of the participants reached 90% maximum heart rate of their age-calculated maximum heart rate ($HR_{max} = 220-$

age), (2) the participants could not continue running, and (3) a rating on the Borg scale exceeded RPE > 17 (very hard).

0–10 Borg Rating of Perceived Exertion Scale	
0	Rest
1	Really easy
2	Easy
3	Moderate
4	Sort of hard
5	Hard
6	
7	Really hard
8	
9	Really, really, hard
10	Maximal: just like my hardest race

Figure 19 Borg Scale RPE.

(8) Finite element simulation of running

This research created a foot FE model with 3D plantar fascia geometry based on the foot CT. The ground reaction force and muscle force were measured from the gait analysis and musculoskeletal stimulation. More information regarding the workflow of the customized foot modeling is available in Figure 20 and Figure 21. As for the model building, including the running gait data collection, geometry reconstruction, material properties, boundary conditions, and model validation.

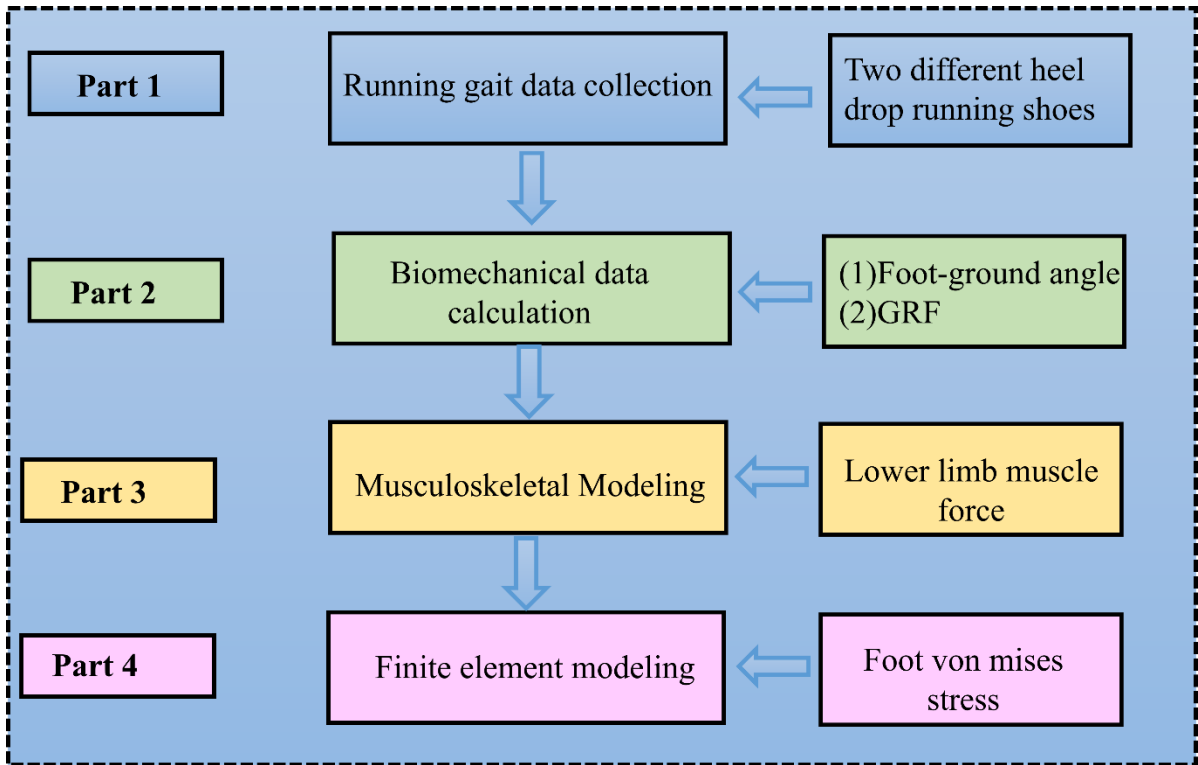


Figure 20 Workflow of finite element in this study.

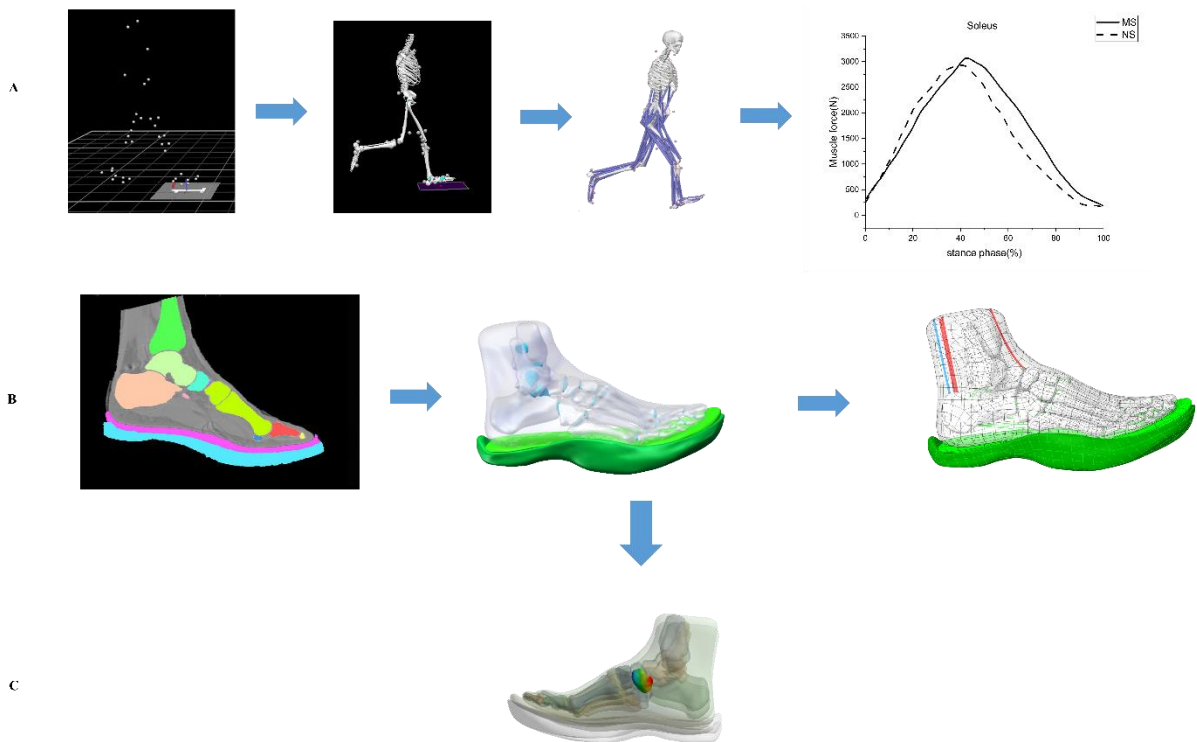


Figure 21 Data collection and foot model simulation in the FE analysis section, A: kinematics parameters collection, B:FE model building, C: FE model with the minimalist shoes.

2.2 Musculoskeletal modeling

2.2.1 Subject-specific musculoskeletal model building

Opensim is an open software based on the C++ and JAVA programming languages for developing, simulating, and analyzing muscle models. OpenSim software, like other motion simulation software, must combine a kinematic capture system and force measurement table to obtain kinematic and mechanical data during human motion and then substitute the measured data into the established human musculoskeletal model for forward or inverse optimization calculation to obtain the force of each muscle in the model during the motion to comprehend the role of each muscle in the motion process.

2.2.2 Model validation

EMG activation variables were compared qualitatively to OpenSim simulated muscle activations to evaluate OpenSim model reliability. Figure 22. depicts the comparison results, which indicate that the predicted muscle activation and EMG during the running stance phase were in good agreement.

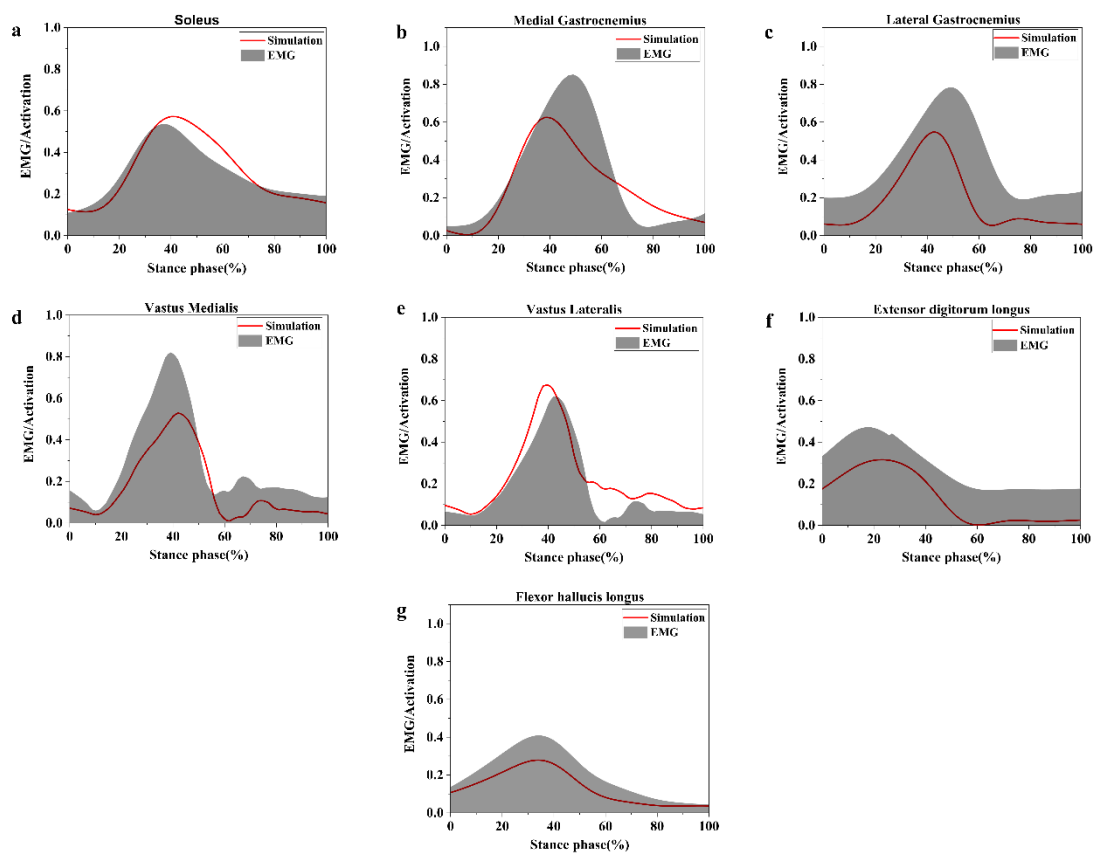


Figure 22 Comparison of muscle activations from static optimization estimated (blue line) and filtered electromyography (EMG) signals measured from the subjects during the same trial of normal walking, jogging

and running. Note. EMG and activations were normalized from zero to one for each subject based upon the minimum and maximum values over the stance phase.

2.3 Data analysis

2.3.1 Joint Kinematics

The kinematic data were preprocessed using Vicon Nexus software, capturing a full running stance phase, completing any missing mark points, and removing any incorrect or redundant mark points. After preprocessing, the biomechanical data was imported into Visual3D software (v6; C-Motion, Inc., Germantown, MD, USA) for processing and calculation. The kinematic and kinetic data were processed using a fourth-order Butterworth low-pass filter with 15 Hz and 50 Hz cutoff frequencies, respectively. Joint angles, moments, power, and work were normalized to the gait cycle over 101-time points. Ankle, knee, and hip angles were calculated using Cardan angles in the sagittal, frontal, and transverse planes.

2.3.2 Joint Kinetics

The joint moments, including the maximum moment values of the ankle, knee, and hip joints, were calculated using an inverse dynamics approach. Joint power, including the maximum power values of the ankle, knee, and hip joints, was defined as the dot product of the joint moment and the angular velocity. The ankle joint dorsiflexion moment, knee joint flexion moment, and hip flexion moment are positive (+), and the corresponding ankle joint plantarflexion moment and hip joint extension moment are negative (-). The positive value (+) of the ankle, knee, and hip joint power indicates energy production. The negative value (-) of the ankle, knee and hip joint power indicates the energy absorption of the ankle, knee, and hip joints.

$$P_j = M_j \cdot \omega_j$$

M_j is the joint moment of the ankle, knee, and hip joint, while ω_j is the joint angular velocity of the ankle, knee, or hip. The joint work is obtained by integrating the joint power over time. In this paper, the trapezoidal method was used for numerical integration. Energy generation (E_g) or energy absorption (E_a) was calculated by the integral of the positive and negative areas of joint angular power at a time using a custom program over the stance phase in MATLAB (Version: R2019a, The MathWorks, Natick, MA, USA). Total joint work was calculated by integrating the joint power time curves over the stance phase, respectively [57,156].

$$E_i = W_i = \int_{t_1}^{t_2} P_j \cdot dt = \int_{t_1}^{t_2} M_j \cdot \omega_j \cdot dt$$

Where $i = a$ as absorption or g as generation, t_1 to t_2 is the time of running stance; W is the total work on a joint during the running stance; P_j is the instantaneous power of a joint. The joint moment, power, and work were all divided by body weight for normalization.

2.3.3 Partial least squares regression (PLSR) method

Partial least squares regression (PLSR) is a regression mathematical modeling approach applied to multiple independent variables to various dependent variables (responses Y) and multiple independent variables (predictors X) to a single dependent variable [157]. There are many advantages of PLSR rather than the traditional classical regression analysis method. Compared with conventional regression analysis, PLSR has no special requirements for sample size, higher utilization of independent variable information. At the same time, it exhibits better modeling accuracy and predictive effect than traditional regression analysis. Partial least squares regression (PLSR) was used to compare four predictors, including initial joint angle and joint motion of the knee and ankle, and six responses, including positive and negative joint work, total joint work of the knee, and the ankle. The predictive variables included initial ankle joint angle ($X1$), initial knee joint angle ($X2$), range motion of the ankle ($X3$), and range motion of the knee ($X4$). The response variables included ankle positive work ($Y1$), ankle negative work ($Y2$), total work of the ankle ($Y3$), knee positive work ($Y4$), knee negative work ($Y5$) and total work of the knee ($Y6$).

Data standardization processing was carried out on the original data matrix X , Y to facilitate the use of formulas in subsequent operations and to express the corresponding data while reducing the error. The corresponding matrix was obtained after processing. Considering a $(N \times K)$ matrix of the mean-centered input space (X) and a $(N \times J)$ matrix of the mean-centered output space (Y), where K is the number of independent variables (factors) per observation (4 joint angles), J is the number of dependent variables per observation (6 joint work), and N is the number of the observations (50 training samples from the total of runners in this study) and subscript L is the number of components. \mathbf{P} matrix and \mathbf{Q} matrix are the so-called loading matrices, \mathbf{E} and \mathbf{F} are the residual matrices. \mathbf{T} and \mathbf{U} are the projection matrices. PLSR method decomposes the \mathbf{X} and \mathbf{Y} matrices into a bilinear structural model, consisting of a linear combination of the score and the loading matrix.

$$\mathbf{X}_{NK} = \mathbf{T}_{NL} \cdot \mathbf{P}_{KL}^T + \mathbf{E}_{NK}$$

$$\mathbf{Y}_{NJ} = \mathbf{U}_{NL} \cdot \mathbf{Q}_{JL}^T + \mathbf{F}_{NJ}$$

Step 1: The original data matrix X , Y will be normalized to facilitate the expression of the corresponding data by the formula in the subsequent operation while reducing the error

between data volumes, and the corresponding matrix will be obtained after processing. The $\mathbf{E}_{\mathbf{N}\mathbf{K}}$ is the corresponding matrix for $\mathbf{X}_{\mathbf{N}\mathbf{K}}$ and $\mathbf{F}_{\mathbf{N}\mathbf{J}}$ is the corresponding matrix for $\mathbf{Y}_{\mathbf{N}\mathbf{J}}$ for repeated iterative operations.

Step 2: After obtaining the corresponding normalized matrix, the corresponding components need to be extracted. In this regression PLSR model, the number k principal components extracted for modeling is determined by the cross-validity test. Thus, H principal components are extracted, where Y_j is the j^{th} dependent variable. The squared sum of the prediction error is shown in the following equation, where p is the total number of reaction factors:

$$PRESS(H) = \sum_{i=k}^p PRESS_j(H)$$

The squared sum of errors of the dependent variable set Y is:

$$SS(H) = \sum_{j=k}^p SS_j(H)$$

According to the principal component analysis, the corresponding components should satisfy $PRESS(H)$ while it reaches the minimum value. Generally, $PRESS(H)$ is larger than $SS(H)$, While $SS(H)$ is lesser than $SS(H-1)$. Consequently, the smaller $PRESS(H)/SS(H-1)$ is the better. The limit value is commonly set as 0.05.

$$Q_H^2 = 1 - PRESS(H)/SS(H - 1) = 1 - 0.952 = 0.0975$$

For this reason, the model meets the accuracy requirement when the cross validity $Q_H^2 < 0.0975$, while the extraction of components is stopped.

This PLSR algorithm model (Version: R2019a, The MathWorks, Natick, MA, USA) uses 80% of the data set sample size as the training set, and 20% sample size as the test set. Firstly, the training set is cross-checked by leave-one-out cross-validation analysis. Second, the new data set was used to verify the model after cross-checking the model's training set. The average X_{ave} , maximum X_{max} , minimum X_{min} , the difference between the maximum and minimum X_{dif} ($X_{\text{max}} - X_{\text{min}}$) of each predictive variable is shown in Table 2. The incremental perturbation action of a predictor variable was taken to $X_{\text{min}} - 10\% X_{\text{dif}}$, X_{min} , $X_{\text{min}} + 10\% X_{\text{dif}}$, $X_{\text{min}} + 20\% X_{\text{dif}}$, $X_{\text{min}} + 30\% X_{\text{dif}}$, $X_{\text{min}} + 40\% X_{\text{dif}}$, $X_{\text{min}} + 50\% X_{\text{dif}}$, $X_{\text{min}} + 60\% X_{\text{dif}}$, $X_{\text{min}} + 70\% X_{\text{dif}}$, $X_{\text{min}} + 80\% X_{\text{dif}}$, $X_{\text{min}} + 90\% X_{\text{dif}}$, X_{max} , $X_{\text{max}} + 100\% X_{\text{dif}}$ in Table 3.

Table 2 The average value (X_{ave}), maximum value (X_{max}), minimum value (X_{min}) and the difference between the maximum and minimum values (X_{dif}) of predictive variables X.

X	X1 (ankle IC)	X2 (knee IC)	X3 (ROM ankle)	X4 (ROM knee)
X_{ave}	8.21	19.22	43.82	27.01
X_{max}	16.58	29.85	80.41	37.51
X_{min}	1.97	8.44	22.53	18.34
X_{dif}	14.61	21.41	57.88	19.17

Table 3 The predictors of each predictive variable.

X	X1 (ankle IC)	X2 (knee IC)	X3 (ROM ankle)	X4 (ROM knee)
$X_{min}-10\% X_{dif}$	1.78	7.60	20.27	16.51
X_{min}	1.97	8.44	22.53	18.34
$X_{min}+10\% X_{dif}$	3.44	10.58	28.31	20.26
$X_{min}+20\% X_{dif}$	4.90	12.73	34.10	22.18
$X_{min}+30\% X_{dif}$	6.36	14.87	39.89	24.09
$X_{min}+40\% X_{dif}$	7.82	17.01	45.68	26.01
$X_{min}+50\% X_{dif}$	9.28	19.15	51.47	27.93
$X_{min}+60\% X_{dif}$	10.74	21.29	57.25	29.84
$X_{min}+70\% X_{dif}$	12.20	23.43	63.04	31.76
$X_{min}+80\% X_{dif}$	13.66	25.57	68.83	33.68
$X_{min}+90\% X_{dif}$	15.12	27.71	74.62	35.59
X_{max}	16.58	8.44	80.41	37.51
$X_{max}+110\% X_{dif}$	33.16	16.89	160.81	75.02

Note: X: predictor variables, X1: initial ankle angle, X2: initial knee angle, X3: range motion of ankle angle, X4: range motion of knee angle.

2.4 Finite element modeling simulation

2.4.1 Geometry acquisition and reconstruction

The subject's right foot was scanned using an Optima CT540 scanner at a hospital while wearing minimalist running shoes. The images were imported into MIMICS 21.0 for further processing. A three-dimensional model of the right foot with minimalist running shoes was reconstructed using medical image processing software. The model included various soft tissues and bones, with a total of 30 bone segments. Boundary surfaces were processed using SolidWorks, which was also used to construct solid bone and soft tissue models. The material characteristics of the foot's bony, ligamentous, and ground plate components were idealized as homogeneous, isotropic, and linear elastic materials. The insole and midsole materials were the same, improving the efficiency of the finite element simulation solution calculation. The coefficient of friction between the midsole and the ground plate was set at 0.6. The interactions between bone and cartilage and bone and soft tissue were defined as frictionless with non-linear contact. The material properties of the components in the finite element model are detailed in Table 4.

Table 4 Material properties of the components in the finite element model.

Component	Elastic modules (MPa): E	Poisson's ratio: ν	Destiny(kg/m ³)	Referrence
Skin	Hyperelastic (first-order Ogden model, $\mu = 0.122 \text{ kPa}, \alpha = 18$)	N/A	950	[158]
Bulk soft tissue	Hyperelastic (second-order polynomial strain, $C_{10} = 0.8556, C_{01} = 0.05841, C_{20} = 0.03900, C_{11} = 0.02319, C_{02} = 0.00851, D_1 = 3.65273$)	N/A	950	[159]
Aterior Crucial Ligament	Hyperelastic (first-order polynomial strain, $C_1 = 1.95, D = 0.00683$)	N/A	1000	[160]
Posterior Crucial Ligament	Hyperelastic (first-order polynomial strain, $C_1 = 3.25, D = 0.0041$)	N/A	1000	
Foot Bones	7300	0.3	1500	[161]
Foot Cartilages	1	0.4	1050	
Foot Ligaments	260	0.4	1000	[162]
Plantar Fascia	350	0.4	1000	[163]
Plate	17000	0.4	1000	[150]
Mid-sole	1.45	0.2	169	/
Sole	1.45	0.2	169	/

2.4.2 Loads and boundary conditions

This study used the Transient Structural module in ANSYS 17.0 software to simulate the interaction between the foot and the ground in different running events. The study aimed to compare the mechanical behavior of the foot when using minimalist shoes (MS) versus normal shoes (NS). A previous study has shown that minimalist shoes might change the rear-foot strike pattern into the mid-foot strike pattern [155]. Therefore, to better compare the running foot mechanical between the MS and NS. This study uniformly selected 20%, 40%, 60%, and 80% of the transient phases of the two running shoes as the target conditions for finite element simulation, resulting in eight simulation models (Figure 23). Therefore, to better compare the mechanical running foot between the MS and NS, this study uniformly selected 20%, 40%, 60%, and 80% of the transient phases of the two running shoes as the target conditions for finite element simulation, resulting in eight simulation models (Figure 23). In order to compare the running foot mechanics between the MS and NS, this study selected 20%, 40%, 60%, and 80% of the transient phases of the two running shoes as the target conditions for finite element simulation. This resulted in eight simulation models (Figure 4). The boundary condition for the finite element model involved fixing the proximal surfaces of the foot's tibia, fibula, and soft tissue. The plantar surface of the ground plate was loaded with a net vertical ground reaction force for different running stance phases [164]. In addition, the muscle forces, including the soleus, gastrocnemius medialis, gastrocnemius lateralis, tibialis anterior, and tibialis posterior, were used as inputs to drive the FE model. These muscle forces were estimated using the musculoskeletal model based on experimental gait data. The simulations were conducted using the standard static solver in Workbench 2021 (ANSYS, Inc., Canonsburg, PA, USA).

MS strike pattern



NS strike pattern



Initial contact

Midstance

Push off

Toe off

Figure 23 FE simulations at four different running gait instants: initial contact(at 20% of the stance phase), midstance stance (40% of the stance phase), push-off (60% of the stance phase), toe-off (80% of the stance phase).

2.5 Data analysis

(i) Statistical analyses were performed to determine significant differences in ankle and knee joint work, joint angle, joint moment, and joint power during the stance phase. Shapiro–Wilk’s tests were performed for normal distribution. The paired t-test in SPSS 23.0 (SPSS Inc., Chicago, IL) was used to assess data differences for kinematic and kinetic parameters. The significance level was set at $p \leq 0.05$. One-dimensional, one-way repeated measures Statistical Parametric Mapping (SPM) ($\alpha = 0.05$) was used to assess differences in joint angle, joint moment, and joint power throughout the running stance.

(ii) Statistical analyses were performed in SPSS version 25.0 (SPSS Science, Chicago, IL, USA). Applying the Shapiro-Wilk normality tests to determine the strike index in different running shoe conditions. Paired-sampled T-tests were used to compare the strike index. The effect size (Cohen's d) of the strike index variable was computed in this study. The means and standard deviations of the six valid trials from each subject were calculated for the two different running shoe measurements. The significance level was set at $p > 0.05$. Matlab was used to compare the joint angle, moment, and muscle force waveforms using the open-source one-dimensional statistical parametric mapping (SPM) program. We created a time series curve with 101 data points using a custom MATLAB script based on data collected during the running phases for statistical parametric mapping (SPM) analysis. The SPM test, equivalent to the paired t-test, was used.

3 Results

3.1 Gait fatigue biomechanics variables

3.1.1 Kinematic variables

Ankle dorsiflexion angle at initial contact significantly decreased when the pre-fatigue condition and post-prolonged running condition were compared ($p=0.002$) (Figure 24A). The maximum dorsiflexion angle was also significantly greater than post-prolonged running in the sagittal ankle plane. Due to the dorsiflexion angle decrease, the ROM of the ankle was significantly larger after prolonged running ($p=0.001$). There were no differences present in the knee flexion angle and in ROM regarding the sagittal plane. At the hip fatigue, prolonged running had a more significant effect on the max hip extension, and the max hip extension angle was decreased when all participants after prolonged running ($p=0.026$) (Figure 24C), but hip flexions observed no change. The range of motion of the hip was increased during the post-prolonged running ($p=0.001$).

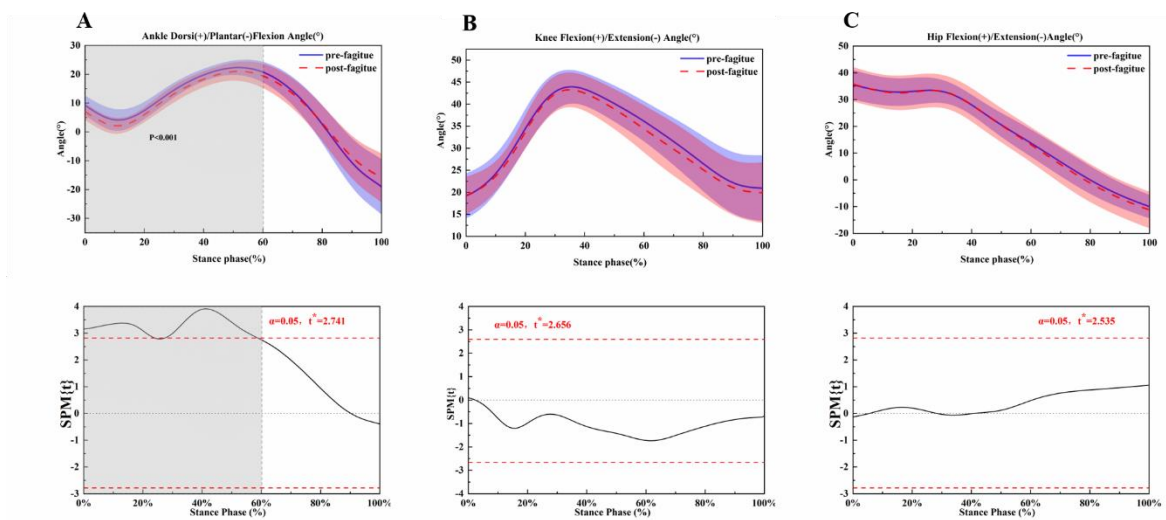


Figure 24 Comparing the mean values of ankle, knee and hip joint angle from all participants between fatigue conditions (pre-fatigue; post-fatigue). * $P \leq 0.05$.

Table 5 Lower extremity joint kinematics pre-fatigue running and post-prolonged fatigue running ($\bar{x} \pm$ SD).

Variables	Pre-fatigue	Post-fatigue	P-value
Ankle IC ($^{\circ}$)	9.23 \pm 3.44	7.19 \pm 3.00	0.002*

Max dorsiflexion angle (°)	22. 20.66±3.31	20.66±3.31	0.001*
Max plantarflexion angle (°)	-19.16±9.43	-18.52±8.24	0.513
Range of ankle joint motion (°)	41.74±8.28	39.18±13.00	0.023*
Knee IC (°)	19.17±5.12	19.27±4.24	0.902
Max flexion angle (°)	44.13±3.87	43.54±3.83	0.271
Range of knee joint motion (°)	27.23±4.28	26.78±4.29	0.511
Max hip flexion angle (°)	35.87±5.24	36.15±6.47	0.693
Max hip extension angle (°)	-9.98±4.39	-11.26±6.86	0.026*
Range of hip joint motion (°)	45.86±4.03	47.41±4.49	0.001*

Note: *significant difference between pre-fatigue running and post-fatigue running ($p \leq 0.05$). IC: initial contact angle

3.1.2 Peak torque and power

Moderate reductions in peak positive ankle power ($p=0.034$) (Figure 25D) were observed following the prolonged running fatigue protocol in Table 4. During running, a significantly higher knee negative power ($p=0.05$) (Figure 25E) was found after the prolonged running fatigue protocol in Table 6. For the hip, the positive power ($p=0.045$) (Figure 25F) was significantly increased in the fatigue and prolonged running condition, respectively (Table 6). All other peak joint moments and peak positive and negative joint powers remained unchanged following the prolonged running fatigue protocol.

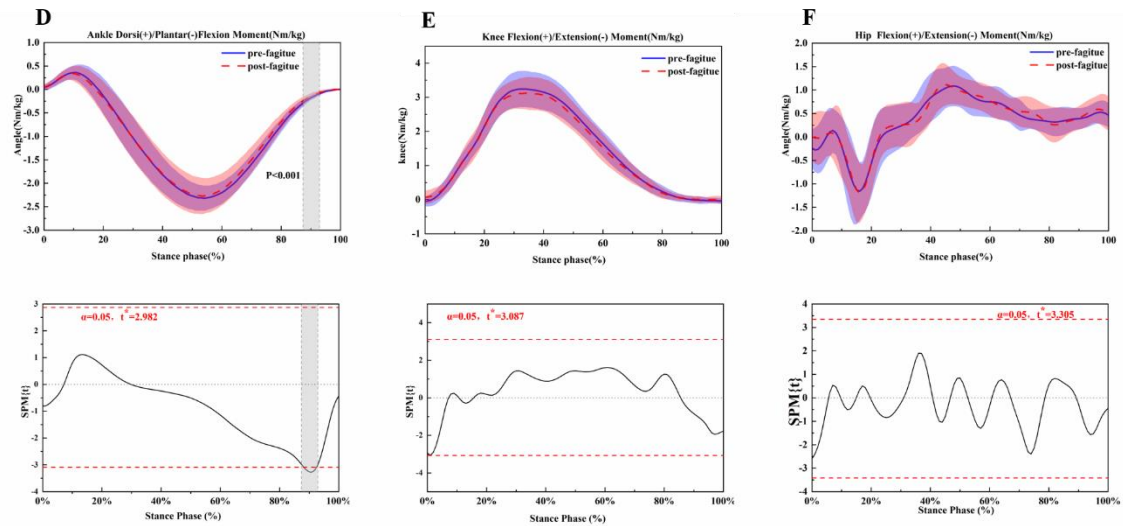


Figure 25 Comparing the mean values of ankle, knee and hip joint moment from all participants between fatigue conditions (pre-fatigue; post-fatigue). * $P \leq 0.05$.

Table 6 Lower extremity joint moment, power pre-fatigue running and post-prolonged fatigue running (\pm SD).

Variables	Pre-fatigue	Post-fatigue	P-value
Max ankle PF moment (Nm/kg)	-2.34 \pm 0.07	-2.30 \pm 0.39	0.337
Max ankle DF moment (Nm/kg)	0.42 \pm 0.12	0.40 \pm 0.14	0.385
Max knee flexion moment (Nm/kg)	3.34 \pm 0.51	3.24 \pm 0.41	0.093
Max hip flexion moment (Nm/kg)	1.37 \pm 0.44	1.38 \pm 0.36	0.885
Max hip extension moment (Nm/kg)	-1.58 \pm 0.56	-1.57 \pm 0.42	0.982
Max ankle positive power (Watt/kg)	9.42 \pm 2.44	8.74 \pm 2.89	0.034*

Max ankle negative power (Watt/kg)	-5.27±1.13	-5.43±1.71	0.535
Max knee positive power (Watt/kg)	9.48±3.97	9.91±4.53	0.455
Max knee negative power (Watt/kg)	-21.45±6.02	-23.65±6.43	0.050*
Max hip positive power (Watt/kg)	2.63±2.24	3.61±2.74	0.045
Max hip negative power (Watt/kg)	-7.80±2.73	-7.43±3.90	0.521

Note: *significant difference between pre-fatigue running and post-fatigue running ($p \leq 0.05$).

3.1.3 Joint work

Relative positive ankle work was significantly increased after prolonged running ($p=0.044$). A moderate reduction in the absolute total of ankle work was observed after prolonged running ($p=0.046$). Relative negative knee work and knee positive work were moderately unchanged following the prolonged running fatigue protocol (Table 7). In addition, the hip positive work was significantly greater when participants after prolonged running ($p=0.050$).

Table 7 Lower extremity joint work pre- fatigue running and post-prolonged fatigue running ($\bar{x} \pm SD$).

Variables	Pre-fatigue	Post-fatigue	P-value
Ankle positive work (J/kg)	0.63±0.17	0.53±0.17	0.044*
Ankle negative work(J/kg)	-0.32±0.08	-0.33±0.08	0.733
Ankle total work (J/kg)	0.31±0.21	0.25±0.16	0.046*
Knee positive work (J/kg)	0.60±0.16	0.55±0.16	0.273
Knee negative work (J/kg)	-0.78±0.21	-0.81±0.21	0.223

Knee total work (J/kg)	0.28±0.17	0.26±0.18	0.543
Hip positive work (J/kg)	0.06±0.05	0.09±0.06	0.050*
Hip negative wok (J/kg)	-0.57±0.18	-0.55±0.28	0.590
Hip total work (J/kg)	-0.51±0.20	-0.46±0.28	0.203

Note: *significant difference between pre-fatigue running and post-fatigue running ($p \leq 0.05$).

3.1.4 PLSR model

PLSR models for female amateur runners (Figure 4) were trained separately for ankle positive work (Y1), ankle negative work (Y2), total work of the ankle (Y3), knee positive work (Y4), knee negative work (Y5) and total work of the knee (Y6). A ‘leave-one-out’ analysis showed a response variable prediction accuracy of 93.31% for the training set and 91.73% for the test set. The results of the sensitivity analysis of the PLSR model based on the independent variable set disturbance factor are shown in Figure 26.

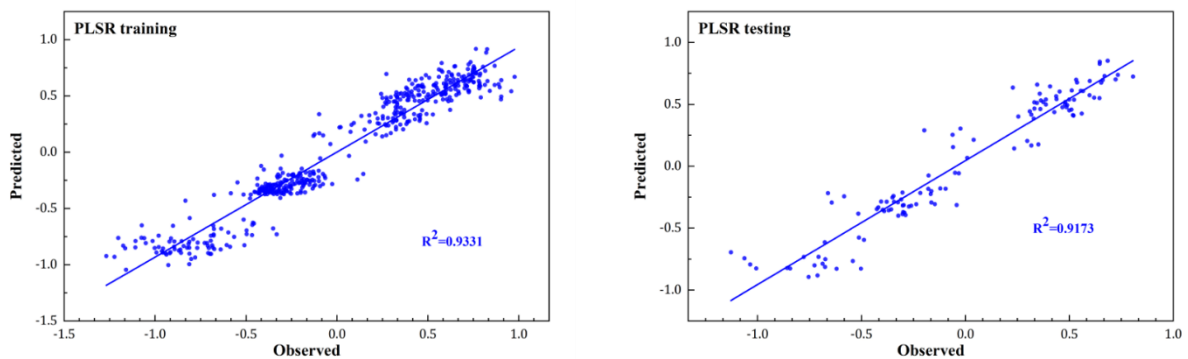


Figure 26 Training (left) and testing (right) accuracy of special skills assessment results of observed and predicted from the PLSR model in the female runners.

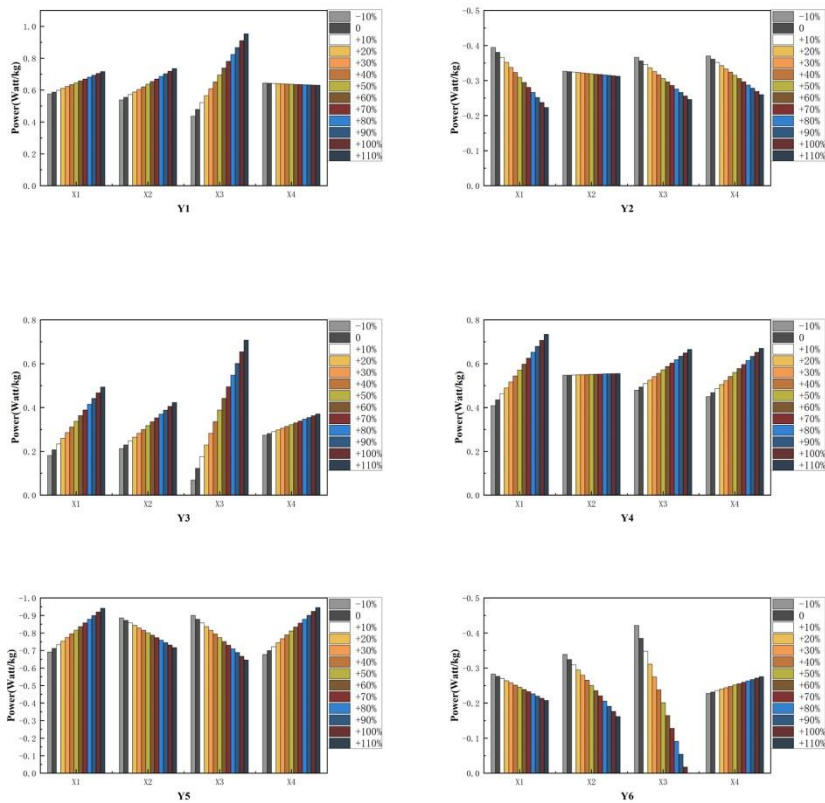


Figure 27 The predicted results of the response variables base on the PLSR model. Ankle positive work (Y1), ankle negative work(Y2), total work of the ankle (Y3), knee positive work (Y4), knee negative work (Y5) and total work of the knee (Y6).

Under the control of other independent variable sets, it can find (1) with increased initial ankle angle, under the same conditions, the joint work for runners after fatigue running, Y2 and Y6 were reduced, and the joint work for runners after fatigue running Y1, Y3, Y4 and Y5 were increased. (2) with increased initial knee angle, under the same conditions, the joint work for runners after fatigue running Y5 and Y6 were reduced, and the joint work for runners after fatigue running Y1, Y3 were increased. (3) with the increased motion of the ankle, under the same conditions, the joint work for runners after fatigue running Y2, Y5, and Y6 were reduced, and the joint work for runners after fatigue running Y1, Y3 and Y4 were increased. (4) with the increased motion of the knee, under the same conditions, the joint work for runners after fatigue running Y2 was reduced, and the joint work for runners after fatigue running Y3, Y4, Y5 and Y6 were increased.

3.2 Gait analysis of Minimalist and normal shoes

3.2.1 Lower extremity kinematics

Through the strike index calculation, Table 8 presents significant differences between minimalist and normal shoes. Compared to normal shoes, the foot strike pattern was shifted 21.65% in minimalist shoes. At the ankle joint, dorsiflexion angle increased at 0-15% ($p=0.038$) and 38%-84% ($p=0.005$) in normal shoes (Figure 28a). The ankle eversion angle was higher during the running stance at 28%-100% ($p<0.001$) with normal shoes (Figure 28b). As for the ankle internal rotation angle, which was decreased at 9%-45% ($p<0.001$) in normal shoes (Figure 28c). However, at 65%-89% ($p<0.001$), the external rotation angle was significantly increased in normal shoes. Peak ankle angles in the sagittal, frontal and transverse planes were shown in Table 9, with increased peak dorsiflexion angle ($p<0.01$) and eversion angle ($p<0.001$) in normal shoes. Nevertheless, there was a significantly decreased peak ankle eversion ($p<0.001$) angle, peak internal rotation ($p<0.001$), and peak external rotation angle ($p=0.001$) in normal shoes.

At the knee joint angle, the knee flexion angle decreased at 0-18% ($p=0.004$) in normal shoes condition (Figure 28d). Compared to minimalist shoes, knee flexion angle was higher during the running stance phase at 27%-100% ($p<0.001$) in normal shoes (Figure 28d). Decreased knee inversion angle was observed at 0-10% ($p=0.004$) (Figure 24e) in the normal shoes. However, knee inversion angle was increased at 42%-63% ($p=0.0019$) and 69%-100% ($p=0.006$) (Figure 28e) when running in normal shoes condition. But there was a significantly greater knee internal rotation angle during the running stance at 0-25% ($p=0.004$) and 36%-100% ($p<0.001$) in normal shoes (Figure 28f). Table 8 presents significantly greater peak knee flexion ($p=0.001$) and smaller peak knee internal rotation angle ($p=0.001$) during the running stance phase in normal shoes.

At the hip joint angle, the dorsiflexion angle increased at 11%-100% ($p<0.001$) in normal shoes (Figure 28g). Compared to minimalist shoes, hip inversion angle at 0-23% ($p=0.004$) and 84%-100% ($p=0.043$) were significantly smaller in normal shoes (Figure 28h). Increased internal rotation angle was observed during the running stance at 4%-88% ($p<0.001$) in normal shoes (Figure 28i). Table 8 presents the peak hip flexion angle ($p=0.004$) and peak hip internal rotation ($p<0.001$) were greater in the normal shoes. However, the peak hip extension angle ($p=0.001$), peak hip abduction angle ($p=0.045$), and peak external rotation angle ($p<0.001$) were significantly smaller in the normal shoes.

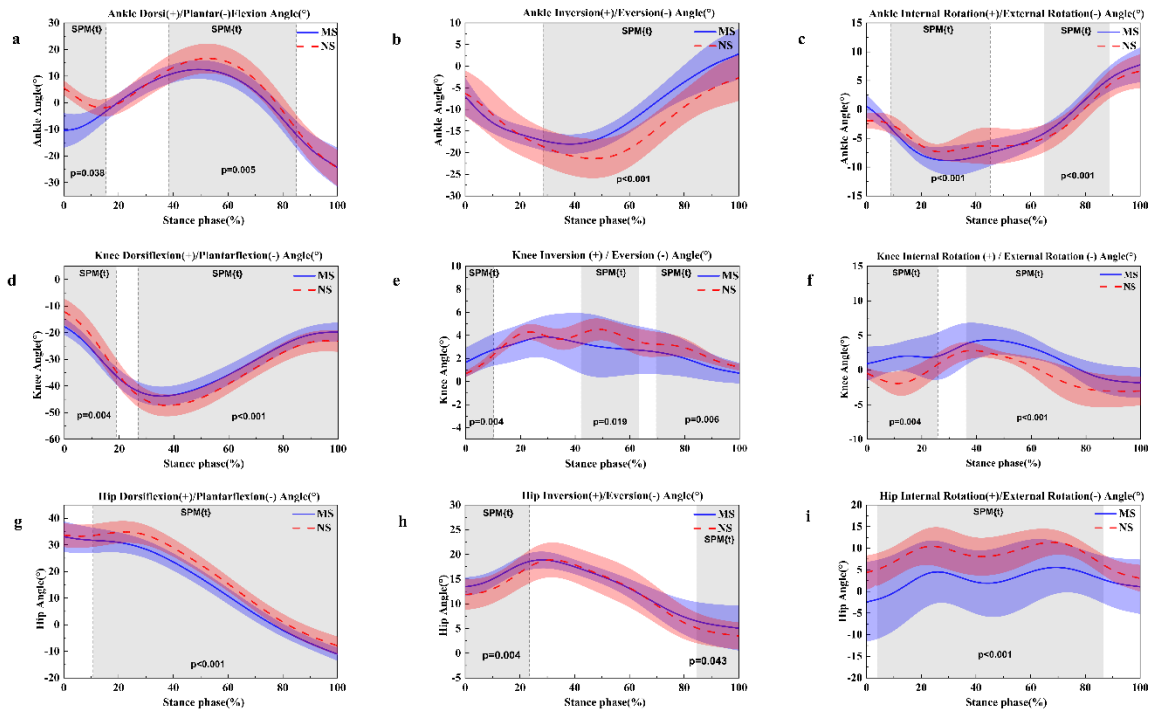


Figure 28 Illustration of the MS and NS lower limb results shows the statistical parametric mapping outputs for the angle of the ankle, knee, and hip during the running stance phase. MS, minimalist shoes, NS, normal shoes.

Table 8 Lower limb joint kinematics during the running stance of two running shoes (minimalist vs. normal shoes).

	Variables	MS	NS	P value	Cohen's d
Ankle(degree)	Strike index (%)	47.58±13.39	25.93±12.03	0.001*	1.70
	Dorsiflexion	12.62±3.55	16.79±6.63	<.001*	0.78
	Plantar flexion	-24.39±7.33	-24.65±6.87	0.803	0.04
	Inversion	2.86±5.82	-1.83±5.12	<.001*	0.19
	Eversion	-18.07±2.23	-21.44±4.56	<.001*	0.94
	Internal Rotation	7.77±3.00	6.66±2.92	<.001*	0.37
	External Rotation	-9.21±2.18	-7.92±1.75	0.001*	0.65
Knee(degree)	Flexion	-43.96±3.51	-47.36±4.09	0.001*	0.89
	Adduction	4.25±1.88	4.73±0.82	0.074	0.33
	Abduction	0.50±1.27	0.67±0.27	0.244	0.19
	Internal Rotation	5.08±1.79	3.00±1.06	0.001*	1.41
	External Rotation	-3.04±2.20	-3.53±1.88	0.123	0.24
Hip(degree)	Flexion	33.46±5.45	35.23±4.10	0.004*	0.37
	Extension	-11.06±2.49	-7.91±5.00	0.001*	0.80
	Adduction	18.95±1.67	19.02±3.49	0.843	0.03
	Abduction	5.06±4.52	3.49±2.74	0.045*	0.42
	Internal Rotation	6.42±6.37	12.69±3.41	<.001*	1.23
	External Rotation	-3.22±8.58	2.44±3.31	<.001*	0.12

Note: MS, minimalist shoes; NS, normal shoes; Max., maximum; Min., minimum; * Significant difference between minimalist shoes and normal shoes ($p < 0.05$).

3.2.2 Lower extremity kinetics

At the ankle joint moment, dorsiflexion moment and plantarflexion moment were increased at 2-42% ($p < 0.001$) and 50%-82% ($p < 0.001$) in normal shoes (Figure 29a). Decreased ankle inversion moment was presented during the running stance at 0%-48% ($p < 0.001$) in normal shoes (Figure 29b). However, ankle inversion moment was significantly greater at 60%-80% ($p < 0.001$) in normal shoes condition. As for the ankle internal rotation moment, which was decreased at 7%-27% ($p < 0.001$) in normal shoes (Figure 29c), however, when at the 45%-70% ($p < 0.001$), the ankle internal rotation moment was significantly greater in normal shoes. As shown in Table 9, the peak ankle dorsiflexion moment ($p < 0.001$), peak plantarflexion moment ($p < 0.001$), and peak eversion moment ($p < 0.001$) were significant increases in normal shoes. Compared to the minimalist shoes, normal shoes showed a smaller peak ankle inversion moment ($p < 0.001$).

At the knee joint moment, compared to minimalist shoes, the knee flexion moment decreased at 4%-23% ($p < 0.001$) (Figure 29d), and the knee flexion moment was significantly increased at 35%-81% ($p < 0.001$) in normal shoes. Decreased knee inversion moment was observed at 0-12% ($p = 0.002$) in the normal shoes (Figure 29e). However, compared to minimalist shoes, knee inversion moment was increased at 19%-28% ($p = 0.001$) and 87%-98% ($p = 0.003$) in normal shoes (Figure 29e). There was a significantly smaller knee internal rotation moment during the running stance at 0-18% ($p < 0.001$) in normal shoes (Figure 29f). The knee internal rotation moment was significantly increased during the running stance at 22%-37% ($p < 0.001$) and 40-65% ($p < 0.001$) in normal shoes condition. Table 9 presents significantly greater peak knee flexion ($p < 0.001$), peak knee abduction ($p = 0.042$), and peak knee internal rotation moment ($p < 0.001$) during the running stance phase in normal shoes.

At the hip joint moment, dorsiflexion angle was observed to increase the 29%-83% ($p < 0.001$) in normal shoes (Figure 29g). There was significant smaller hip eversion angle at 0-10% ($p < 0.001$), 12%-23% ($p < 0.001$) and 32%-33% ($p < 0.001$) in normal shoes (Figure 29h). Decreased external rotation angle was observed during the running stance at 2%-24% ($p < 0.001$) in normal shoes (Figure 29i). Compared to minimalist shoes, hip external rotation angle increased at the running stance at 67%-84% ($p < 0.001$) in normal shoes. Table 9 presents the peak hip abduction moment ($p = 0.001$) and peak hip external rotation moment ($p = 0.002$) were significantly smaller in the normal shoes.

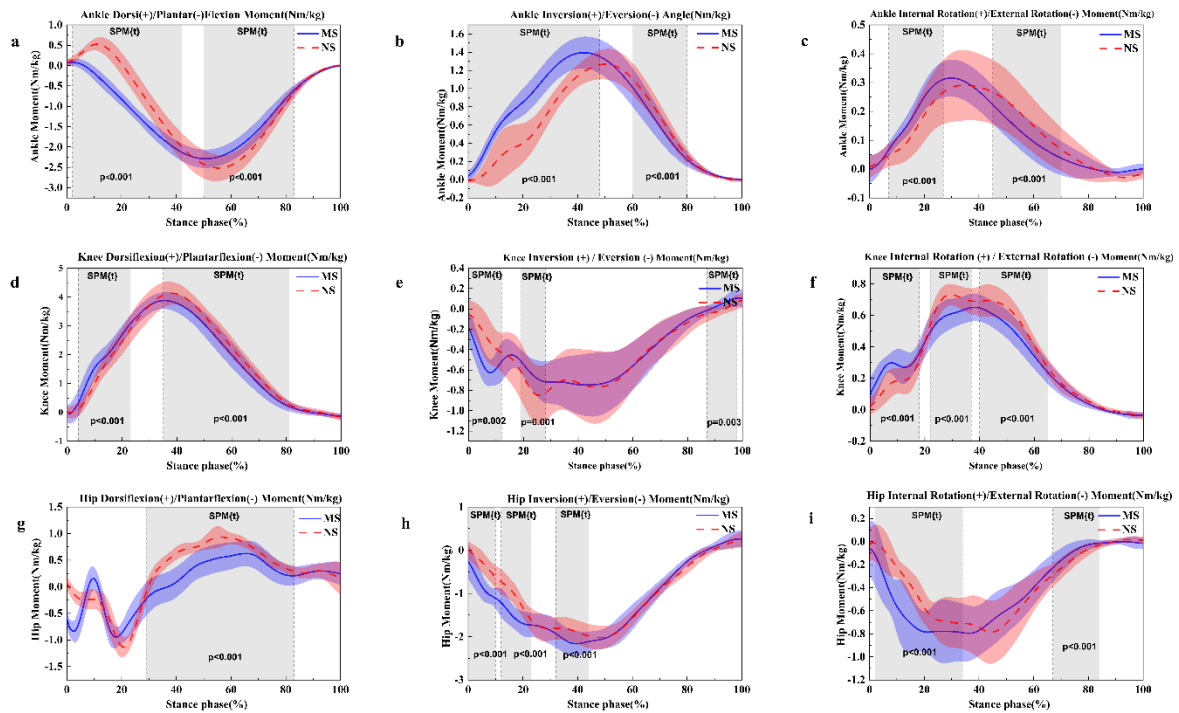


Figure 29 Illustration of the MS and NS lower limb results showing the statistical parametric mapping outputs for the moment of the ankle, knee, and hip during the running stance phase. MS, minimalist shoes, NS, normal shoes.

Table 9 Lower limb joint moment during the running stance of two running shoes (minimalist vs. normal shoes).

Joint	Variables	MS	NS	P value	Cohen's d
Ankle(xBW)	Dorsiflexion	0.11±0.08	0.56±0.13	<.001*	4.17
	Plantar flexion	-2.30±0.23	-2.53±0.32	<.001*	0.83
	Inversion	1.40±0.18	1.28±0.16	<.001*	0.70
	Eversion	-0.01±0.01	-0.05±0.06	<.001*	0.93
	Internal Rotation	0.32±0.06	0.31±0.11	0.341	0.11
	External Rotation	-0.03±0.02	-0.04±0.02	0.136	0.71
Knee(xBW)	Flexion	3.92±0.28	4.17±0.38	<.001*	0.75
	Adduction	0.13±0.09	0.11±0.07	0.067	0.25
	Abduction	-0.88±0.20	-0.94±0.27	0.042*	0.25
	Internal Rotation	0.67±0.08	0.75±0.07	<.001*	1.06
	External Rotation	-0.04±0.02	-0.05±0.02	0.516	0.5
	Flexion	0.69±0.28	1.00±0.17	<.001*	1.33
Hip(xBW)	Extension	-1.12±0.23	-1.18±0.19	0.091	0.28
	Adduction	0.33±0.23	0.29±0.14	0.204	0.21
	Abduction	-2.25±0.25	-2.10±0.26	0.001*	0.59
	Internal Rotation	0.10±0.11	0.09±0.09	0.293	0.10
	External Rotation	-0.94±0.24	-0.84±0.24	0.002*	0.42

Note: MS, minimalist shoes; NS, normal shoes; Max., maximum; Min., minimum; * Significant difference between minimalist shoes and normal shoes ($p < 0.05$).

3.2.3 Musculoskeletal modeling estimation

As shown in Figure 30, the characteristic muscle force pattern for running was similar between the normal shoes and minimalist shoes. The largest shift in muscle force across the running stance was observed for the soleus muscle force at 0-48% ($p < 0.001$), medial gastrocnemius force at 0-29% ($p < 0.001$), 30%-52% ($p < 0.001$) and 63%-100% ($p < 0.001$), which reduced in normal shoes. Simultaneously, lateral gastrocnemius force was also observed to decrease at 0-41% ($p < 0.001$) and 72%-100% ($p < 0.001$) during the running stance in normal shoes. There was significantly smaller Achilles tendon force at 0-51% ($p < 0.001$) and flexor hallucis longus force at 0-57% ($p < 0.001$) in normal shoes. However, there was a significantly increased vastus medialis force at 0-47% ($p < 0.001$) and vastus lateral force at 0-42% ($p < 0.001$) in normal shoes.

Table 10. presents peak vastus medialis force ($p < 0.001$), peak vastus lateralis force ($p < 0.001$), peak lateral gastrocnemius force ($p < 0.001$) and extensor digitorum longus force ($p < 0.001$) were significant greater in normal shoes. The peak soleus force ($p < 0.001$), Achilles tendon force ($p = 0.002$) and Flexor hallucis longus ($p = 0.001$) were significant smaller in normal shoes.

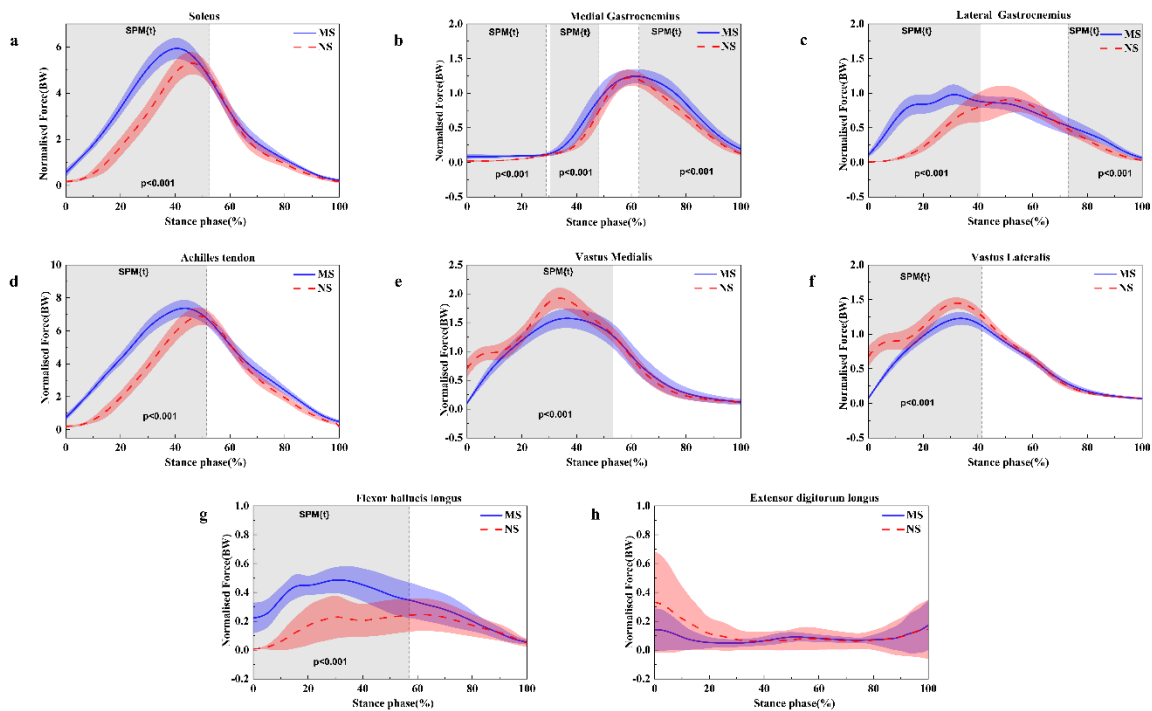


Figure 30 Illustration of the results between the MS and NS lower limb showing the statistical parametric mapping outputs for the muscle force during the running stance phase. MS, minimalist shoes, NS, normal shoes.

Table 10 Normalized peak muscle force data during the running stance of two running shoes (minimalist vs. normal shoes).

Muscle	MS	NS	P value	Cohen's d
Vastus Medialis (BW)	1.59±0.18	1.93±0.18	<.001	1.89
Vastus Lateralis (BW)	1.23±0.09	1.45±0.08	<.001	2.58
Medial Gastrocnemius (BW)	1.27±0.10	1.23±0.16	0.057	0.30
Lateral Gastrocnemius (BW)	0.62±0.05	0.93±0.18	<.001	2.35
Soleus (BW)	5.96±0.45	5.33±0.48	<.001	1.35
Achilles tendon (BW)	7.40±0.50	6.93±0.52	0.002*	0.92
Flexor hallucis longus (BW)	0.53±0.07	0.29±0.14	0.004*	2.17
Extensor digitorum longus (BW)	0.23±0.17	0.39±0.31	<.001	0.64

Note: MS, minimalist shoes; NS, normal shoes; * Significant difference between minimalist shoes and normal shoes ($p < 0.05$).

3.3 Finite element model simulation

3.3.1 FE modeling validation

In order to evaluate and validate the FE model, the simulated ground reaction force (GRF) was compared with the experimental data. Figure 31 shows high correlations between the simulated GRF and experimental data for both the MS condition ($R=0.9767$) and NS condition ($R=0.9821$). The results of the GRF demonstrate a good agreement. Table 11 presents the experimental and simulated GRF values for the MS and NS conditions during the different stance phases.

Table 11 Ground reaction force variables of MS and NS conditions between FE prediction and experimental measurement.

Shoe condition	variables	20%	40%	60%	80%
MS	Ground reaction force(N)-Measurement	1154.04	1648.41	1304.49	487.57
	Ground reaction force(N)-FE	1046.93	1421.03	1254.01	339.25
NS	Ground reaction force(N)-Measurement	956.1	1648.4	1229.9	494.1
	Ground reaction force(N)-FE	808.84	1591.84	985.9	329.5

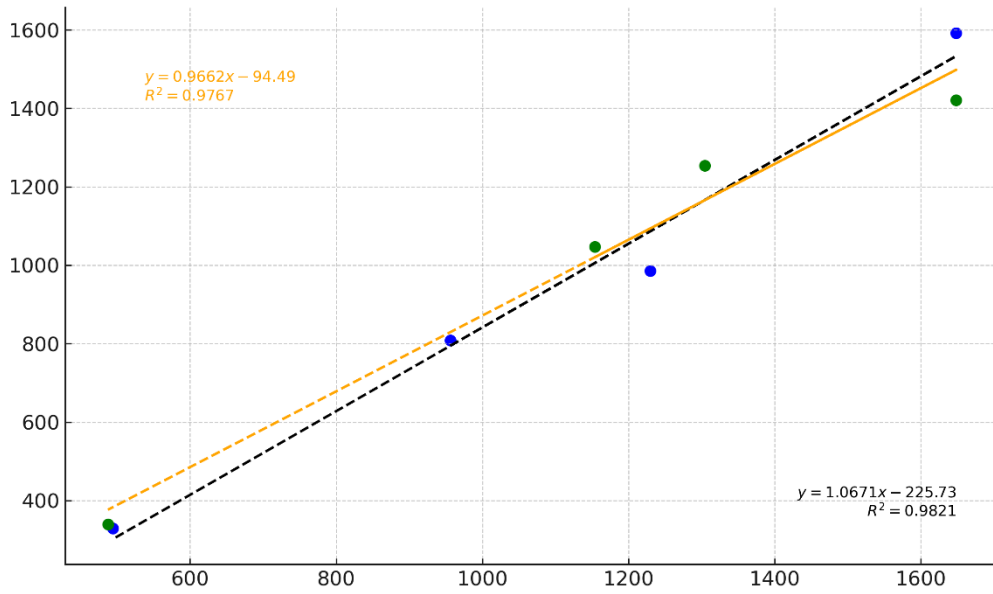


Figure 31 Validation of the FE foot model by comparing the predicted ground reaction force with experimental measurement.

3.3.2 Gait variables

Table 12 presents the running gait variables, such as running speed, contact time, and foot-ground angle. It was observed that the FSA angle significantly decreased when running in minimalist shoes. Furthermore, the FSA value fell within the MSF range, which indicates that the MFS = $-1.68^\circ < \text{FSA} < 8.0^\circ$, RFS = $\text{FSA} > 8.0^\circ$, and FFS = $\text{FSA} < -1.6^\circ$ [165]. However, the NS exhibited the FSA value within the RFS range (Figure 32).

Table 12 Running gait variable during the running stance.

	MS	NS
Running speed (m/s)	3.27	3.15
Contact time (s)	0.21	0.24
Foot-ground angle ($^\circ$)	0.96	18.74

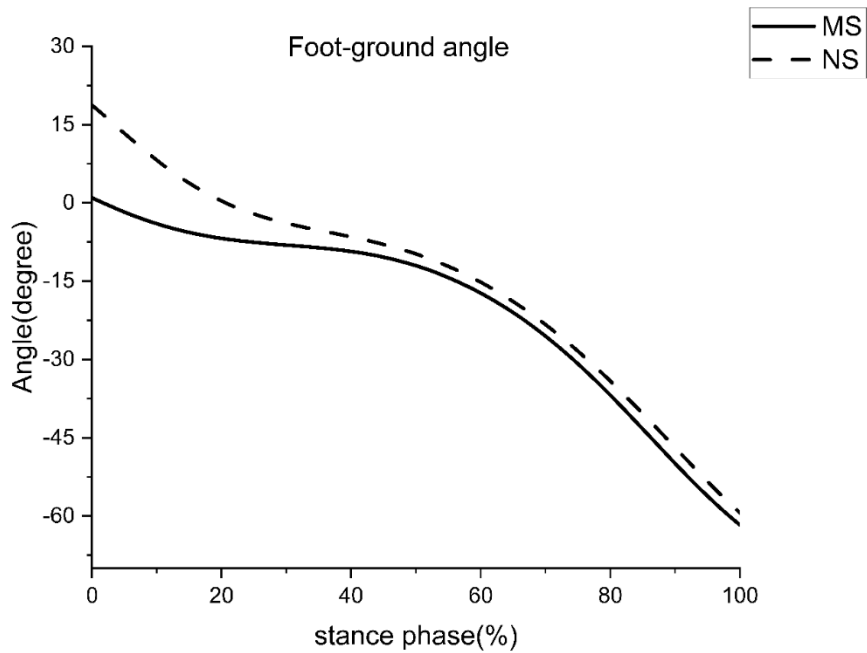


Figure 32 Foot-ground angle between the two running shoes condition. MS: minimalist running shoes, NS: normal shoes.

3.3.3 Boundary conditions from the musculoskeletal model

The two running shoe conditions showed significant muscle force differences during the running stance phase (Figure 33). In addition, we calculated the different running stance phase muscle forces by the musculoskeletal modeling. All the muscle force values were shown in Table 13 and Table 14, which were used to define the boundary condition for the FE model simulations.

Table 13 The musculoskeletal model calculated muscle forces used to define the loading and boundary conditions of the FE model at four different gait instants in the running stance phase of MS.

Muscle force(N)	20%	40%	60%	80%
Soleus	1648.63	2935.74	2329.35	942.89
Medial gastrocnemius	51.14	260.13	740.33	474.17
Lateral gastrocnemius	553.87	503.79	411.72	206.26
Tibialis anterior	369.15	463.29	411.66	297.46
Tibialis posterior	1610.83	1747.61	1574.82	802.57

Table 14 Musculoskeletal model calculated muscle forces used to define the loading and boundary conditions of the FE model at four different gait instants in the running stance phase of NS.

Muscle force(N)	20%	40%	60%	80%
Soleus	1973.47	2925.85	1762.08	626.02
Medial gastrocnemius	39.89	101.04	671.03	428.22
Lateral gastrocnemius	172.92	639.48	497.28	147.02
Tibialis anterior	300.93	397.52	506.79	264.87
Tibialis posterior	1423.38	1699.90	1626.12	921.05

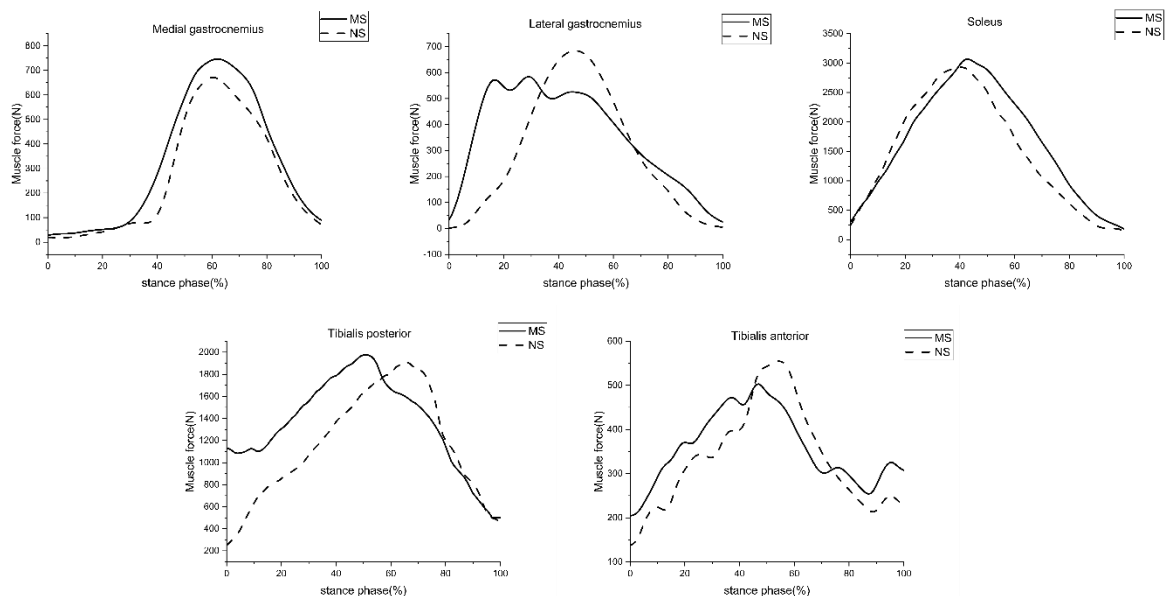


Figure 33 Extrinsic lower limb muscle force estimated by the OpenSim musculoskeletal model. MS: minimalist shoes, NS: normal shoes.

3.3.4 Metatarsal von mises stress

As shown in Figure 34, the heel drop significantly influences the metatarsal von Miss stress. The maximum von Miss stress of the metatarsal was larger in the MS than in the NS during the four running phases. According to the results, it can be found that the peak metatarsal von Miss stress occurred in the push-off. The peak von Mises stress was 44.775 MPa, especially in the fourth metatarsal. Table 15 and Figure 35 showed the first metatarsal von mises stress to the fifth metatarsal von mises stress distribution during the different running stances between the MS and NS conditions. The first metatarsal von mises stress to fifth metatarsal von mises stress

distribution was significantly larger than the NS during the mid-stance and push-off phases.

In the NS simulation, the max metatarsal von Miss stress was the fifth metatarsal during the mid-stance phase, 33.14 MPa. The peak metatarsal von Miss stress in the NS was reduced during the running passes compared to the MS. It also demonstrated that running with negative shoes might increase the risks of metatarsal stress fracture.

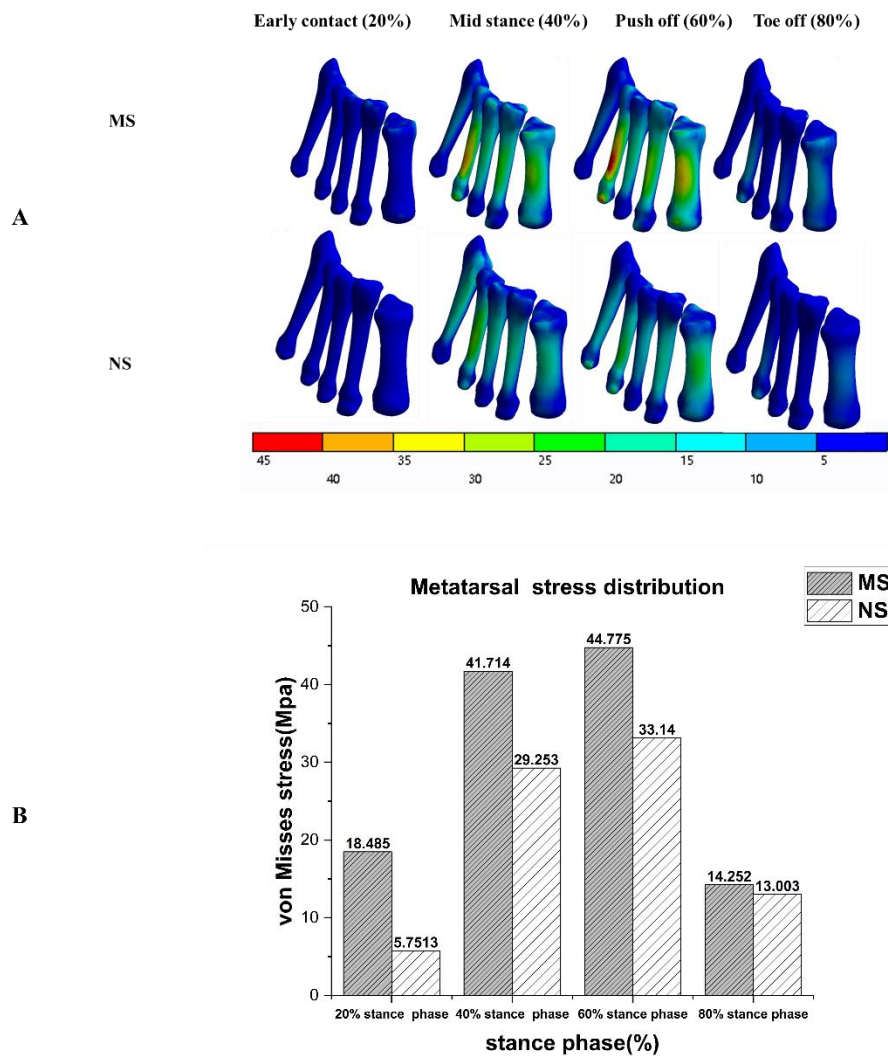


Figure 34 Metatarsal von mises stress distribution during the different running stances between the MS and NS conditions.

Table 15 First metatarsal von mises stress to fifth metatarsal von mises stress distribution during the different running stances between the MS and NS conditions.

	variables	20%	40%	60%	80%
MS	M1	12.192	26.168	35.444	10.638
	M2	7.5594	26.956	32.31	14.252
	M3	18.485	41.714	22.046	3.6189
	M4	13.579	39.322	44.775	14.165

	M5	4.9475	8.2842	6.7443	5.5295
	M1	5.0294	20.836	29.032	8.2951
	M2	4.0185	21.185	17.819	4.8414
NS	M3	2.9474	19.712	12.635	1.3527
	M4	5.7513	29.253	28.904	13.003
	M5	1.9001	18.714	33.14	0.45162

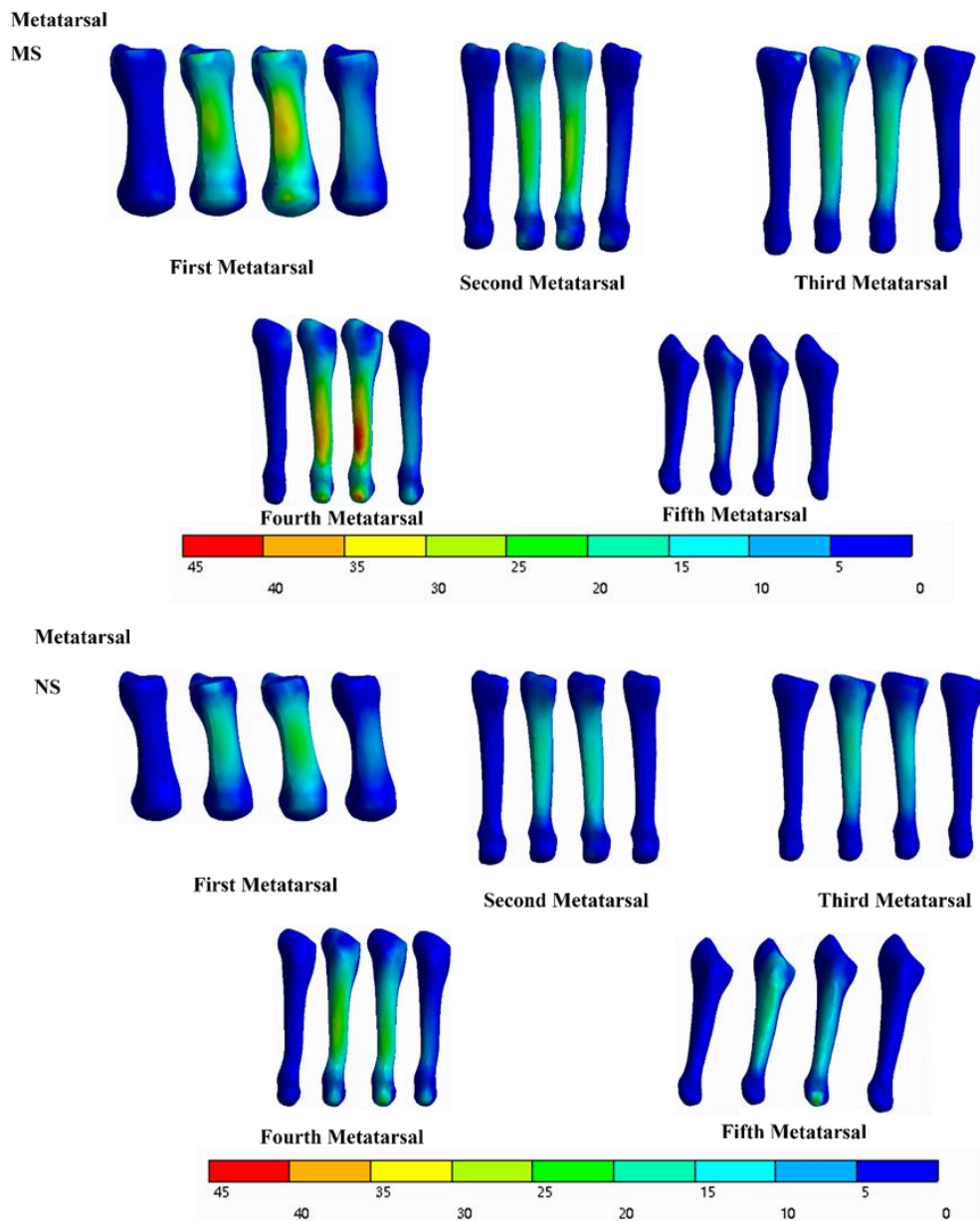


Figure 35 First metatarsal von mises stress to fifth metatarsal von mises stress distribution during the different running stances between the MS and NS conditions.

The von Mises stress of mid-bone for MS and NS conditions simulations is shown in Figure 37. The midfoot bones include the navicular bone, three cuneiform bones, and the cuboid bone.

The MS simulation showed that the maximum von Mises stress of the midfoot bone occurred at push-off. The navicular bone peak von Mises stress was 28.622 MPa during the push-off phases. Moreover, the navicular bone peak von Mises stress was the highest in the four running phases. Figure 2 found that the max von Mises stress during the MS four stance phase was 8.522 MPa, 39.503 MPa, 28.622 MPa, and 14.03 MPa.

The NS simulation showed that the maximum von Mises stress of the midfoot bone occurred at the push-off phase. The navicular bone peak von Mises stress was 22.732 MPa during the push-off phases. MS and NS condition, mid-stance phases, and push-off von Mises stress are concentrated on the navicular bone and the three cuneiform bones. In the early stance phase, the Von Mises stress peak values of midfoot bones are similar.

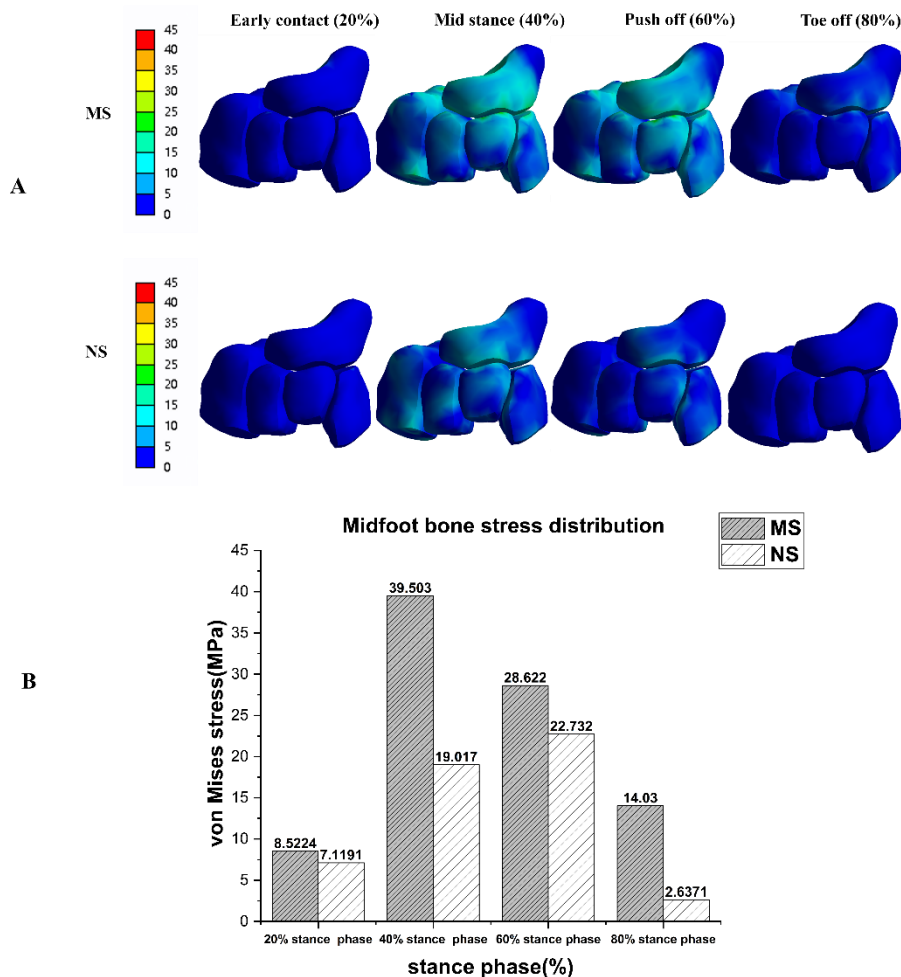


Figure 36 Mid-bone von mises stress distribution during the different running stances between the MS and NS conditions.

4 Discussion

4.1 Gait fatigue biomechanics variables

In this part, the main purpose was to describe and examine the kinematic and joint mechanical parameters of female recreational runners who sustained prolonged running until reaching the point of fatigue. The main findings of this part are the following: decreased ankle initial contact angle and range of motion of the ankle were found following fatigue running, which agrees with our hypothesis. At the hip joint, the extension angle was significantly decreased, but the motion of the hip increased in the fatigue-prolonged running condition. Furthermore, skeletal joint work was significantly reduced regarding the kinetics, including positive ankle work and total ankle work. However, fatigue running resulted in increased hip positive power. When comparing the knee parameters, negative knee power was higher following prolonged running compared to the initial status. However, there was no significant change in the joint angle, positive power, and joint work of knee parameters in this study.

In the section study, significant fatigue effects on lower limb kinematics and kinetics were found following prolonged running as highlighted in the lower limb kinematics: pre-running and post-fatigue running presented different joint angles, joint power, and joint work change trends. A recent study has compared joint work following prolonged running and found that joint work decreased in the distal lower limb joints[71]. After prolonged running, the ankle plantar flexor muscle activity was significantly reduced, which led to joint work redistribution in the ankle joint. Our results are consistent with this finding. With the distal ankle work decreased proximally, hip power significantly increased in the fatigue running condition. Several factors were identified as the underlying mechanisms that caused joint work redistribution following fatigue-induced prolonged running. First, the initial contact angle, max dorsiflexion angle, and range of ankle motion during the stance were significantly decreased in the prolonged fatigue condition compared with the pre-fatigue condition. The decrease in ankle dorsiflexion angle will reduce the moment arm of the ankle joint. A combination of smaller dorsiflexion initial contact and a smaller range of motion of the ankle resulted in smaller positive power, and therefore more minor positive joint work and total energy dissipation at the joint. Moreover, the running distance, sex, and the runner's ability level might affect joint work redistribution following prolonged fatigue running. During the stance of running, the energy distribution of the lower limbs follows the conservation of energy. After fatigue and prolonged running, a decrease in the work done by the distal ankle joint results in an increase in the work and power done by the hip joint. In this study finding, the hip ROM was significantly increased when runners in post-fatigue prolonged running. The study by

Winter et al. shows that the ROM of the hip joint increases significantly after fatigue, which also supports this result[166].

However, there was no change in knee joint work moment and angle in our study. After fatigue prolonged running, the knee flexion with no changes might be due to fatigue running not being associated with knee flexion. Accordingly, the knee was a vital joint during the running stance, absorbing shock and dissipating the ground reaction force[167]. In the current study, it has been found that knee negative power was increased in the fatigue-prolonged running condition. It has also been demonstrated that well-trained runners are examined, then the knee and hip joint positive work showed no changes following a fatiguing treadmill run[74].

In addition, it has been noted that following prolonged running, the muscle of the foot also undergoes modification[168], which inverts or dorsiflexes following fatigue. It has been found that prolonged fatigue running might lead to dorsiflexor fatigue, increasing the lower extremity attenuation capability to heel impacts[169]. Therefore, if the dorsiflexors are fatigued, the initial dorsiflexion contact angle and max dorsiflexion angle are smaller in the fatigue condition, which was consistent with our results. The decreased positive joint work and total joint work of the ankle may result from muscular fatigue. However, we did not collect any muscle change data prior to and after the prolonged running fatigue protocol. In the future, researchers should consider muscle fatigue and investigate the relationship between joint work redistribution.

It should be noted that while the PLSR method has been used to predict plantar pressure[170], foot posture, joint kinematics, joint moments, and joint contact forces in gait analysis[171], this is the first study that applies PLSR models to correlate initial angles with prolonged running fatigue joint work in amateur female runners.

Our model observed that the ankle angle at IC decreased in the fatigue-prolonged running, and the joint work showed a high linear correlation, which is consistent with the previous study. Furthermore, with the dorsiflexion decreased, the ankle work and total ankle work were also smaller than the pre-fatigue condition[71,74]. Moreover, after prolonged fatigue running, knee flexion may increase more than pre-running. The increased knee flexion angle will decrease the arm of the proximal joint, and the knee joint work will also be smaller than pre-running. This model can be used to analyze the angle changes after fatigued running, which can predict the redistribution and alteration of the work of the ankle and knee joints. Using this prediction model, it is possible to understand the change of work in lower limb joints following prolonged running.

There are also some limitations to this section. First, all subjects were amateur female runners. Therefore, I need to consider different levels of runners to compare the joint work before and after prolonged running in the future. A considerable variance existed in knee

outcome measures. Additional measurement trials may help to overcome this problem. In the future, more attention needs to be paid to muscle fatigue and running economy tests. We used a subjective measure (RPE) and heart rate to rate physical fatigue following treadmill running. While these measures are accurate and valid, we cannot be 100% certain that all participants were exhausted at the end of the running fatigue protocol.

4.2 Gait analysis of Minimalist and normal shoes

In this section, firstly, we used the simulation technology to compare the muscle activity and muscle force running in the MS and NS. In addition, we also compared the stress distribution during the running mid-stance phase. We found that when running in minimalist shoes, runners might adjust the running strike pattern from rearfoot strike to forefoot strike. The result of the present study supports our hypothesis that plantar flexor and Achilles tendon force might increase when running in minimalist shoes. Similarly, the changes in biomechanics parameters were associated with the heel-to-toe drop of footwear. Ultimate, There are also significant differences in the stress distribution of the calcaneus, talus, and midfoot.

A previous study showed that a decreased drop in running shoes would alter the running gait into a midfoot strike pattern [83]. Previous research also observed some main differences in kinematics parameters between minimalist and normal running shoes[172]. In general, according to the strike index calculation, all the participants in the present study participants used midfoot strike patterns when running in minimalist shoes during the running stance. Our results were also consistent with the findings of others [88,107]. The lower drops of running shoes would increase the ankle's initial dorsiflexion angle and decrease the contact time during the running stance. Thus, the reduced contact time and initial plantarflexion angle of the joint ankle might cause the strike pattern to midfoot strike pattern. In our study, the heel-to-toe drop of the minimalist shoes was negative 8mm, which caused the adjustment from the rearfoot strike pattern to the midfoot strike pattern.

Different drops of running shoes were the primary factors influencing the kinematics parameters during the running stance. The minimalist shoes demonstrated less ankle dorsiflexion, ankle eversion, knee flexion, hip flexion, hip internal rotation and hip external rotation angle than the normal shoes. One of the main elements for the kinematic changes of the knee and hip joints is the kinematic changes of the ankle joint during different striking patterns. In the present study, the ankle dorsiflexion angle decreased in minimalist shoes, which also caused the larger plantarflexion angle during the running stance. Due to the lower heel-to-toe drop, the larger ankle plantarflexion angle might decrease the shoe surface angle in the running stance. Compared with runners using the forefoot strike pattern, running using the rearfoot strike pattern condition has a small ankle range motion in the ankle sagittal plane and

more significantly greater hip and knee range motion in the sagittal plane[173]. With the decreased heel-to-toe drop, the runners indicated a lower plantar flexion angle and a larger knee range motion to absorb the energy for the toe-off phase [174]. In addition, in FFS running, negative work was greater in the ankle and less in the knee. The forefoot strike pattern decreased during the running stance. In FFS running, the stride length and the center of mass were significantly smaller than the RFS, reducing the work output of the quadriceps [175]. Moreover, the hip flexion and internal rotation angles were more different when running in minimalist shoes and normal shoes. The larger hip flexion and internal rotation angles were observed in the normal shoes during the running stance. A previous study has shown that a greater hip internal rotation angle might increase the iliotibial band friction syndrome [176]. These findings suggested that normal running shoes might increase the running injury rate.

There was a considerable joint moment difference between the minimalist running shoes and the normal running shoes. The ankle joint moment in minimalist shoes was the most noticeable difference in our study. In the minimalist shoes, ankle dorsiflexion, plantar flexion, and eversion moments were dramatically reduced. In the sagittal plane, a significantly larger initial plantarflexion angle was found in the forefoot strike pattern, which might increase the dorsiflexion moment [173]. Similarly, ankle dorsiflexion and rearfoot eversion angles were also observed to increase in the forefoot strike pattern during the running stance[98]. It has been shown that the forefoot strike pattern with shorter stride lengths, larger ankle ROM and knee ROM may increase knee injuries[177]. In addition, the minimalist shoes with the negative heel-to-toe drop need the participant's triceps to decrease the dorsiflexion angle during the running stance. Then, the Achilles tendon force and ankle plantarflexion moment were all increased[178]. Compared to normal shoes, the knee flexion moment was decreased in the minimalist shoes. Forefoot runners are subjected to less ground reaction and less range motion of lower limb than rearfoot runners, thus the moment in the sagittal plane of the knee joint is also reduction. Simultaneously, hip abduction and hip external rotation moment was significantly increased in minimalist shoes.

In this section, our findings showed that lateral gastrocnemius force was significantly greater in minimalist shoes. The lateral and medial gastrocnemius muscle forces have been reported to be greater during barefoot running than in shod running. When running barefoot, the gastrocnemius muscle force would be increased than running shod [179]. Another study also measured muscle activation and calculated the iEMG of the gastrocnemius, which found that the gastrocnemius medialis were significantly smaller when running in the shoes using rearfoot strike patterns [90]. In addition, Divert et al. found values of 24 % and 14 % greater in the medial and lateral gastrocnemius muscle pre-activation amplitude, respectively, while barefoot

compared to the RFS style shoed condition [180]. In our study, when participants run in minimalist shoes, the negative heel-to-toe drop of running shoes might cause the ankle plantar flexor muscles to enter into a pre-activation condition before touching the ground, which increased the lateral gastrocnemius muscle force [91]. As soleus muscle force and Achilles tendon force were increased with the lower heel-to-toe drop of running shoe in the current study. Kulmala et al. report that data has shown that mid/forefoot runners exhibited larger Achilles tendon force (ATF) and reduced knee loading than rearfoot runners [178]. The result of the current study consisted of the previous research. That can explain this due to the negative heel-to-toe drop of running shoes, and participants might use the midfoot strike pattern to contact the ground. The gastrocnemius and soleus muscles would be in pre-activation during the running stance in order to decrease the impact force, and the soleus force may be greater during the running stance in minimalist shoes. According to a recent study, barefoot and barefoot-inspired running shoes were related to increased Achilles tendon force compared to conventional shoes [111]. As such, the finds suggested that the negative heel-to-toe drop of running shoes may not be adapted for runners who suffer Achilles tendon injuries.

In addition, the flexor hallucis longus muscle and extensor digitorum longus muscle should be taking into consideration the increased ankle plantarflexion angle and moment, normally resulted from minimalist shoes. The results of our study demonstrated the large flexor hallucis longus muscle force and less extensor digitorum longus muscle force when running in minimalist shoes. During the initial contact ground phase of the forefoot strike pattern, the arch is subjected to a three-point force load, and to better control the deformation of the arch and the elastic potential energy, the muscle group of the foot will be more strength [123,150,181,182]. Therefore, whilst the increase in flexor hallucis longus muscle was adapted deformation of the arch of the foot and the play of elastic potential energy. Thus, minimalist shoes can also enhance the function of the foot.

This section only compared the difference in muscle force between minimalist and normal shoes for recreational runners, which is a limitation. Future research should consider analyzing the different running levels of runners, such as experienced and novice runners. Additionally, although the small sample size in this study was statistically powered correctly, it is still a limitation and should be increased in future studies. Another vital factor to consider in future studies is the foot strike pattern, which influences running musculoskeletal injuries. Therefore, future studies should include habitual forefoot or midfoot strike pattern runners. Lastly, investigating female runners would provide valuable insights for future research.

4.3 Finite element model simulation

The popularity of the running strike pattern has increased globally, with more runners opting for minimalist running shoes over traditional shoes. However, this technique may lead to higher internal foot injuries. Previous studies have primarily focused on kinematics and kinetic variable changes, with limited attention given to the foot's internal biomechanics. Therefore, this section aimed to develop a 3D-foot shoe finite element (FE) model to analyze the internal foot biomechanics during the four running stance phases using different running heel-drop shoes. A subject-specific musculoskeletal multibody driven-foot model was developed to analyze internal foot biomechanics. The study found that the maximum von Mises stress in the metatarsal was significantly higher in minimalist shoes compared to normal shoes. This difference was most pronounced during the push-off phase, where a 12% increase in von Mises stress was observed. Regarding stress distribution, the midfoot bone experienced a 74% higher von Mises stress during the mid-stance phase when minimalist shoes were compared to normal shoes.

The foot finite model validation used the comparison of FE-simulation GRF and experiment measurements during running with RFS and FFS[154]. As for the model validation results in this section, there are high correlations between the simulated GRF and experimental for the MS condition($R=0.9767$) and NS conditions (0.9821), indicating that the MS and NS measured model's GRF agreed well with the FE simulation results. The results demonstrate that the developed FE model provides an accurate approach to analyzing foot stress distributions in the model of the foot and minimalist running shoes under running stance phase conditions, facilitating biomechanical investigations.

The metatarsophalangeal joint plays a crucial role in activities like walking, running, and jumping, serving as the terminal joint where movement occurs. To achieve full extension, the plantar flexor muscles of the ankle joint work together with the toe flexor muscles. This coordinated action of the ankle plantar flexor muscles and the toe flexor muscles, while maintaining distal fixation, allows for the completion of the stretching movement[183]. Previous studies have reported a correlation between running and metatarsal stress fractures in individuals with multiple sclerosis (MS)[184,185]. However, it is essential to note that there is currently no evidence linking an increased incidence of metatarsal stress fractures specifically to MS. A recent study comparing foot plantar pressure during running in individuals with MS and NS found that forefoot plantar pressure was significantly higher in the MS group than in the NS group[186]. This suggests that MS may contribute to increased plantar pressure in the metatarsal region, potentially increasing the risk of stress fractures. I examined the effects of heel drop on metatarsal strains during four different phases of running stances: (1) initial

contact, (2) midstance phase, (3) push-off, and (4) toe-off. The results indicated that running with the MS led to a higher von Mises stress in the metatarsal.

Furthermore, the push-off phase exhibited the highest metatarsal von Mises stress when running in MS. During this phase, the foot plays an active role in propelling the body forward, requiring significant force to be transmitted through the metatarsals, which act as pivotal fulcrums. The elevated stress levels suggest a greater vulnerability to injuries like metatarsal stress fractures, especially when subjected to repetitive stress without sufficient recovery periods—understanding the metatarsals of von Mises stress can improve running performance and decrease running injuries. Moreover, the mid-stance phase also showed greater metatarsal von Mises stress in MS. During the running mid-stance, the foot mainly absorbs the energy. The larger metatarsal von Mises stress may increase the foot loading in the mid-stance phase. Moreover, the highest von Mises stress was found in the 4th metatarsal when running in minimalist shoes. This result corresponds with the other authors' findings, who pointed out that lower-drop shoes might elevate the risk of metatarsal stress fracture.

The present FE results showed significantly larger midfoot von Mises stress in the mid-stance phase and push-off in MS. The midfoot bone plays a crucial role in distributing the load from the tibia, fibula, and heel bone to the five metatarsal rows and the forefoot. Specifically, the navicular bone and cuneiform bone in the middle of the foot are significant in transmitting mechanical forces. The simulation results indicated that the maximum von Mises stress on the navicular, medial cuneiform, intermediate cuneiform, lateral cuneiform, and cuboid bones was significantly higher when running in MS than in NS. The navicular bone, located in the midfoot, is particularly susceptible to mechanical risks, and an increase in stress on this bone can also raise the likelihood of stress fractures. Since the three cuneiform bones in the midfoot are connected to the navicular bone, an increase in stress on any one of the bones connected to the navicular can cause compression between the navicular and the other cuneiform bones due to the lever principle, resulting in stress concentration and amplification. Therefore, this section's results showed that the midfoot von Mises stress in the mid-stance and push-off may increase the stress fracture risk of the navicular bone.

5 Conclusions and future work

5.1 Conclusions

The first section of the thesis shows an investigation of the changes in joint mechanics, joint kinematics, joint moments, and joint power in the lower extremity following a fatiguing treadmill run in fifty female recreational runners. A relationship between knee and ankle initial angles and joint work was developed. It was found that moderate reductions in absolute positive ankle power, total ankle energy dissipation, dorsiflexion at initial contact, max dorsiflexion angle, and range of motion of the joint ankle were observed after fatigue following prolonged running. Knee joint mechanics, joint angle, and joint power were unchanged following prolonged running. However, with decreased ankle joint work, negative knee power, increased hip positive work, and hip positive power, initial foot contact following running increased due to fatigue. These results suggest no proximal shift in knee joint mechanics in female recreational runners following a prolonged run. The joint work redistribution was associated with running fatigue changes. To improve running performance, long-distance runners should include ankle muscle strength training to avoid running-related injuries.

Shoes with varying heel-to-toe drops might affect biomechanical variables during the running stance. In addition, negative heel-to-toe drop running shoes increase the lateral gastrocnemius, Achilles tendon, and extensor hallucis longus muscles. This may increase the potential for Achilles tendonitis and ankle flexor injuries. Furthermore, running with a low heel-to-toe drop transitions from a rearfoot strike pattern to a midfoot strike pattern. According to this finding, we suggest that athletes without Achilles tendon injuries and strong calf muscles can choose minimalist footwear for running. However, pay attention to strengthening exercises to strengthen the foot muscles. In Ultimate, we also investigated the foot strain and stress in MS and NS during the running mid-stance phase. The main finding of this section has shown increased calcaneus, talus, and midfoot stress during the running mid-stance phase. These results may suggest that runners who choose MS shoes enhance their foot strength. Although the MS shoes may decrease the GRF during the run, the larger stress on the foot could increase the RRI.

Finally, I developed a subject-specific musculoskeletal multibody driven-foot model to investigate the effect of heel drop on internal foot biomechanics. Thus, through creative the 3D-foot shoe FE model to analyze the internal foot biomechanical during four running stance phases. As for the model validation results in this section, there are high correlations between the simulated GRF and experimental for the MS condition($R=0.9767$) and NS conditions (0.9821), indicating that the MS and NS measured model's GRF agreed well with the FE

simulation results. According to the numerical results, the minimalist shoes showed larger von Mises stresses in the metatarsal segment during the four running stance phases compared to normal shoes. This difference was the most significant in the push-off phase, where 12% higher von Mises stress was found compared to normal shoes. Moreover, the highest von Mises stress was found in the 4th metatarsal when running in minimalist shoes. It mentioned that running with the MS may increase the metatarsal stress fracture. It also found that 74% higher von Mises stress was found in the midfoot when running in minimalist shoes compared to normal shoes during the mid-stance phase. This suggests that the design of minimalist shoes should consider midfoot support and cushioning to reduce the pressure distribution during running.

5.2 Recommendations for future works

The first part of this study examines the influence of running fatigue on the redistribution of lower limb work in amateur female runners. The study employs the PLSR machine learning method to analyze the IC angle in conjunction with joint work. Subsequent research can build upon the findings of this study. By utilizing an ultrasonic instrument to assess the impact on deep muscles before and after fatigue, a deeper understanding of the relationship between fatigue mechanics and injury can be obtained. Additionally, future studies should aim to collect a large sample size to explore and predict the effects of different landing methods on the biomechanics of lower limb joints using deep machine learning. Moreover, in order to provide a theoretical reference for runners and shoe design with different landing methods, it is recommended to combine dynamic finite element analysis with finite element analysis of stress distribution within the foot. This will allow for an exploration and analysis of stress changes in the knee joint and foot, as well as the forces exerted on ligaments during dynamic running.

Thesis points

1st Thesis point:

Based on my experiments, I could prove that a linear relationship can be found between the angle of the ankle at the initial contact and the joint work. This result demonstrates that the ankle angle at the initial contact decreases when fatigue arises due to prolonged running.

More importantly, I could deduce that an approximately 30% decrease in the angle of the ankle at the initial contact caused approximately 20% and 25% decrease in the positive work of the ankle and a 30% increase in the positive work of the hip joint when fatigue arose in case of female runners.

Since I detected no significant changes in the knee joint power, this result suggests that no proximal shift appears in knee joint mechanics in the case of female recreational runners following a prolonged run.

In conclusion, this experimental result proves that joint work redistribution takes place when fatigue arises due to prolonged running, slowly shifting more power to the hip joint to maintain equilibrium during running.

Related article to the 1st thesis point:

¹ **Wenjing Quan**, Ren Feng, Datao Xu, Gusztav, Julien S. BAKER, Yaodong Gu. (2021). Effects of Fatigue Running on Joint Mechanics in Female Runners: A Prediction Study Based on a Partial Least Squares Algorithm. *Frontiers in Bioengineering and Biotechnology*, 880. **Q1, IF = 5.890**

2nd Thesis point:

Based on my experiments on minimalist running shoes, I concluded that a decrease from 8 mm to -8 mm in the heel-to-toe drop resulted in a 12% increase in the soleus force, a 7% increase in Achilles tendon force and an 8% increase in the flexor hallucis longus force.

The obvious increment in these forces implies that the decrease in heel-to-toe drop potentially increases the risk of Achilles tendonitis and ankle flexor injuries in the case of running shoes.

In addition, since the strike index is significantly greater in the case of these minimalist shoes, I could prove that these shoes can change the foot strike pattern during running gait.

Furthermore, I also concluded that these minimalist running shoes decrease the knee flexion moment by 6% compared to normal shoes. Therefore, the knee joint loading is lower, resulting in less injury probability.

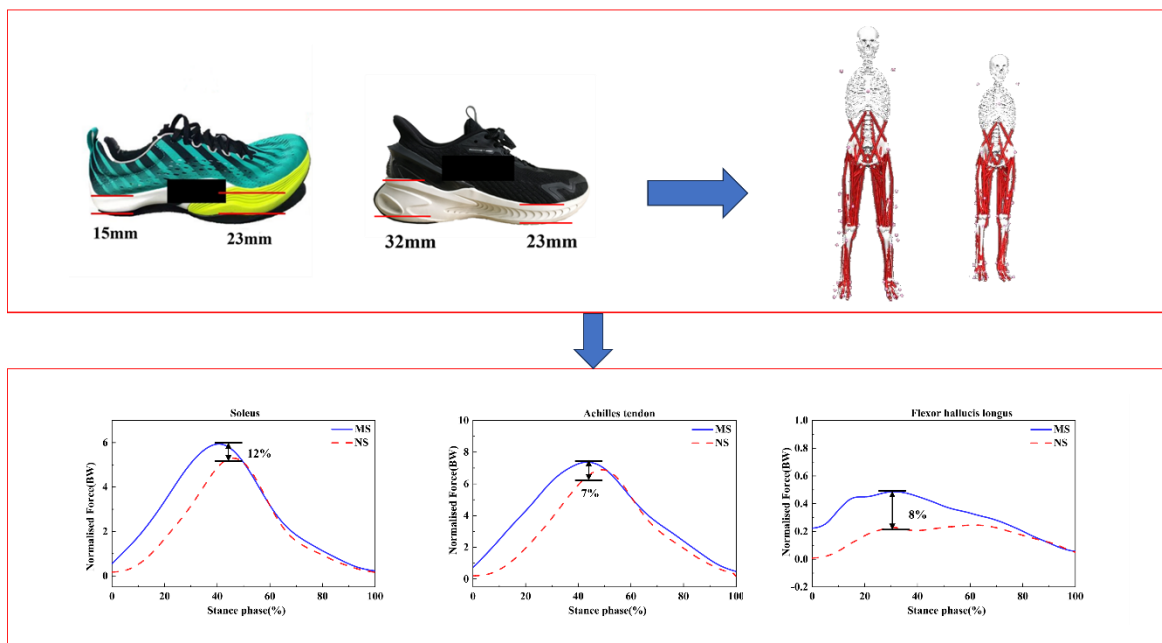


Figure 37 Muscle force changed between the MS and NS running.

Related article to the 2nd thesis point:

¹ Wenjing Quan, Linna Gao, Datao Xu, Huiyu Zhou, Tamás Korim, Shirui Shao, Julien S Baker, Yaodong Gu. 2023. Simulation of Lower Limb Muscle Activation Using Running Shoes with Different Heel-to-Toe Drops Using Opensim. Healthcare, 11(9), 1243, Q2, IF = 3.160

3rd Thesis point:

I created a finite element model with different heel-drop shoes (normal and minimalist shoes) to study stress distribution during the four different running stance phases.

According to the numerical results, the minimalist shoes showed larger von Mises stresses in the metatarsal segment during the four running stance phases compared to normal shoes. This difference was the most significant in the push-off phase, where 12% higher von Mises stress was found compared to normal shoes.

Moreover, the highest von Mises stress was found in the 4th metatarsal when running in minimalist shoes. This result corresponds with the other authors' findings, who pointed out that lower-drop shoes might elevate the risk of metatarsal stress fracture.

Concerning stress distribution, 74% higher von Mises stress was found in the midfoot when running in minimalist shoes compared to normal shoes during the mid-stance phase. This suggests that the design of minimalist shoes should consider midfoot support and cushioning to reduce the pressure distribution during running.

Therefore, I could generally conclude that shoes with lower drop increase stress levels in the metatarsal and midfoot, particularly during the push-off phase.

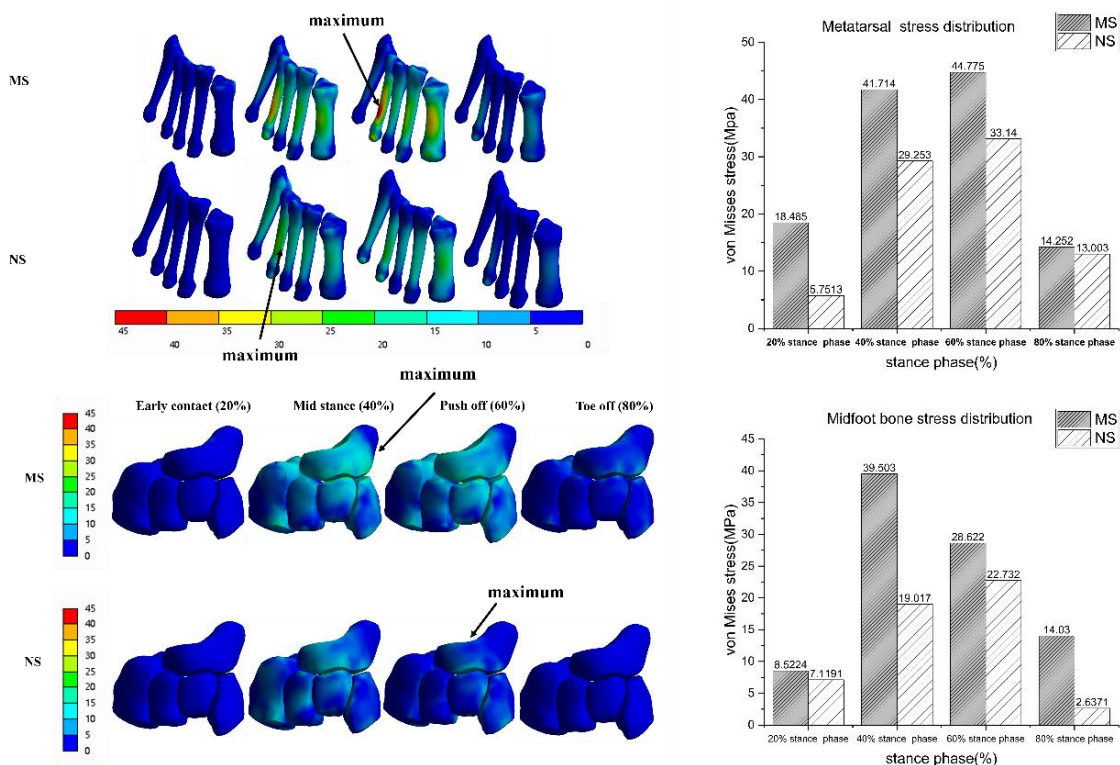


Figure 38 3D-footwear Finite Element model analysis.

Related articles to the 3rd thesis point:

¹ **Wenjing Quan**, Huiyu Zhou, Datao Xu, Shudong Li, Julien S. BAKER, Yaodong Gu. (2021, October). Competitive and Recreational Running Kinematics Examined Using Principal Components Analysis. In Healthcare (Vol. 9, No. 10, p. 1321). **Q2, IF = 2.645**

² **Wenjing Quan**, Feng Ren, Dong Sun, Gusztáv Fekete, Yuhuan He. (2021). Do Novice Runners Show Greater Changes in Biomechanical Parameters? Applied Bionics and Biomechanics, 2021. **Q3, IF = 1.781**

³ Huiyu Zhou, Datao Xu, **Wenjing Quan**, Ukadike Chris Ugbohue, Zhanyi Zhou, Yaodong Gu. Journal: Journal of Human Kinetics. 2023(accept). Can the entire function of the foot be concentrated in the forefoot area during the running stance phase? A finite element study of different shoe soles. **Q1, IF = 2.3**

List of publications

Referred articles related to this thesis:

1. **Wenjing Quan**, Ren Feng, Datao Xu, Gusztav, Julien S. BAKER, Yaodong Gu. (2021). Effects of Fatigue Running on Joint Mechanics in Female Runners: A Prediction Study Based on a Partial Least Squares Algorithm. *Frontiers in Bioengineering and Biotechnology*, 880. **Q1 IF=5.890**
2. **Wenjing Quan**, Linna Gao, Datao Xu, Huiyu Zhou, Tamás Korim, Shirui Shao, Julien S Baker, Yaodong Gu. 2023. Simulation of Lower Limb Muscle Activation Using Running Shoes with Different Heel-to-Toe Drops Using Opensim. *Healthcare* **Q2 IF=3.160**
3. **Wenjing Quan**, Huiyu Zhou, Datao Xu, Shudong Li, Julien S. BAKER, Yaodong Gu. (2021, October). Competitive and Recreational Running Kinematics Examined Using Principal Components Analysis. In *Healthcare* (Vol. 9, No. 10, p. 1321). **Q2 IF=2.645**
4. **Wenjing Quan**, Feng Ren, Dong Sun, Gusztáv Fekete, Yuhuan He. (2021). Do Novice Runners Show Greater Changes in Biomechanical Parameters? *Applied Bionics and Biomechanics*, 2021. **Q3 IF=1.781**
5. Huiyu Zhou, Datao Xu, **Wenjing Quan**, Ukadike Chris Ugbohue, Zhanyi Zhou, Yaodong Gu. *Journal: Journal of Human Kinetics*. 2023(accept). Can the entire function of the foot be concentrated in the forefoot area during the running stance phase? A finite element study of different shoe soles. **Q1 IF=2.3**

International conference abstracts related to this thesis:

1. **Wenjing Quan**, Datao Xu, Xinyan Jiang, Yanan Huang. 2021. Lower limb biomechanical analysis of heel shock absorption and stability in running shoes with different midsole stiffness. The 21st National Sports Biomechanics Academic Exchange Conference. At: Taiyuan, China.
2. **Wenjing Quan**, Datao Xu, Yaodong Gu, Gusztáv Fekete. 2021. Effects of a Triple Density Midsole with Lateral Windows on Lower Limb Kinematics and Kinetics of runners in Comparison to a Conventional Running. The 8th Asian Sport Biomechanics Conference. At: Taiwan, China.
3. **Wenjing Quan**, Huiyu Zhou, Yaodong Gu, Gusztáv Fekete. 2021. Running shoe effects on knee and ankle loading during running in Male Recreational Runner. The 8th Asian Sport Biomechanics Conference. At: Taiwan, China

Other publications:

1. **Wenjing Quan**, Meizi Wang, Gongju Liu, Gusztáv Fekete, Julien S. BAKER, Feng Ren, Yaodong Gu. (2020). Comparative Analysis of Lower Limb Kinematics between the Initial and Terminal Phase of 5km Treadmill Running. *JoVE (Journal of Visualized Experiments)*, (161), e61192. **Q2 IF=1.26**
2. Meizi Wang, Julien S. BAKER. Siqin Shen, **Wenjing Quan**, Gusztáv Fekete, Yaodong Gu. (2020). A preventive role of exercise across the coronavirus 2 (SARS-CoV-2) pandemic. *Frontiers in Physiology*, 1139. **Q2 IF=4.566**
3. Huiyu Zhou, Datao Xu, **Wenjing Quan**, Minjun Liang, Ukadike Chris Ugbole, Julien S. BAKER, Yaodong Gu. (2021, October). A Pilot Study of Muscle Force between Normal Shoes and Bionic Shoes during Men Walking and Running Stance Phase Using Opensim. In *Actuators* (Vol. 10, No. 10, p. 274). **Q2 IF=1.994**
4. Xinyan Jiang, Huiyu Zhou, **Wenjing Quan**, Qiuli Hu, Julien S. BAKER, Yaodong Gu. (2021). Ground Reaction Force Differences between Bionic Shoes and Neutral Running Shoes in Recreational Male Runners before and after a 5 km Run. *International Journal of Environmental Research and Public Health*, 18(18), 9787. **Q2 IF=3.390**
5. Datao Xu, **Wenjing Quan**, Huiyu Zhou, Dong Sun, Julien S. BAKER, Yaodong Gu. (2022). Explaining the differences of gait patterns between high and low-mileage runners with machine learning. *Scientific Reports*, 12(1), 1-12. **Q1 IF=4.379**
6. **Wenjing Quan**, Qichang Mei, Yaodong Gu, Feng Ren, Sterzing, T., & Fernandez, J. (2018). Biomechanical Variations in Female Runner's Pre and Post Treadmill Running. In *Journal of Biomimetics, Biomaterials and Biomedical Engineering* (Vol. 37, pp. 1-11). **Q4 IF=0.64**
7. Jingying Lu, Datao Xu, **Wenjing Quan**, Julien S. Baker, Yaodong Gu. (2022) Effects of Forefoot Shoe on Knee and Ankle Loading during Running in Male Recreational Runners (Vol. 19, No.2). **Q4 IF=0.338**
8. Huiyu Zhou , Datao Xu , **Wenjing Quan** , Ukadike Chris Ugbole , Nicholas F. Sculthorpe , Julien S. Baker , Yaodong Gu.(2022) A foot joint and muscle force assessment of the running stance phase whilst wearing normal shoes and bionic shoes. *Acta of Bioengineering and Biomechanics*. **Q3 IF=1.265**
9. Dong Sun, Yang Song, **Wenjing Quan**, Jianshe Li, Yaodong Gu, 2022.The effect of running shoes bending stiffness alteration on lower extremity biomechanical performance and running economy. *China Sport Science and Technology*.
10. Jinpeng Zhang, **Wenjing Quan**, Yuhuan He. 2022 The effect of running surface on the lower limb biomechanical. *Zhejiang Sport Science*.

11. Datao Xu, **Wenjing Quan**, Huiyu Zhou, Dong Sun, Julien S. BAKER, Yaodong Gu. 2022. Exploring the gait pattern of "high-low" mileage runners based on deep neural network and layer-by-layer correlation propagation technology difference. Journal of Medical Biomechanics. Vol.37, No.5.
12. Datao Xu, Huiyu Zhou, **Wenjing Quan**, Fekete Gusztav, Meizi Wang, Julien S Baker, Yaodong Gu.2023. Accurately and effectively predict the ACL force: Utilizing biomechanical
13. landing pattern before and after-fatigue. Computer Methods and Programs in Biomedicine. **Q1 IF=6.1**
14. Huiyu Zhou, Datao Xu, **Wenjing Quan**, Ukadike Chris Ugbole, Zhanyi Zhou, Yaodong Gu. Journal: Journal of Human Kinetics. 2023(accept). Can the entire function of the foot be concentrated in the forefoot area during the running stance phase? A finite element study of different shoe soles.**Q1 IF=2.3**
15. Datao Xu, Huiyu Zhou, **Wenjing Quan**, Fekete Gusztav, Julien S Baker, Yaodong Gu. 2023. Adaptive Neuro-Fuzzy Inference System model driven by the Non-Negative Matrix Factorization-extracted muscle synergy patterns to estimate lower limb joint movements. Computer Methods and Programs in Biomedicine. **Q1 IF=6.1**
16. Datao Xu, Huiyu Zhou, **Wenjing Quan**, Xinyan Jianga, Minjun Liang, Shudong Li, Ukadike Chris Ugbole, Julien S. Baker, Fekete Gusztav, Xin Mag, Li Chen, Yaodong Gu. 2023. A new method proposed for realizing human gait pattern recognition: Inspirations for the application of sports and clinical gait analysis. Gait poster.**Q1 IF=2.4**

Reviewer for international journal articles:

1. BMC Musculoskeletal Disorders
2. Physical Activity and Health
- 3.PLOS One

ORCID: <http://orcid.org/0000-0002-3881-518X>

Total independent citations (Scopus): 58

<https://www.scopus.com/authid/detail.uri?authorId=57202351906>

Independent Hirsch index: 3

Total Impact Factor (Web of Science): 50.508

References

1. Hespanhol Junior, L.C.; Pillay, J.D.; van Mechelen, W.; Verhagen, E. Meta-analyses of the effects of habitual running on indices of health in physically inactive adults. *Sports medicine* **2015**, *45*, 1455-1468.
2. Murr, S.; Pierce, B. How aging impacts runners' goals of lifelong running. *Physical Activity and Health* **2019**, *3*.
3. Huang, Z.; Rusanova, O.M. Cardiorespiratory system in the context of regular exercise in kayaking. *Physical Activity and Health* **2022**, *6*.
4. Costa, R.J.; Knechtle, B.; Tarnopolsky, M.; Hoffman, M.D. Nutrition for ultramarathon running: trail, track, and road. *International journal of sport nutrition and exercise metabolism* **2019**, *29*, 130-140.
5. Kapri, E.; Mehta, M.; Singh, K. Biomechanics of running: An overview on gait cycle. *International Journal of Physical Education, Fitness and Sports* **2021**, *10*.
6. Bridgman, C.F. *Biomechanical evaluation of distance running during training and competition*; University of Salford (United Kingdom): 2015.
7. Dugan, S.A.; Bhat, K.P. Biomechanics and analysis of running gait. *Physical Medicine and Rehabilitation Clinics* **2005**, *16*, 603-621.
8. Novacheck, T.F. The biomechanics of running. *Gait & posture* **1998**, *7*, 77-95.
9. Slijepcevic, D.; Horst, F.; Lapuschkin, S.; Horsak, B.; Raberger, A.-M.; Kranzl, A.; Samek, W.; Breiteneder, C.; Schöllhorn, W.I.; Zeppelzauer, M. Explaining machine learning models for clinical gait analysis. *ACM Transactions on Computing for Healthcare (HEALTH)* **2021**, *3*, 1-27.
10. Hasegawa, H.; Yamauchi, T.; Kraemer, W.J. Foot strike patterns of runners at the 15-km point during an elite-level half marathon. *The Journal of Strength & Conditioning Research* **2007**, *21*, 888-893.
11. Butler, R.J.; Davis, I.S.; Hamill, J. Interaction of arch type and footwear on running mechanics. *The American journal of sports medicine* **2006**, *34*, 1998-2005.
12. Dixon, S. Use of pressure insoles to compare in-shoe loading for modern running shoes. *Ergonomics* **2008**, *51*, 1503-1514.
13. Paolini, G.; Della Croce, U.; Riley, P.O.; Newton, F.K.; Kerrigan, D.C. Testing of a tri-instrumented-treadmill unit for kinetic analysis of locomotion tasks in static and dynamic loading conditions. *Medical engineering & physics* **2007**, *29*, 404-411.
14. Ndermann, A.; Nigg, B.M.; Humble, R.N.; Stefanyshyn, D.J. Orthotic comfort is related to kinematics, kinetics, and EMG in recreational runners. *Med Sci Sports Exerc* **2003**, *195*, 3510-1710.

15. Milner, C.E.; Ferber, R.; Pollard, C.D.; Hamill, J.; Davis, I.S. Biomechanical factors associated with tibial stress fracture in female runners. *Medicine & Science in Sports & Exercise* **2006**, *38*, 323-328.
16. Stafilidis, S.; Arampatzis, A. Track compliance does not affect sprinting performance. *Journal of sports sciences* **2007**, *25*, 1479-1490.
17. Derrick, T.R.; Dereu, D.; McLean, S.P. Impacts and kinematic adjustments during an exhaustive run. *Medicine & Science in Sports & Exercise* **2002**, *34*, 998-1002.
18. Karamanidis, K.; Arampatzis, A.; Brüggemann, G.-P. Reproducibility of electromyography and ground reaction force during various running techniques. *Gait & posture* **2004**, *19*, 115-123.
19. Van Gent, R.; Siem, D.; van Middelkoop, M.; Van Os, A.; Bierma-Zeinstra, S.; Koes, B. Incidence and determinants of lower extremity running injuries in long distance runners: a systematic review. *British journal of sports medicine* **2007**, *41*, 469-480.
20. Videbæk, S.; Bueno, A.M.; Nielsen, R.O.; Rasmussen, S. Incidence of running-related injuries per 1000 h of running in different types of runners: a systematic review and meta-analysis. *Sports medicine* **2015**, *45*, 1017-1026.
21. Tonoli, C.; Cumps, E.; Aerts, I.; Verhagen, E.; Meeusen, R. Running related injuries in long-distance running: Incidence, risk factors and prevention. *Sport en Geneeskunde* **2010**, *43*, 12.
22. Fields, K.B.; Sykes, J.C.; Walker, K.M.; Jackson, J.C. Prevention of running injuries. *Current sports medicine reports* **2010**, *9*, 176-182.
23. Lopes, A.D.; Hespanhol, L.C.; Yeung, S.S.; Costa, L.O.P. What are the main running-related musculoskeletal injuries? A systematic review. *Sports medicine* **2012**, *42*, 891-905.
24. Hespanhol Junior, L.C.; Costa, L.O.; Carvalho, A.C.; Lopes, A.D. A description of training characteristics and its association with previous musculoskeletal injuries in recreational runners: a cross-sectional study. *Brazilian Journal of Physical Therapy* **2012**, *16*, 46-53.
25. Franke, T.P.; Backx, F.J.; Huisstede, B.M. Running themselves into the ground? Incidence, prevalence, and impact of injury and illness in runners preparing for a half or full marathon. *Journal of orthopaedic & sports physical therapy* **2019**, *49*, 518-528.
26. Raghunandan, A.; Charnoff, J.N.; Matsuwaka, S.T. The epidemiology, risk factors, and nonsurgical treatment of injuries related to endurance running. *Current sports medicine reports* **2021**, *20*, 306-311.

27. Callahan, L.R.; Sheon, R. Overview of running injuries of the lower extremity. *UpToDate* **2014**, *10*, 1-34.
28. Ferber, R.; Davis, I.M.; Williams Iii, D.S. Gender differences in lower extremity mechanics during running. *Clinical biomechanics* **2003**, *18*, 350-357.
29. Sinclair, J.; Selfe, J. Sex differences in knee loading in recreational runners. *Journal of biomechanics* **2015**, *48*, 2171-2175.
30. Faulkner, J.A.; Larkin, L.M.; Claflin, D.R.; Brooks, S.V. Age-related changes in the structure and function of skeletal muscles. *Clinical and Experimental Pharmacology and Physiology* **2007**, *34*, 1091-1096.
31. Nonaka, H.; Mita, K.; Watakabe, M.; Akataki, K.; Suzuki, N.; Okuwa, T.; Yabe, K. Age-related changes in the interactive mobility of the hip and knee joints: a geometrical analysis. *Gait & posture* **2002**, *15*, 236-243.
32. DeVita, P.; Fellin, R.E.; Seay, J.F.; Ip, E.; Stavro, N.; Messier, S.P. The relationships between age and running biomechanics. *Medicine and science in sports and exercise* **2016**, *48*, 98-106.
33. Koplman, J.P.; Powell, K.E.; Sikes, R.K.; Shirley, R.W.; Campbell, C. An epidemiologic study of the benefits and risks of running. *Jama* **1982**, *248*, 3118-3121.
34. Macera, C.A.; Pate, R.R.; Powell, K.E.; Jackson, K.L.; Kendrick, J.S.; Craven, T.E. Predicting lower-extremity injuries among habitual runners. *Archives of internal medicine* **1989**, *149*, 2565-2568.
35. Taunton, J.E.; Ryan, M.B.; Clement, D.; McKenzie, D.C.; Lloyd-Smith, D.; Zumbo, B. A retrospective case-control analysis of 2002 running injuries. *British journal of sports medicine* **2002**, *36*, 95-101.
36. Marti, B.; Vader, J.P.; Minder, C.E.; Abelin, T. On the epidemiology of running injuries: the 1984 Bern Grand-Prix study. *The American Journal of Sports Medicine* **1988**, *16*, 285-294.
37. Nielsen, R.O.; Buist, I.; Parner, E.T.; Nohr, E.A.; Sørensen, H.; Lind, M.; Rasmussen, S. Predictors of running-related injuries among 930 novice runners: a 1-year prospective follow-up study. *Orthopaedic journal of sports medicine* **2013**, *1*, 2325967113487316.
38. Nielsen, R.O.; Buist, I.; Sørensen, H.; Lind, M.; Rasmussen, S. Training errors and running related injuries: a systematic review. *International journal of sports physical therapy* **2012**, *7*, 58.

39. Winter, S.C.; Gordon, S.; Brice, S.M.; Lindsay, D.; Barrs, S. A multifactorial approach to overuse running injuries: a 1-year prospective study. *Sports Health* **2020**, *12*, 296-303.
40. Sun, X.; Lam, W.-K.; Zhang, X.; Wang, J.; Fu, W. Systematic review of the role of footwear constructions in running biomechanics: Implications for running-related injury and performance. *Journal of sports science & medicine* **2020**, *19*, 20.
41. Messier, S.P.; Legault, C.; Schoenlank, C.R.; Newman, J.J.; Martin, D.F.; DeVita, P. Risk factors and mechanisms of knee injury in runners. *Medicine & Science in Sports & Exercise* **2008**, *40*, 1873-1879.
42. Luedke, L.E.; Heiderscheit, B.C.; Williams, D.B.; Rauh, M.J. Association of isometric strength of hip and knee muscles with injury risk in high school cross country runners. *International Journal of Sports Physical Therapy* **2015**, *10*, 868.
43. Daoud, A.I.; Geissler, G.J.; Wang, F.; Saretsky, J.; Daoud, Y.A.; Lieberman, D.E. Foot strike and injury rates in endurance runners: a retrospective study. *Med Sci Sports Exerc* **2012**, *44*, 1325-1334.
44. Xu, Y.; Yuan, P.; Wang, R.; Wang, D.; Liu, J.; Zhou, H. Effects of foot strike techniques on running biomechanics: a systematic review and meta-analysis. *Sports Health* **2021**, *13*, 71-77.
45. Sinclair, J.; Taylor, P.; Vincent, H. The influence of barefoot and shod running on plantar fascia strain during the stance phase of running. *The Foot and Ankle Online Journal* **2015**, *8*, 4.
46. Lieberman, D.E.; Venkadesan, M.; Werbel, W.A.; Daoud, A.I.; D'andrea, S.; Davis, I.S.; Mang'Eni, R.O.; Pitsiladis, Y. Foot strike patterns and collision forces in habitually barefoot versus shod runners. *Nature* **2010**, *463*, 531-535.
47. Ceysens, L.; Vanelderen, R.; Barton, C.; Malliaras, P.; Dingenen, B. Biomechanical risk factors associated with running-related injuries: a systematic review. *Sports medicine* **2019**, *49*, 1095-1115.
48. Dudley, R.I.; Pamukoff, D.N.; Lynn, S.K.; Kersey, R.D.; Noffal, G.J. A prospective comparison of lower extremity kinematics and kinetics between injured and non-injured collegiate cross country runners. *Human Movement Science* **2017**, *52*, 197-202.
49. Noehren, B.; Hamill, J.; Davis, I. Prospective evidence for a hip etiology in patellofemoral pain. *Medicine and science in sports and exercise* **2013**, *45*, 1120-1124.
50. Noehren, B.; Davis, I.; Hamill, J. ASB Clinical Biomechanics Award Winner 2006: Prospective study of the biomechanical factors associated with iliotibial band syndrome. *Clinical biomechanics* **2007**, *22*, 951-956.

51. Hein, T.; Janssen, P.; Wagner-Fritz, U.; Haupt, G.; Grau, S. Prospective analysis of intrinsic and extrinsic risk factors on the development of Achilles tendon pain in runners. *Scandinavian Journal of Medicine & Science in Sports* **2014**, *24*, e201-e212.
52. Messier, S.P.; Martin, D.F.; Mihalko, S.L.; Ip, E.; DeVita, P.; Cannon, D.W.; Love, M.; Beringer, D.; Saldana, S.; Fellin, R.E. A 2-year prospective cohort study of overuse running injuries: the runners and injury longitudinal study (TRAILS). *The American journal of sports medicine* **2018**, *46*, 2211-2221.
53. Vieira, M.F.; e Souza, G.S.d.S.; Lehen, G.C.; Rodrigues, F.B.; Andrade, A.O. Effects of general fatigue induced by incremental maximal exercise test on gait stability and variability of healthy young subjects. *Journal of electromyography and kinesiology* **2016**, *30*, 161-167.
54. Stutzig, N.; Siebert, T. Muscle force compensation among synergistic muscles after fatigue of a single muscle. *Human movement science* **2015**, *42*, 273-287.
55. Kellis, E.; Zafeiridis, A.; Amiridis, I.G. Muscle coactivation before and after the impact phase of running following isokinetic fatigue. *Journal of athletic training* **2011**, *46*, 11-19.
56. Radzak, K.N.; Putnam, A.M.; Tamura, K.; Hetzler, R.K.; Stickley, C.D. Asymmetry between lower limbs during rested and fatigued state running gait in healthy individuals. *Gait & posture* **2017**, *51*, 268-274.
57. Koblbauer, I.F.; van Schooten, K.S.; Verhagen, E.A.; van Dieën, J.H. Kinematic changes during running-induced fatigue and relations with core endurance in novice runners. *Journal of science and medicine in sport* **2014**, *17*, 419-424.
58. Dierks, T.A.; Davis, I.S.; Hamill, J. The effects of running in an exerted state on lower extremity kinematics and joint timing. *Journal of biomechanics* **2010**, *43*, 2993-2998.
59. Bazuelo-Ruiz, B.; Durá-Gil, J.V.; Palomares, N.; Medina, E.; Llana-Belloch, S. Effect of fatigue and gender on kinematics and ground reaction forces variables in recreational runners. *PeerJ* **2018**, *6*, e4489.
60. Willson, J.D.; Loss, J.R.; Willy, R.W.; Meardon, S.A. Sex differences in running mechanics and patellofemoral joint kinetics following an exhaustive run. *Journal of biomechanics* **2015**, *48*, 4155-4159.
61. Elliot, B.; Ackland, T. Biomechanical effects of fatigue on 10,000 meter running technique. *Research quarterly for exercise and sport* **1981**, *52*, 160-166.
62. Dutto, D.; Levy, M.; Lee, K.; Sidthalaw, S.; Smith, G. Effect of fatigue and gender on running mechanics 469. *Medicine & Science in Sports & Exercise* **1997**, *29*, 82.

63. Brown, A.M.; Zifchock, R.A.; Hillstrom, H.J. The effects of limb dominance and fatigue on running biomechanics. *Gait & posture* **2014**, *39*, 915-919.
64. Borgia, B.; Dufek, J.S.; Silvernail, J.F.; Radzak, K.N. The effect of fatigue on running mechanics in older and younger runners. *Gait & Posture* **2022**, *97*, 86-93.
65. García-Pinillos, F.; Cartón-Llorente, A.; Jaén-Carrillo, D.; Delgado-Floody, P.; Carrasco-Alarcón, V.; Martínez, C.; Roche-Seruendo, L.E. Does fatigue alter step characteristics and stiffness during running? *Gait & Posture* **2020**, *76*, 259-263.
66. Möhler, F.; Fadillioglu, C.; Stein, T. Fatigue-related changes in spatiotemporal parameters, joint kinematics and leg stiffness in expert runners during a middle-distance run. *Frontiers in Sports and Active Living* **2021**, *3*, 634258.
67. Willwacher, S.; Sanno, M.; Brüggemann, G.-P. Fatigue matters: An intense 10 km run alters frontal and transverse plane joint kinematics in competitive and recreational adult runners. *Gait & posture* **2020**, *76*, 277-283.
68. Mizrahi, J.; Verbitsky, O.; Isakov, E. Fatigue-related loading imbalance on the shank in running: a possible factor in stress fractures. *Annals of biomedical engineering* **2000**, *28*, 463-469.
69. Benson, L.C.; O'Connor, K.M. The effect of exertion on joint kinematics and kinetics during running using a waveform analysis approach. *Journal of applied biomechanics* **2015**, *31*, 250-257.
70. Winter, D.A. *Biomechanics and motor control of human movement*; John Wiley & Sons: 2009.
71. Sanno, M.; Willwacher, S.; Epro, G.; Brüggemann, G.-P. Positive work contribution shifts from distal to proximal joints during a prolonged run. *Medicine and science in sports and exercise* **2018**, *50*, 2507-2517.
72. Kelly, L.A.; Cresswell, A.G.; Farris, D.J. The energetic behaviour of the human foot across a range of running speeds. *Scientific reports* **2018**, *8*, 10576.
73. Cigoja, S.; Firminger, C.R.; Asmussen, M.J.; Fletcher, J.R.; Edwards, W.B.; Nigg, B.M. Does increased midsole bending stiffness of sport shoes redistribute lower limb joint work during running? *Journal of Science and Medicine in Sport* **2019**, *22*, 1272-1277.
74. Melaro, J.A.; Gruber, A.H.; Paquette, M.R. Joint work is not shifted proximally after a long run in rearfoot strike runners. *Journal of Sports Sciences* **2021**, *39*, 78-83.
75. Giandolini, M.; Munera, M.; Chimentin, X.; Bartold, S.; Horvais, N. Footwear influences soft-tissue vibrations in rearfoot strike runners. *Footwear Science* **2017**, *9*, S25-S27.

76. Chambon, N.; Rao, G.; Guéguen, N.; Berton, E.; Delattre, N. Foot angle at touchdown is not linearly related to the loading rate during running. *Footwear Sci* **2015**, *7*, S37-38.
77. Breine, B.; Malcolm, P.; Van Caekenberghe, I.; Fiers, P.; Frederick, E.C.; De Clercq, D. Initial foot contact and related kinematics affect impact loading rate in running. *Journal of Sports Sciences* **2017**, *35*, 1556-1564.
78. Nigg, B.M.; Cole, G.K.; Brüggemann, G.-P. Impact forces during heel-toe running. *Journal of applied biomechanics* **1995**, *11*, 407-432.
79. Frederick, E.; Hagy, J.L.; Mann, R.A. The prediction of vertical impact force during running. *Journal of Biomechanics* **1981**, *14*, 498.
80. Clarke, T.; Frederick, E.; Hamill, C. The study of rearfoot movement in running. *Sport shoes and playing surfaces. Champaign, IL: Human Kinetics* **1984**, 166-189.
81. Cavanagh, P.R. *The running shoe book*; Anderson World: 1980.
82. Nigg, B. Biomechanical aspects of running, in biomechanics of running shoes. *Human Kinetics Publishers* **1986**, *3*, 1-25.
83. Chambon, N.; Delattre, N.; Guéguen, N.; Berton, E.; Rao, G. Is midsole thickness a key parameter for the running pattern? *Gait & posture* **2014**, *40*, 58-63.
84. Zhang, M.; Zhou, X.; Zhang, L.; Liu, H.; Yu, B. The effect of heel-to-toe drop of running shoes on patellofemoral joint stress during running. *Gait & Posture* **2022**, *93*, 230-234.
85. Malisoux, L.; Chambon, N.; Urhausen, A.; Theisen, D. Influence of the heel-to-toe drop of standard cushioned running shoes on injury risk in leisure-time runners: a randomized controlled trial with 6-month follow-up. *The American journal of sports medicine* **2016**, *44*, 2933-2940.
86. Chambon, N.; Delattre, N.; Guéguen, N.; Berton, E.; Rao, G. Shoe drop has opposite influence on running pattern when running overground or on a treadmill. *European journal of applied physiology* **2015**, *115*, 911-918.
87. Horvais, N.; Samozino, P. Effect of midsole geometry on foot-strike pattern and running kinematics. *Footwear Science* **2013**, *5*, 81-89.
88. Yu, P.; He, Y.; Gu, Y.; Liu, Y.; Xuan, R.; Fernandez, J. Acute effects of heel-to-toe drop and speed on running biomechanics and strike pattern in male recreational runners: application of statistical nonparametric mapping in lower limb biomechanics. *Frontiers in Bioengineering and Biotechnology* **2022**, *9*, 1441.
89. Yong, J.R.; Silder, A.; Delp, S.L. Differences in muscle activity between natural forefoot and rearfoot strikers during running. *Journal of biomechanics* **2014**, *47*, 3593-3597.

90. Ervilha, U.F.; Mochizuki, L.; Figueira Jr, A.; Hamill, J. Are muscle activation patterns altered during shod and barefoot running with a forefoot footfall pattern? *Journal of Sports Sciences* **2017**, *35*, 1697-1703.
91. Ahn, A.; Brayton, C.; Bhatia, T.; Martin, P. Muscle activity and kinematics of forefoot and rearfoot strike runners. *Journal of Sport and Health Science* **2014**, *3*, 102-112.
92. Hall, J.P.; Barton, C.; Jones, P.R.; Morrissey, D. The biomechanical differences between barefoot and shod distance running: a systematic review and preliminary meta-analysis. *Sports Medicine* **2013**, *43*, 1335-1353.
93. Esculier, J.-F.; Dubois, B.; Dionne, C.E.; Leblond, J.; Roy, J.-S. A consensus definition and rating scale for minimalist shoes. *Journal of foot and ankle research* **2015**, *8*, 1-9.
94. Coetzee, D.R.; Albertus, Y.; Tam, N.; Tucker, R. Conceptualizing minimalist footwear: an objective definition. *Journal of sports sciences* **2018**, *36*, 949-954.
95. Rothschild, C.E. Primitive running: a survey analysis of runners' interest, participation, and implementation. *The Journal of Strength & Conditioning Research* **2012**, *26*, 2021-2026.
96. Bertelsen, M.; Hulme, A.; Petersen, J.; Brund, R.K.; Sørensen, H.; Finch, C.; Parner, E.T.; Nielsen, R. A framework for the etiology of running-related injuries. *Scandinavian journal of medicine & science in sports* **2017**, *27*, 1170-1180.
97. Squadrone, R.; Gallozzi, C. Biomechanical and physiological comparison of barefoot and two shod conditions in experienced barefoot runners. *Journal of sports medicine and physical fitness* **2009**, *49*, 6.
98. Sinclair, J.; Greenhalgh, A.; Brooks, D.; Edmundson, C.J.; Hobbs, S.J. The influence of barefoot and barefoot-inspired footwear on the kinetics and kinematics of running in comparison to conventional running shoes. *Footwear Science* **2013**, *5*, 45-53.
99. Firminger, C.R.; Edwards, W.B. The influence of minimalist footwear and stride length reduction on lower-extremity running mechanics and cumulative loading. *Journal of science and medicine in sport* **2016**, *19*, 975-979.
100. Fredericks, W.; Swank, S.; Teisberg, M.; Hampton, B.; Ridpath, L.; Hanna, J.B. Lower extremity biomechanical relationships with different speeds in traditional, minimalist, and barefoot footwear. *Journal of Sports Science & Medicine* **2015**, *14*, 276.
101. Hollander, K.; Argubi-Wollesen, A.; Reer, R.; Zech, A. Comparison of minimalist footwear strategies for simulating barefoot running: a randomized crossover study. *PloS one* **2015**, *10*, e0125880.

102. Firminger, C.R.; Fung, A.; Loundagin, L.L.; Edwards, W.B. Effects of footwear and stride length on metatarsal strains and failure in running. *Clinical Biomechanics* **2017**, *49*, 8-15.
103. Gillinov, S.M.; Laux, S.; Kuivila, T.; Hass, D.; Joy, S.M. Effect of minimalist footwear on running efficiency: A randomized crossover trial. *Sports health* **2015**, *7*, 256-260.
104. MCCALLION, P. Acute differences in foot strike and spatiotemporal variables for shod, barefoot or minimalist male runners. **2014**.
105. Fuller, J.T.; Thewlis, D.; Tsiros, M.D.; Brown, N.A.; Buckley, J.D. Effects of a minimalist shoe on running economy and 5-km running performance. *Journal of Sports Sciences* **2016**, *34*, 1740-1745.
106. Jandová, S.; Volf, P.; Vaverka, F. The influence of minimalist and conventional sports shoes and lower limbs dominance on running gait. *Acta of bioengineering and biomechanics* **2018**, *20*.
107. Squadrone, R.; Rodano, R.; Hamill, J.; Preatoni, E. Acute effect of different minimalist shoes on foot strike pattern and kinematics in rearfoot strikers during running. *Journal of sports sciences* **2015**, *33*, 1196-1204.
108. Izquierdo-Renau, M.; Queralt, A.; Encarnación-Martínez, A.; Perez-Soriano, P. Impact acceleration during prolonged running while wearing conventional versus minimalist shoes. *Research Quarterly for Exercise and Sport* **2021**, *92*, 182-188.
109. Zhang, X.; Deng, L.; Yang, Y.; Li, L.; Fu, W. Acute shoe effects on Achilles tendon loading in runners with habitual rearfoot strike pattern. *Gait & Posture* **2020**, *82*, 322-328.
110. Sinclair, J.; Atkins, S.; Taylor, P.J. The effects of barefoot and shod running on limb and joint stiffness characteristics in recreational runners. *Journal of Motor Behavior* **2016**, *48*, 79-85.
111. Sinclair, J. Effects of barefoot and barefoot inspired footwear on knee and ankle loading during running. *Clinical biomechanics* **2014**, *29*, 395-399.
112. Lu, J.; Xu, D.; Quan, W.; Baker, J.S.; Gu, Y. Effects of Forefoot Shoe on Knee and Ankle Loading during Running in Male Recreational Runners. *Molecular & Cellular Biomechanics* **2022**, *19*, 61.
113. Cheung, R.; Ngai, S.P. Effects of footwear on running economy in distance runners: A meta-analytical review. *Journal of science and medicine in sport* **2016**, *19*, 260-266.
114. Nordin, A.D.; Dufek, J.S. Footwear and footstrike change loading patterns in running. *Journal of Sports Sciences* **2020**, *38*, 1869-1876.

115. Paquette, M.R.; Zhang, S.; Baumgartner, L.D. Acute effects of barefoot, minimal shoes and running shoes on lower limb mechanics in rear and forefoot strike runners. *Footwear Science* **2013**, *5*, 9-18.
116. Rice, H.M.; Jamison, S.T.; Davis, I.S. Footwear matters: influence of footwear and foot strike on load rates during running. **2016**.
117. Hoitz, F.; Vienneau, J.; Nigg, B.M. Influence of running shoes on muscle activity. *PloS one* **2020**, *15*, e0239852.
118. Roca-Dols, A.; Losa-Iglesias, M.E.; Sánchez-Gómez, R.; Becerro-de-Bengoa-Vallejo, R.; López-López, D.; Palomo-López, P.; Rodríguez-Sanz, D.; Calvo-Lobo, C. Electromyography activity of triceps surae and tibialis anterior muscles related to various sports shoes. *Journal of the Mechanical Behavior of Biomedical Materials* **2018**, *86*, 158-171.
119. Willson, J.D.; Bjorhus, J.S.; Williams III, D.B.; Butler, R.J.; Porcari, J.P.; Kernozek, T.W. Short-term changes in running mechanics and foot strike pattern after introduction to minimalistic footwear. *Pm&r* **2014**, *6*, 34-43.
120. Warne, J.; Kilduff, S.; Gregan, B.; Nevill, A.; Moran, K.; Warrington, G. A 4-week instructed minimalist running transition and gait-retraining changes plantar pressure and force. *Scandinavian journal of medicine & science in sports* **2014**, *24*, 964-973.
121. Divert, C.; Mornieux, G.; Freychat, P.; Baly, L.; Mayer, F.; Belli, A. Barefoot-shod running differences: shoe or mass effect? *International journal of sports medicine* **2008**, *29*, 512-518.
122. Lussiana, T.; Fabre, N.; Hébert-Losier, K.; Mourot, L. Effect of slope and footwear on running economy and kinematics. *Scandinavian Journal of Medicine & Science in Sports* **2013**, *23*, e246-e253.
123. Perl, D.P.; Daoud, A.I.; Lieberman, D.E. Effects of footwear and strike type on running economy. *Med Sci Sports Exerc* **2012**, *44*, 1335-1343.
124. Warne, J.P.; Moran, K.A.; Warrington, G.D. Eight weeks gait retraining in minimalist footwear has no effect on running economy. *Human movement science* **2015**, *42*, 183-192.
125. Warne, J.P.; Smyth, B.P.; Fagan, J.O.C.; Hone, M.E.; Richter, C.; Nevill, A.M.; Moran, K.A.; Warrington, G.D. Kinetic changes during a six-week minimal footwear and gait-retraining intervention in runners. *Journal of Sports Sciences* **2017**, *35*, 1538-1546.

126. Khowailed, I.A.; Petrofsky, J.; Lohman, E.; Daher, N. Six weeks habituation of simulated barefoot running induces neuromuscular adaptations and changes in foot strike patterns in female runners. *Medical Science Monitor: International Medical Journal of Experimental and Clinical Research* **2015**, *21*, 2021.
127. Johnson, A.; Myrer, J.; Mitchell, U.; Hunter, I.; Ridge, S. Response to the Letter to the Editor for article: The Effects of a Transition to Minimalist Shoe Running on Intrinsic Foot Muscle Size. *International Journal of Sports Medicine* **2016**, *37*, 917-917.
128. Campitelli, N.A.; Spencer, S.A.; Bernhard, K.; Heard, K.; Kidon, A. Effect of Vibram FiveFingers minimalist shoes on the abductor hallucis muscle. *Journal of the American Podiatric Medical Association* **2016**, *106*, 344-351.
129. Delp, S.L.; Anderson, F.C.; Arnold, A.S.; Loan, P.; Habib, A.; John, C.T.; Guendelman, E.; Thelen, D.G. OpenSim: open-source software to create and analyze dynamic simulations of movement. *IEEE transactions on biomedical engineering* **2007**, *54*, 1940-1950.
130. Yu, J.; Zhang, S.; Wang, A.; Li, W. Human gait analysis based on OpenSim. In Proceedings of the 2020 International Conference on Advanced Mechatronic Systems (ICAMechS), 2020; pp. 278-281.
131. Thelen, D.G.; Anderson, F.C. Using computed muscle control to generate forward dynamic simulations of human walking from experimental data. *Journal of biomechanics* **2006**, *39*, 1107-1115.
132. Liu, M.Q.; Anderson, F.C.; Schwartz, M.H.; Delp, S.L. Muscle contributions to support and progression over a range of walking speeds. *Journal of biomechanics* **2008**, *41*, 3243-3252.
133. van der Krogt, M.M.; Delp, S.L.; Schwartz, M.H. How robust is human gait to muscle weakness? *Gait & posture* **2012**, *36*, 113-119.
134. Trinler, U.; Leboeuf, F.; Hollands, K.; Jones, R.; Baker, R. Estimation of muscle activation during different walking speeds with two mathematical approaches compared to surface EMG. *Gait & posture* **2018**, *64*, 266-273.
135. Kim, H.K.; Mei, Q.; Gu, Y.; Mirjalili, A.; Fernandez, J. Reduced joint reaction and muscle forces with barefoot running. *Computer Methods in Biomechanics and Biomedical Engineering* **2021**, *24*, 1263-1273.
136. Zhou, H.; Xu, D.; Quan, W.; Liang, M.; Ugbolue, U.C.; Baker, J.S.; Gu, Y. A pilot study of muscle force between normal shoes and bionic shoes during men walking and running stance phase using opensim. In Proceedings of the Actuators, 2021; p. 274.

137. Yu, L.; Mei, Q.; Mohamad, N.I.; Gu, Y.; Fernandez, J. An exploratory investigation of patellofemoral joint loadings during directional lunges in badminton. *Computers in Biology and Medicine* **2021**, *132*, 104302.
138. Scarton, A.; Jonkers, I.; Guiotto, A.; Spolaor, F.; Guarneri, G.; Avogaro, A.; Cobelli, C.; Sawacha, Z. Comparison of lower limb muscle strength between diabetic neuropathic and healthy subjects using OpenSim. *Gait & posture* **2017**, *58*, 194-200.
139. Peterson, C.L.; Hall, A.L.; Kautz, S.A.; Neptune, R.R. Pre-swing deficits in forward propulsion, swing initiation and power generation by individual muscles during hemiparetic walking. *Journal of biomechanics* **2010**, *43*, 2348-2355.
140. Lerner, Z.F.; Browning, R.C. Compressive and shear hip joint contact forces are affected by pediatric obesity during walking. *Journal of biomechanics* **2016**, *49*, 1547-1553.
141. Scott, G.; Menz, H.B.; Newcombe, L. Age-related differences in foot structure and function. *Gait & posture* **2007**, *26*, 68-75.
142. Schünke, M.; Ross, L.M.; Schulte, E.; Schumacher, U.; Lamperti, E.D. *General anatomy and musculoskeletal system*; Thieme: 2010.
143. Kelikian, A.S.; Sarrafian, S.K. *Sarrafian's anatomy of the foot and ankle: descriptive, topographic, functional*; Lippincott Williams & Wilkins: 2011.
144. Golanó, P.; Vega, J.; De Leeuw, P.A.; Malagelada, F.; Manzanares, M.C.; Götzens, V.; Van Dijk, C.N. Anatomy of the ankle ligaments: a pictorial essay. *Knee Surgery, Sports Traumatology, Arthroscopy* **2010**, *18*, 557-569.
145. Park, D.-J.; Hwang, Y.-I. Comparison of the intrinsic foot muscle activities between therapeutic and three-dimensional foot-ankle exercises in healthy adults: An explanatory study. *International Journal of Environmental Research and Public Health* **2020**, *17*, 7189.
146. McKeon, P.O.; Hertel, J.; Bramble, D.; Davis, I. The foot core system: a new paradigm for understanding intrinsic foot muscle function. *British journal of sports medicine* **2015**, *49*, 290-290.
147. Cho, J.-R.; Park, S.-B.; Ryu, S.-H.; Kim, S.-H.; Lee, S.-B. Landing impact analysis of sports shoes using 3-D coupled foot-shoe finite element model. *Journal of mechanical science and technology* **2009**, *23*, 2583-2591.
148. Yang, Z.; Cui, C.; Wan, X.; Zheng, Z.; Yan, S.; Liu, H.; Qu, F.; Zhang, K. Design feature combinations effects of running shoe on plantar pressure during heel landing: A finite element analysis with Taguchi optimization approach. *Frontiers in Bioengineering and Biotechnology* **2022**, *10*.

149. Peng, Y.; Wang, Y.; Wong, D.W.-C.; Chen, T.L.-W.; Chen, S.F.; Zhang, G.; Tan, Q.; Zhang, M. Different design feature combinations of flatfoot orthosis on plantar fascia strain and plantar pressure: A muscle-driven finite element analysis with taguchi method. *Frontiers in Bioengineering and Biotechnology* **2022**, *10*.
150. Xiang, L.; Mei, Q.; Wang, A.; Shim, V.; Fernandez, J.; Gu, Y. Evaluating function in the hallux valgus foot following a 12-week minimalist footwear intervention: A pilot computational analysis. *Journal of Biomechanics* **2022**, *132*, 110941.
151. Li, Y.; Leong, K.F.; Gu, Y. Construction and finite element analysis of a coupled finite element model of foot and barefoot running footwear. *Proceedings of the Institution of Mechanical Engineers, Part P: Journal of Sports Engineering and Technology* **2019**, *233*, 101-109.
152. Li, S.; Zhang, Y.; Gu, Y.; Ren, J. Stress distribution of metatarsals during forefoot strike versus rearfoot strike: A finite element study. *Computers in biology and medicine* **2017**, *91*, 38-46.
153. Ellison, M.; Fulford, J.; Javadi, A.; Rice, H. Do non-rearfoot runners experience greater second metatarsal stresses than rearfoot runners? *Journal of Biomechanics* **2021**, *126*, 110647.
154. Chen, T.L.-W.; Wong, D.W.-C.; Wang, Y.; Lin, J.; Zhang, M. Foot arch deformation and plantar fascia loading during running with rearfoot strike and forefoot strike: a dynamic finite element analysis. *Journal of Biomechanics* **2019**, *83*, 260-272.
155. Quan, W.; Gao, L.; Xu, D.; Zhou, H.; Korim, T.; Shao, S.; Baker, J.S.; Gu, Y. Simulation of Lower Limb Muscle Activation Using Running Shoes with Different Heel-to-Toe Drops Using Opensim. In *Proceedings of the Healthcare, 2023*; p. 1243.
156. Xu, D.; Lu, Z.; Shen, S.; Gus, F.; Ukadike, C.; Gu, Y. The Differences in Lower Extremity Joints Energy Dissipation Strategy during Landing between Athletes with Symptomatic Patellar Tendinopathy (PT) and without Patellar Tendinopathy (UPT). *Mol. Cell. Biomech* **2021**, *18*.
157. Wu, T.; Martens, H.; Hunter, P.; Mithraratne, K. Emulating facial biomechanics using multivariate partial least squares surrogate models. *International journal for numerical methods in biomedical engineering* **2014**, *30*, 1103-1120.
158. Pailler-Mattei, C.; Bec, S.; Zahouani, H. In vivo measurements of the elastic mechanical properties of human skin by indentation tests. *Medical engineering & physics* **2008**, *30*, 599-606.

159. Gu, Y.; Ren, X.; Li, J.; Lake, M.; Zhang, Q.; Zeng, Y. Computer simulation of stress distribution in the metatarsals at different inversion landing angles using the finite element method. *International orthopaedics* **2010**, *34*, 669-676.
160. Pena, E.; Calvo, B.; Martinez, M.; Doblare, M. A three-dimensional finite element analysis of the combined behavior of ligaments and menisci in the healthy human knee joint. *Journal of biomechanics* **2006**, *39*, 1686-1701.
161. Cheung, J.T.-M.; Zhang, M.; Leung, A.K.-L.; Fan, Y.-B. Three-dimensional finite element analysis of the foot during standing—a material sensitivity study. *Journal of biomechanics* **2005**, *38*, 1045-1054.
162. Siegler, S.; Block, J.; Schneck, C.D. The mechanical characteristics of the collateral ligaments of the human ankle joint. *Foot & ankle* **1988**, *8*, 234-242.
163. Chen, W.-M.; Lee, T.; Lee, P.V.-S.; Lee, J.W.; Lee, S.-J. Effects of internal stress concentrations in plantar soft-tissue—a preliminary three-dimensional finite element analysis. *Medical engineering & physics* **2010**, *32*, 324-331.
164. Cheung, J.T.-M.; Zhang, M.; An, K.-N. Effects of plantar fascia stiffness on the biomechanical responses of the ankle-foot complex. *Clinical Biomechanics* **2004**, *19*, 839-846.
165. Altman, A.R.; Davis, I.S. A kinematic method for footstrike pattern detection in barefoot and shod runners. *Gait & posture* **2012**, *35*, 298-300.
166. Winter, S.; Gordon, S.; Watt, K. Effects of fatigue on kinematics and kinetics during overground running: a systematic review. *The Journal of Sports Medicine and Physical Fitness* **2016**, *57*, 887-899.
167. Zhang, S.-N.; Bates, B.T.; Dufek, J.S. Contributions of lower extremity joints to energy dissipation during landings. *Medicine and science in sports and exercise* **2000**, *32*, 812-819.
168. Christina, K.A.; White, S.C.; Gilchrist, L.A. Effect of localized muscle fatigue on vertical ground reaction forces and ankle joint motion during running. *Human movement science* **2001**, *20*, 257-276.
169. Duquette, A.M.; Andrews, D.M. Tibialis anterior muscle fatigue leads to changes in tibial axial acceleration after impact when ankle dorsiflexion angles are visually controlled. *Human movement science* **2010**, *29*, 567-577.
170. Mei, Q.; Gu, Y.; Xiang, L.; Yu, P.; Gao, Z.; Shim, V.; Fernandez, J. Foot shape and plantar pressure relationships in shod and barefoot populations. *Biomech. Model. Mechanobiol.* **2019**, 1-14.

171. Mei, Q.; Gu, Y.; Xiang, L.; Baker, J.S.; Fernandez, J. Foot pronation contributes to altered lower extremity loading after long distance running. *Front. Physiol.* **2019**, *10*, 573.
172. Cheung, R.T.; Rainbow, M.J. Landing pattern and vertical loading rates during first attempt of barefoot running in habitual shod runners. *Human movement science* **2014**, *34*, 120-127.
173. Valenzuela, K.A.; Lynn, S.K.; Mikelson, L.R.; Noffal, G.J.; Judelson, D.A. Effect of acute alterations in foot strike patterns during running on sagittal plane lower limb kinematics and kinetics. *Journal of sports science & medicine* **2015**, *14*, 225.
174. Hamill, J.; Gruber, A.H.; Derrick, T.R. Lower extremity joint stiffness characteristics during running with different footfall patterns. *European journal of sport science* **2014**, *14*, 130-136.
175. Lieberman, D.E. What we can learn about running from barefoot running: an evolutionary medical perspective. *Exercise and sport sciences reviews* **2012**, *40*, 63-72.
176. Ferber, R.; Noehren, B.; Hamill, J.; Davis, I. Competitive female runners with a history of iliotibial band syndrome demonstrate atypical hip and knee kinematics. *journal of orthopaedic & sports physical therapy* **2010**, *40*, 52-58.
177. Altman, A.R.; Davis, I.S. Barefoot running: biomechanics and implications for running injuries. *Current sports medicine reports* **2012**, *11*, 244-250.
178. Kulmala, J.-P.; Avela, J.; Pasanen, K.; Parkkari, J. Forefoot strikers exhibit lower running-induced knee loading than rearfoot strikers. *Medicine & Science in Sports & Exercise* **2013**, *45*, 2306-2313.
179. Sinclair, J.; Atkins, S.; Richards, J.; Vincent, H. Modelling of muscle force distributions during barefoot and shod running. *Journal of Human Kinetics* **2015**, *47*, 9-17.
180. Divert, C.; Mornieux, G.; Baur, H.; Mayer, F.; Belli, A. Mechanical comparison of barefoot and shod running. *International journal of sports medicine* **2005**, *26*, 593-598.
181. Jenkins, D.W.; Cauthon, D.J. Barefoot running claims and controversies: a review of the literature. *Journal of the American Podiatric Medical Association* **2011**, *101*, 231-246.
182. Kelly, L.A.; Farris, D.J.; Lichtwark, G.A.; Cresswell, A.G. The influence of foot-strike technique on the neuromechanical function of the foot. **2018**.
183. Roy, J.-P.R.; Stefanyshyn, D.J. Shoe midsole longitudinal bending stiffness and running economy, joint energy, and EMG. *Medicine & Science in Sports & Exercise* **2006**, *38*, 562-569.

184. Cauthon, D.J.; Langer, P.; Coniglione, T.C. Minimalist shoe injuries: three case reports. *The foot* **2013**, *23*, 100-103.
185. Salzler, M.J.; Bluman, E.M.; Noonan, S.; Chiodo, C.P.; de Asla, R.J. Injuries observed in minimalist runners. *Foot & Ankle International* **2012**, *33*, 262-266.
186. Bergstra, S.; Kluitenberg, B.; Dekker, R.; Bredeweg, S.; Postema, K.; Van den Heuvel, E.; Hijmans, J.; Sobhani, S. Running with a minimalist shoe increases plantar pressure in the forefoot region of healthy female runners. *Journal of Science and Medicine in Sport* **2015**, *18*, 463-468.